Approaches for Chatter Reduction in
Deep Cavity and Intricate Surface Milling
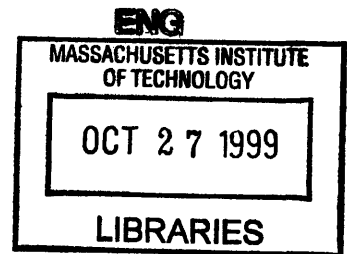
by

Gaurav Rohatgi

B.S. Mechanical Engineering
Massachusetts Institute of Technology, 1996

SUBMITTED TO THE DEPARTMENT OF MECHANICAL ENGINEERING IN
PARTIAL FULFILLMENT OF THE REQUIREMENTS FOR THE DEGREE OF

MASTER OF SCIENCE IN MECHANICAL ENGINEERING
AT THE
MASSACHUSETTS INSTITUTE OF TECHNOLOGY

JUNE 1998

Signature of Author: _____

Department of Mechanical Engineering
May 20, 1998
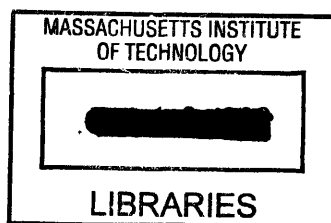
Certified by: _____

Alexander Slocum
Alex & Brit d'Arbeloff Professor of Mechanical Engineering
Thesis Supervisor

Approved by: _____

Ain A. Sonin
Professor of Mechanical Engineering
Chairman, Committee for Graduate Students

Approaches for Chatter Reduction in Deep Cavity and Intricate Surface Milling

by

Gaurav Rohatgi

Submitted to the Department of Mechanical Engineering
on May 20, 1998 in Partial Fulfillment of the
Requirements for the Degree of Master of Science in
Mechanical Engineering

ABSTRACT

The goal of the project was to increase the metal removal rate or improve the surface quality of an intricate surface cut by a long overhang tool. The results of the metal cutting tests show that the surface quality of a finish cut at conventional milling speeds can be improved by approximately 50% by using a stepped or tapered tool. In applications with straight walls or intricate surfaces where the larger diameter base of the tool interferes with the workpiece, a high stiffness 5 axis machine can achieve the desired geometry. Damping treatments such as the squeeze film damped tool and the visocelastic ring were developed that could significantly increase the dynamic stiffness of a long overhang tool. These damping treatments did not improve the workpiece surface finish at conventional milling speeds. However, metal cutting theory indicates that more damping could be beneficial in high speed milling applications in which the vibration amplitude of the tool's resonant cantilever mode limits the stable depth of cut. This study has also produced an analytic model and damping methods that will enable designers to tailor the dynamic response of a tool to attenuate the vibrations that cause chatter at higher spindle speeds.

Thesis Supervisor: Alexander Slocum
Title: Professor of Mechanical Engineering

Acknowledgments

Nothing of consequence can be accomplished without the help of others. I'd like to thank the people who got out and pushed when the car was stalled and cheered as it was racing.

Professor Alex Slocum who has been my guardian angel at MIT and who is a gem of a human being. If we all had his attitude to life and work, we could end crime, world hunger, and social injustice.

Kevin Wasson whose work on the Turbo Tool™ opened the door for this work and whose technical knowledge on the subject greatly accelerated my learning curve.

The sponsors of the project Gary Vrsek, Rodney Tobazinski, Zafar Shaikh Joe Shim of Ford Motor Company and Norman Lawton and Dave Leslie of Star Cutter Company for their infinite patience and willingness to try crazy new ideas.

Dr. Larry Schuette and David Armoza of the Naval Research Laboratory and DanGearing of the Defense Logistics Agency whose generous support of the PERG, help enable this type of research to be conducted.

Maureen Lynch because she's the only one who can keep Alex in line.

Marc, Jerry and Fred for turning the machine shop experience from traumatic to fun.

Martin Culpepper, Abbe Bamberg, Nathan Kane, Jason Jarboe, my lab mates who kicked around ideas, kept the computer network working and let me learn from them.

The National Science Foundation and the Center for Innovation in Product Development who were also sponsors of this work. In particular, I am indebted to Warren Seering, Kamala Grasso, Ana Thornton, Daniel Whitney, Don Clausing, and Maggie.

Charlie Gardiner and Bret Gnall for their guidance and encouragement while I was visiting Xerox. The things I learned from them helped me create the development process for the project.

Burt LaFountain and Marc Ardayfio two friends who, through their example and support, are the reason I stayed in graduate school and finished.

My parents who taught me everything important and stood behind their lessons with unconditional love.

My fiancee, Tara, who kicks me in the butt and lets me hide from the world around me but has the wisdom to know when to do what.

God who created us and gave us the ability to create love and the love to create.

Table of Contents

Chapter 1: Need for a low cost chatter reduction solution

1.1 Chatter in High Speed Machining

In metal cutting, machine spindle speeds are slowly but continuously increasing due to the improved part surface quality and improved metal removal rates that high speed machining provides. The improvement in performance at high speeds is largely due to the reduction in cutting forces as more tooth passes are made to remove a given amount of material (King 1985). The benefits of high speed machining are especially attractive in applications such as mold making and rapid prototyping where complex geometries, smooth surface finishes and fast cycle times are critical to the successful, timely launch of a new product. Due to the widespread applicability and continuous development effort in the area of high speed machining, analysts in the machine tool industry expect that machining speed will show slow but continuous growth into the next century. (Lewis 1996)

To keep pace with customers' desire to machine at faster and faster speeds, machine tools and their complimentary industries will have to develop products that address the special needs in high speed machining. One problem associated with high speed machining is that chatter occurs as the higher frequency modes of vibration associated with the cutting tool are excited.

Chatter is a violent vibration between the cutting tool and the workpiece that results in poor surface quality and damage to the cutting tool or even the machine. Chatter occurs because the damping of the machine tool system is not sufficient to absorb

the portion of the cutting energy transmitted to the system. (Stephenson 1997) The most common approach to eliminate chatter is to lower the excitation energy by reducing the metal removal rate when it is encountered under specific cutting conditions. While this approach is preferred to damaging the part, tool or machine, it too can have far reaching negative economic impact. Procedures and products are available for chatter reduction, but they have limited applicability due to their small range of effectiveness or prohibitive cost.

Due to the lack of widely applicable solution for chatter reduction, high speed machining is only slowly gaining acceptance in those applications where quality and speed greatly outweigh cost considerations. For high speed machining to become a practical reality in common practice, where quality, speed and cost are equally important, an effective low-cost solution for chatter reduction will have to be found.

1.2 The Mechanism of Chatter

Chatter, or self excited vibration, is not induced by external periodic forces but from the dynamic cutting process itself. Figure 1.1 below shows that the cutting forces encountered in milling can be approximated by a saw tooth function.
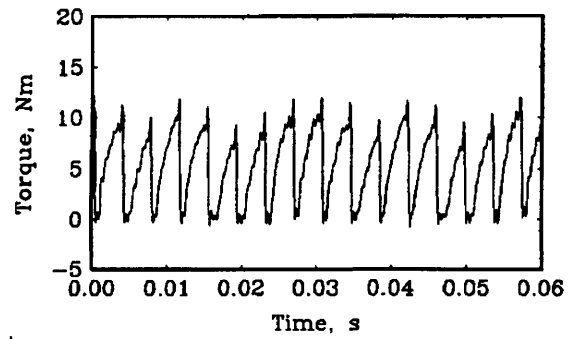
Figure 1.1 Spindle torque measured in up milling. (Smith 1994)

Chatter occurs when forces from the cutting process excite one or more of the natural modes of vibration of the machine tool system. A typical deflection/force transfer function for a carbide endmill in a spindle showing the resonant peak associated with the first cantilever mode is shown in Figure 1.2.
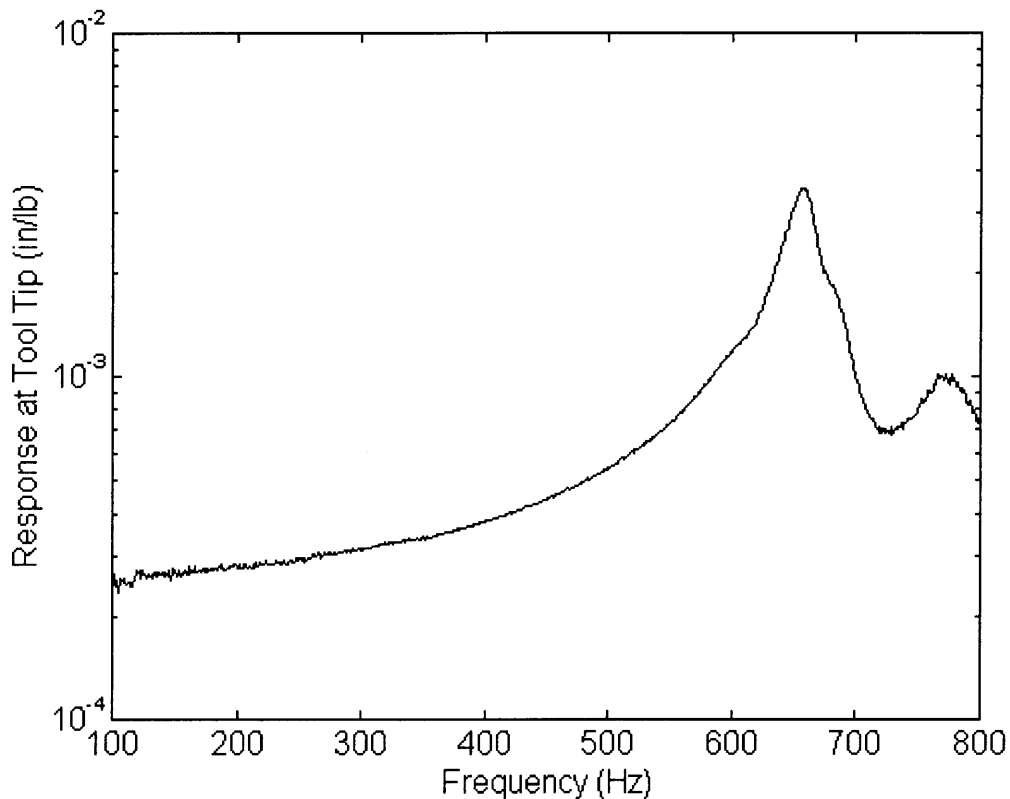
Figure 1.2: Typical dynamic response of a machine tool system. (Q=14)

The force required for this excitation can come from a hard grain in the work piece, the individual cutting edges of the tool entering the work piece, or from deformities in the work piece or cutting tool edge. Such conditions can result in impact forces which feed energy over a broad spectrum of frequencies to the machine tool system. In milling, as the spindle speed increases, the period of the saw tooth cutting force decreases and the cutting forces decrease since more teeth passes are made to remove a given amount of material. At very high spindle speeds, the power required to remove a given amount of material is actually lower than at slow speeds. This results in a further reduction in cutting force at a given feed rate. The reduction in cutting force results in better surface finishes while the ability to increase the feed rate increases the metal removal rate. Figure 1.3

compares the frequency content of several saw tooth trains of equal power but different spindle speeds. Note that as the spindle speed increases and the saw tooth amplitude decreases, the force amplitude at higher frequencies increases relative to the force amplitude at low frequencies. When the feed rate is increased at high spindle speeds, thereby increasing the amplitude of all frequencies in the input spectrum, the high frequency components of the cutting forces input to the system become significant.
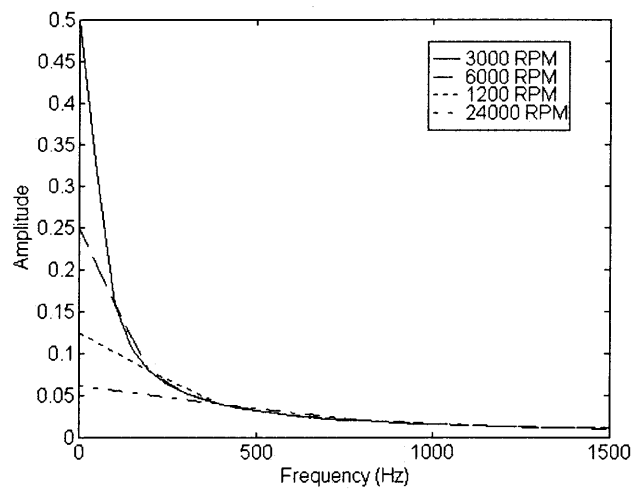
Figure 1.3: Relative frequency spectrum of saw tooth cutting forces at various spindle speeds and constant material removal rate.

This could explain why the high frequency cantilever mode of the tool (around 500-1500 hz) which is inactive in normal machining, can cause vibrations that result in poor surface finish or even chatter in high speed machining.

To help understand how vibration at the tool tip can lead to chatter, a block diagram for the feedback process responsible for chatter, as described in Tlusty's theory (Stephenson 1997), is shown in Figure 1.4. If the impact force associated with cutting contains enough energy at a natural frequency of the system, the system will vibrate at that frequency. This vibration results in the tool cutting a wavy surface (y_i) in the work

piece (primary feedback). Figure 1.5 illustrates the surface waviness generated in various metal cutting operations. Under certain conditions, the next pass of the vibrating tool, or flute in the case of milling, can align with the wavy surface just cut (y_{i-1}) to cause variations in the chip thickness (regenerative feedback).

The degree of constructive or destructive alignment of the vibrations depends on the phase lag (ε) between cutting events at a single point and the overlap factor (μ)[1]. In milling, at a given frequency of vibration, f, in hertz, ε can be calculated from the relation.

$$\varepsilon = 2\pi\left(\frac{f}{nz} - N\right) \qquad\qquad Eqn\ 1.1$$

where n is the spindle speed in revolutions/sec, z is the number of teeth per revolution, and N is the number of whole oscillation cycles between subsequent cuts at a single point (see Figure 1.5). Note that in Figure 1.5 that the largest variation in chip thickness corresponds to $\varepsilon=180°$.

The variation in thickness of the chip formed due to these vibrations causes fluctuations in the cutting force proportional to the width of cut (b) and the cutting stiffness of the material (k_d)[2]. These fluctuations in cutting force can further propagate

---

[1] In general, $\mu=1$ in milling since the surface being cut by the current tooth or flute is entirely the product of the previous tooth or flute. In thread cutting, $\mu=0$ since the cut zone never overlaps the most recently cut surface.

[2] Typically, k_d is 2.9×10^5 psi (2×10^9 Pa) for cutting steel.

the amplitude of vibration and can eventually lead to instability if the vibration is not

sufficiently damped.
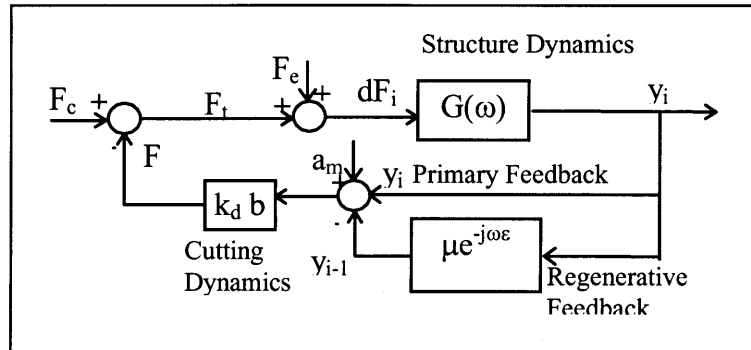
Figure 1.4: Block diagram of machining process characteristics that lead to chatter.(Stephenson 1997)
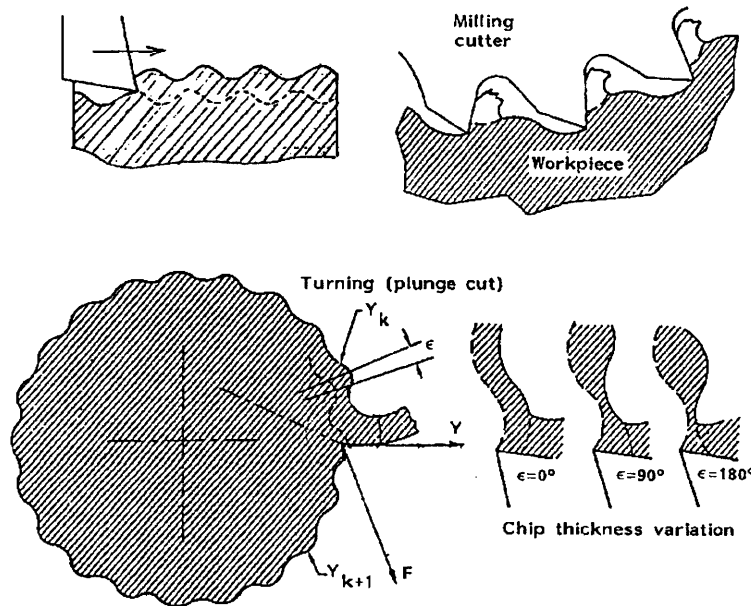
Figure 1.5: Surface waviness generated in metal cutting operations.(Tlusty 1985)

Using this model for the cutting process, the criterion for stability requires that the

current amplitude of vibration, y_i, must be less than or equal to the amplitude of vibration

13

during the previous pass of the cutter, y_{i-1}. Otherwise, the amplitude of vibration

increases in each subsequent pass and the system becomes unstable.

From the transfer function, the ratio of the current amplitude of vibration to the

amplitude of the previous cut is given by:

$$\frac{y_i}{y_{i-1}} = \frac{-G(\omega)}{G(\omega) + \dfrac{1}{k_d \cdot b}} \qquad\qquad Eqn\ 1.2$$

To find the limit width of cut for stability, b_{lim}, we set the magnitude of this ratio equal to

1, the criterion for stability. We also recognize that at any given frequency, the amplitude

of vibration corresponding to $\varepsilon=180$ is just the projection of the magnitude of the transfer

function projected onto the negative real axis as shown in Figure 1.6.
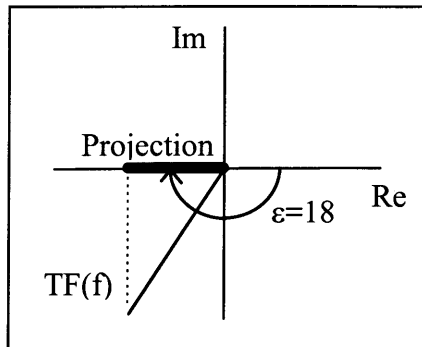
Figure 1.6: Significance of the negative real part of the tool tip deflection/force transfer function.

The resulting expression for the limit width of cut is given by:

$$b_{lim} = \frac{-1}{2 \cdot k_d \cdot \text{Re}\{G(\omega)\}_{(-\max)}} \qquad\qquad Eqn\ 1.3$$

where $\text{Re}\{G(\omega)\}_{(-\max)}$ is the maximally negative value of the real part of the

deflection/force transfer function at the cutter.

14

1.3 The Costs of Chatter

1.3.1 Poor part quality

If a chatter problem in a metal cutting operation goes un-remedied, the part quality suffers. During chatter, vibrations can cause the cutting edge to leave the work piece entirely and upon its return, impact and dig deep into the work piece. This results in a high pitched noise for which the phenomenon is named. It also results in a damaged part surface where the depth of cut varies from the nominal and possibly beyond the acceptable tolerance limits for the part. Even if part damage does not occur, the amplitude of the chatter vibrations can cause surface waviness beyond the tolerance limits of the part.

1.3.2 Accelerated tool wear

Chatter problems impact the manufacturer's costs in other ways as well. The impact between the tool and the workpiece also damages the tool or at the very least causes premature tool wear. As a result, the manufacturer incurs costs of greater tool consumption and tool changes which reduce output.

1.3.3 Accelerated machine wear

In addition to the workpiece and tool, the machine tool can also suffer damage due to chatter. Machine tools are not generally designed to handle high amplitude vibrations on a continuous basis. Chatter vibrations can damage spindle and linear axis bearing surfaces and lead to accelerated aging and high maintenance and depreciation costs.

1.3.4 Reduced output

Since products that fail to meet the customer's specifications cannot be sold, chatter must be avoided. If no other remedy can be found, metal removal rates must be reduced until vibration free performance is obtained. This reduced output increases the machining time required for the part.

One result of longer machining time is a higher manufacturing cost. In competitive markets, increasing the selling price of a product to maintain profits is not an option since it usually leads to reduced market share and revenue which could jeopardize future projects and the health of the business. This means the manufacturer has to accept a smaller margin to maintain the target selling price, thereby reducing or even eliminating the profits.

A potentially more devastating effect of reduced output arises if the increased machining time causes a delay in the critical path to a product launch. For example, consider an injection mold required for a plastic part in a new product. In order to avoid chatter, the metal removal rate in machining the mold is reduced by 50%. If the expected machining time was 200 hours, it would now be 400 hours. Assuming the machine could be run 100 hours a week, this results in a 2 week delay of product launch since the mold is on the project's critical path. Since other companies might be launching competing products at the same time, the delay in product launch could result in lost revenue. In markets with high sales volumes, short product life-cycles and customers who are fast to adopt new products, the difference in profitability due to only a few weeks delay can be staggering. A detailed quantitative analysis of this scenario is given in (Ulrich 1993).

1.4 Currently Available Methods of Chatter Reduction

1.4.1 Universally available methods

Chatter problems are most often the cause of the machine tool or work piece structural dynamics. As a result, the universal methods of chatter reduction discussed below, which do not modify the machine tool structure in any way, are limited in their applicability.

1.4.1.1 Minimizing the tool overhang

In conventional milling, increasing the stiffness of the tool by reducing the overhang length as much as possible reduces the amplitude of vibration. This is due to the fact that the input force spectrum is dominated by low frequency components at conventional speeds. The machine tool system's response to this type of input force is dominated by the static compliance of the system rather than the resonant peak response at one of its natural modal frequencies.

1.4.1.2 Reducing the cutting tool rake angle

The rake angle is the angle of inclination between the leading edge of the cutting tool and the part being cut. As a chip of given thickness is sheared from the work piece, a small angle of inclination generates smaller reaction forces at the tool than a large angle of inclination. For the same reason, variations in cutting force for a given amplitude of vibration are also smaller with a smaller rake angle. As a result, it is common practice to grind tools with as small a rake angle as possible without sacrificing the integrity of the cutting tooth structure.

17

1.4.1.3 Radiusing the cutting tool

Another approach to chatter avoidance taken by experienced machinists is to grind the sharp point of a sharpened cutting tool into a slightly radiused point. A radiused point does not penetrate the workpiece as readily as a sharp point so for a given variation in cutting force, the deflection of the tool tip, and thereby the amount of energy stored in the cantilevered tool that can lead to chatter, is minimized.

1.4.1.4 Damping materials

On a few lucky occasions, machinists can sufficiently dampen the problematic mode of the machine tool system by using visco-elastic damping materials to mount certain components of machine tool. However, more often than not, the small percentage of extra damping does not effect the problematic mode or is not enough to completely eliminate the chatter problems.

1.4.2 Currently available chatter reduction products

Certain products are available to increase the machine tool system's resistance to chatter in cases where the universal approaches to chatter reduction are not sufficient or cutting parameters to yield stable machining cannot be easily found. However, due to the high purchase and implementation costs associated with these solutions, they are only applicable in cases where the part being produced warrants extensive machining process development or the cutting tool facilitates the use of renewable cutting inserts. Again, in mold making or rapid prototyping, where fast cycle times and small diameter milling tools are required, neither of these luxuries exist.

1.4.2.1 CRAC

A system for chatter recognition and control known as CRAC has been developed at the University of Florida and Manufacturing Laboratories, Inc. This system can distinguish the audio signal of a stable cutting process from one that is chattering. Once chatter is detected, the system can automatically adjust the cutting feed rate or spindle speed to return the system to stability. When this system is coupled with an adaptive control system, the machine can automatically catalogue the spindle speeds and axial depth of cut that result in the highest metal removal rate. (Tlusty 1997)

While this system does simplify the practitioner's search for the maximum metal removal rate under stable cutting conditions, it does not improve the damping of the system to make it more resistant to chatter. Hence, the machine tool's maximum productivity rates are simply found, not enhanced.

1.4.2.2 Tuned Tooling

Kennemetal Corporation markets tunable steel boring bars that incorporate an internal damper in the tool overhang. The product is pictured in Figure 1.7. These boring bars can operate from 6:1 to 10:1 length-to-diameter ratios. This concept can also be extended to large diameter milling cutters. The tool overhangs must be tuned for a given ratio by using the tuning device to measure the dynamic response and adjusting the internal damper until the dynamic response is minimized.
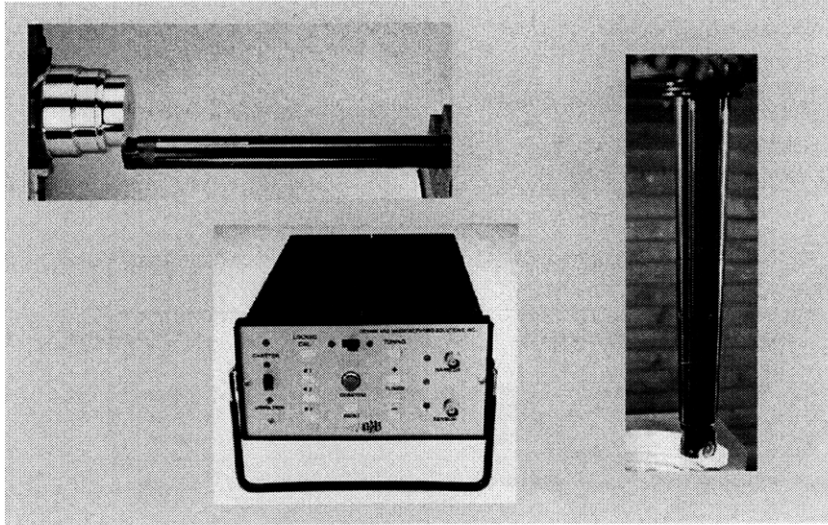
Figure 1.7 Tuned tooling and tuning device from Kennemetal Corporation.

While tuned tooling can help a machine tool achieve better surface finishes and tighter tolerances than it could without the product, it is only applicable in large diameter applications where the cutting edges of the tool can be separated from the tool overhang. To incorporate the internal damper into small diameter, disposable end-mills, and to require that each tool be individually tuned, could be prohibitively expensive.

1.4.2.3 Lanchester Vibration Absorber

The Lanchester Vibration Absorber is another approach used to enhance damping and reduce chatter in boring and large diameter milling. The device consists of a damper mass and damper. A practical example by Hahn is shown in Figure 1.8.
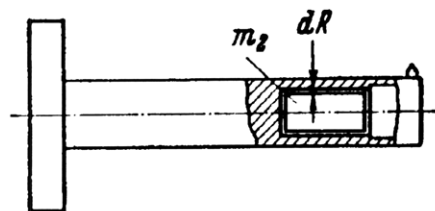
Figure 1.8: Lanchester damper by Hahn (Tobias 1965)

In the example shown, the viscous damper by Hahn consists of a mass m_2 which is

housed in a viscous medium trapped in the bored-out end of a bar near the tool. The

optimal radial clearance dR depends on the viscosity of the damping medium.

Commonly, oil is used as the damping medium. In the practical design of the device, m_2

should be made as large as possible and the damper mass and housing bore should be

held to a high standard of surface finish. (Tobias 1965)

While the device has given good results in large diameter boring and milling, it

would be difficult to satisfy the practical design requirements of mass and surface finish

in the small- diameter, disposable end-mills used in mold making and rapid prototyping.

1.4.2.4 Stiffer Tooling Systems

The stiffness of the tool holder - spindle interface and the tool - tool holder

interface have been areas of major improvements in recent years. There are a number of

competing designs in the tool holder - spindle interface. The traditional taper interface

tends to open as the spindle speed increases, thereby reducing the grip force or drawing

the tool further into the spindle. The HSK design, shown in Figure 1.9, uses interior

clamping which becomes stronger as the speed increases and a separate surface to locate

the tool axially. Due to the face contact between spindle and tool flange the stiffness is 5 -

7 times higher compared to tapered connections (Diebold Goldring Tooling 1997).

However, in long tool applications, the stiffness of the tool is an order of magnitude

lower than the holder anyway, so the stiffness of the tool holder - spindle interface is not a

significant concern.
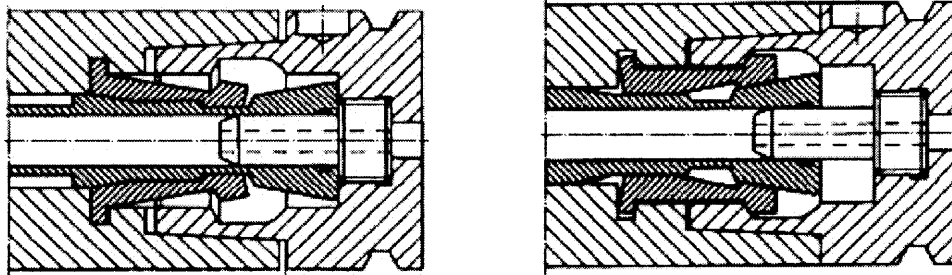
Figure 1.9: An HSK toolholder in the unclamped and clamped position.(WWW 1997)

In the tool-tool holder interface, substantial increases in stiffness and shortening of the overhang have been achieved using shrink fit tooling. A comparison of the static stiffness of three tool holding systems is shown in Figure 1.10.
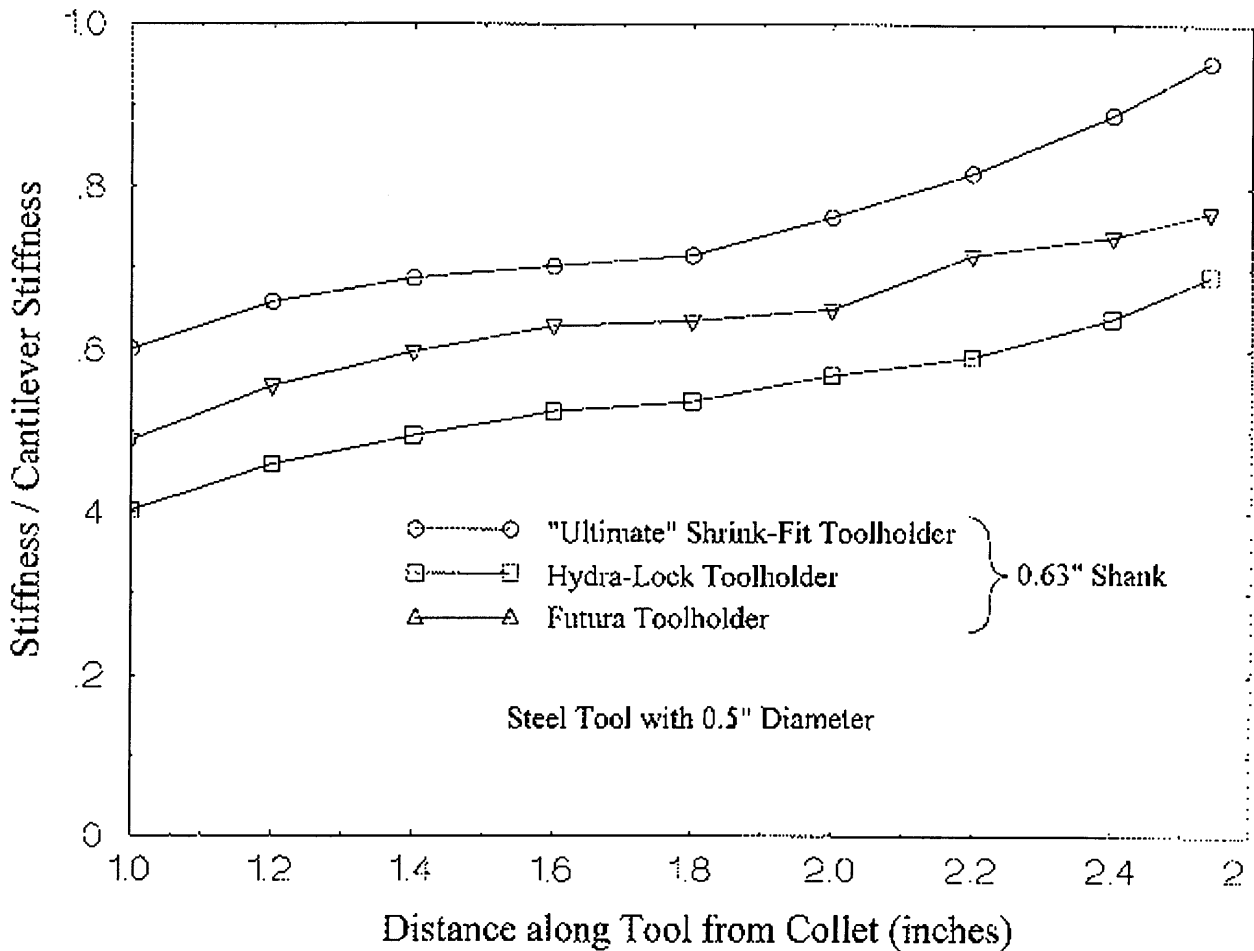
Figure 1.10: Comparison of static stiffness achieved by different tool holding approaches.(Shoffa 1997)

Note that the shrink fit tool holder results in greater static stiffness than the hydraulic or

conventional slit collet from Futura Inc.. One possible explanation for the performance

measured is that the level of pre-load pressure generated to hold the tool is largest in the shrink fit design.

The shrink-fit tool holder system from Universal Tooling Division comes with an induction heating unit that allows the customer to heat only the tool holder so the cooler and temporarily smaller tool can be replaced. The normal cycle time for changing tooling is only 7 seconds, making it as convenient to use as the hydraulic or slit collet designs.

A tool holder design from Universal Engineering, shown in Figure 1.11, incorporates both the HSK spindle interface and the Shrinker™ shrink fit tooling interface into the same tool holder and is quite possibly the most statically stiff tool holding solution available.
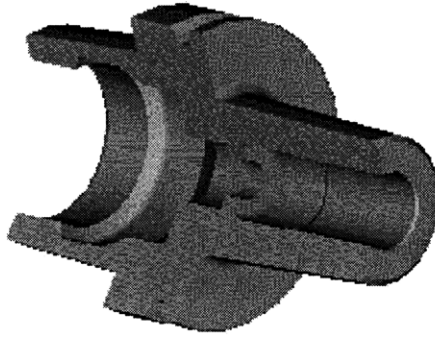
Figure 1.11: Toolholder from Universal Engineering incorporating the HSK and Shrinker™ designs.(WWW 1998)

The design does not, however, incorporate any device to increase the damping of the system. Therefore, at high spindle speeds, the machining process is still susceptible to high frequency chatter at the tool's resonant frequency.

The stiffness of the tooling system can also be increased by using a tapered tool. Tapered tools are much stiffer than standard straight tools of equal length and therefore provide better surface finishes. However, they are more expensive and may require the

23

use of a 5-axis machine to cut parts with straight vertical walls (Stilwell 1998) (See

Appendix D).

1.5 Motivation

Upon analyzing the causes of chatter and the approaches available to eliminate it,

it is apparent that no product or procedure currently exists to enable faster metal removal

rates or improved surface finishes in a wide variety of applications that require small

diameter, long overhang milling cutters.

Chapter 2 Project Planning for Rapid Technology Development

2.1 Balancing Time with Resource Burn

Given the need for tools with improved damping, an efficient method for developing new

technology products is required. The development of new technology products often

differs from the development of new generations of established technologies. The lack

of information about a well defined customer group and performance data for the

technology under consideration often requires that development tasks be delayed until the

design direction is finalized so that development resources can be used most efficiently.

An alternative approach is to conduct many tasks in parallel toward potential and

unidentified opportunities rather than in a serial fashion for maximum development speed

once the desired design direction is finalized. The distinction between Resource Efficient

Technology Development and Fast Technology Development is discussed below. The

following chapters follow the outline set forth in this section and illustrate how the Fast

Technology Development method, with its multiple parallel design directions, was used

to develop the chatter reduction solutions investigated in this project.

2.1.1 Resource Efficient Technology Development

Resource Efficient Technology Development, represented in Figure 2.1, is preferred in projects that require large resource commitments due to the complexity of the technology or the large capital cost incurred in developing the product. In this situation, it is risky to begin developing concepts, prototypes and detailed designs for the product before a design direction is established. The risk can be illustrated by considering a simple break-even analysis. Such an analysis would show that large amounts of money spent early in the project are harder to recover through product sales than large expenditures later in the project. Instead, it is wiser, in the case of large projects, to wait until the company's understanding of the technology and customer are mature so the duration of the resource intensive phases of the project can be kept to a minimum.
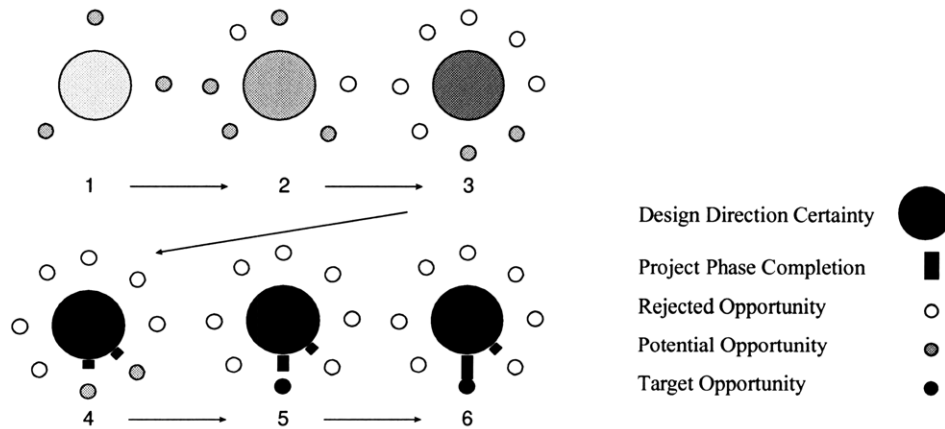
Figure 2.1: Time lapse representation of Resource Efficient Technology Development

2.1.2 Fast Technology Development

Fast Technology Development, represented in Figure 2.2, is preferred in projects that can be completed with a relatively small resource commitment. These projects

generally involve a simple technology, small piece of a complex technology, or a well

differentiated customer group. Most start up companies are founded by these types of

projects. In this case, time to market rather than resource expenditure rate determines the

profitability of the project since being late to market can allow a competitor to take an

early lead in market share or installed base. Since it is relatively cheap to develop

concepts, prototypes and detailed designs, several different design directions can be

explored while knowledge about the technology and customers is built. This knowledge

is required to determine the best opportunity to target, but usually takes a long time to

build in the case of new technologies and markets.
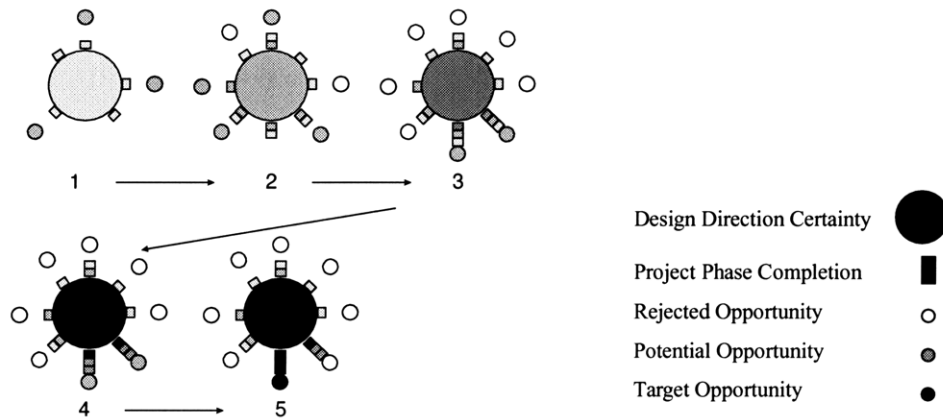
Figure 2.2: Time lapse representation of Fast Technology Development.

In Fast Technology Development, product developers are encouraged to explore

as many design directions as possible, even if there is only a vague understanding of the

potential opportunity. Also, phases are sometimes conducted in parallel as long as the

resource spending is justified by the certainty that there will be an eventual product. Such

an approach has three benefits. First, exploration of a certain design direction might

catalyze the identification of a new opportunity. Secondly, the work done in exploring a particular design direction might be applicable to another design direction for a newly identified potential opportunity. Finally, once the target opportunity is determined, it's likely that many of the phases of development toward that opportunity have already been partially completed thereby reducing the remaining time until product realization.

2.2 Development Process for Chatter Reduction Technology and Product

The Fast Technology Development approach was used in this project. A three phase development process was used for each design direction. In this section, short descriptions of tasks in the *Concept Generation and Evaluation*, *Concept Development*, and *Product Solidification and Release* phases are given.

2.2.1 Concept Generation and Evaluation

<u>2.2.1.1 Benefit Proposition</u>

The benefit proposition is a statement of the product's purpose with respect to the company and its customers that is used to guide the product definition.

<u>2.2.1.2 Functional Requirement Identification</u>

The functional requirements that the product must fulfill are based on testimony from experts and potential customers and an analytic understanding of the activities and parameters important to machining performance.

2.2.1.3 Enabling and Complementary Technologies Identification

Once the factors controlling the functionality of the product are determined, technologies that can deliver the required functionality are identified. Technologies which are currently gaining popularity with the target customer group are also identified to ensure that the product under consideration will take advantage of, rather than contradict, strong trends in the marketplace.

2.2.1.4 Conceptual Design

In conceptual design, the enabling and complementary technologies are arranged into a product architecture. The architectural rules such as the functions of modules within the product and the interactions of modules with each other and the environment are defined. The goal of conceptual design is to arrange the architectural elements in a way that will provide the greatest functionality for the cost incurred. However, designs in this phase do not have to be qualified by detailed cost or performance analysis and relative estimates of performance and costs for the various concepts are sufficient.

2.2.1.5 Concept Pre-Selection

In this phase concepts are selected based on their ability to meet the functional requirements. Only those designs that can be eliminated on the basis of their conceptual design without more detailed analysis are discarded.

2.2.2 Concept Development

2.2.2.1 Critical Parameter Identification

Critical Parameters are the product design attributes that effect the product's ability to meet the functional requirements. These critical parameters are determined by developing an analytic understanding of the fundamental physical principles that govern the product's performance.

2.2.2.2 Performance Modeling

Some Critical Parameters cannot be modeled analytically so they must be numerically simulated on a digital computer. The performance model helps the product development practitioner codify their understanding of the parameters that control the product's performance. The model must be refined as the understanding of the product's performance grows. A well developed performance model can help predict the effect of design changes and tolerance uncertainties.

2.2.2.3 Parametric Solid Modeling

A Parametric Solid Model helps in quickly developing a conceptual design into a realistic detailed design. Because the solid model forces the product development practitioner to consider the realistic constraints in manufacturing and assembling the product, it can help identify critical parameters that were overlooked before. The solid model can also be easily modified to yield production drawings later in the project when the design parameters are finalized.

2.2.2.4 Rapid Prototyping

Before the detailed production design is completed, parts of the product can be made to test the validity of the conceptual design and the accuracy of the performance model in predicting the product's performance. The results of testing on rapid prototypes can indicate that the model needs to include another level of detail to be sufficiently accurate. Testing done with rapid prototypes can also help gauge the performance that can be expected from the product and the customer's acceptance of the product.

2.2.2.5 Critical Parameter Verification

After experiments are conducted with the rapid prototypes, the product development practitioner must verify that the product attributes contributing the functional performance of the product are sufficiently understood. If a product is released without understanding the critical parameters that control the product's performance, solutions may not be readily available when problems are reported in the field. It is not necessary to understand every critical parameter before releasing the product, but the risk associated with the lack of understanding should be assessed before making the decision to release the product.

2.2.3 Product Solidification and Release

2.2.3.1 Model Optimization

Using a reasonably accurate model, the performance of the product can be optimized without building several iterations of the hardware, thereby saving time and money. A numerically simulated model can be optimized by adjusting the values of the

critical parameters and seeking the optimal combination of performance characteristics. An analytic model can be solved to directly output the required critical parameter value for a desired level of performance.

2.2.3.2 Manufacture to Detail Design

Once the performance model is optimized, the resulting critical parameters values can be applied to the solid model. From this model, drawings are quickly generated and parts can be made. For parts that require production tooling with a long lead time, preparations for manufacture are made in parallel to the detail design. To speed the development, long-lead-time tooling is produced in stages as more and more details become available. As a result, only slight modifications to the tool are required and parts can be made available quickly after the design is finalized. In such cases, major design changes that are not required for the functionality of the product are deferred until the next development cycle of the product so as not to delay its initial release.

2.2.3.3 Product Validation Testing

In validation testing, the product is tested under field conditions. This may include tests conducted by the product's developer or by customers chosen by the developer to act as test sites. This phase also includes quality assurance testing in which the developer must verify that the processes used in manufacturing the product can consistently deliver the product attributes required.

2.2.3.4 Risk Analysis Based Product Release

No development project is ever completely finished. In every project, there are unknown critical parameters and possible design improvements that could effect the performance of the product in the market place and in the field. The product developer must balance the risk of releasing the "unfinished" product against the cost of delaying the introduction and subsequent revenue of the product.

Chapter 3 Concept Generation and Evaluation

Concept Generation and Evaluation is the first phase of a new product development program. The activities in this phase are geared toward generating and identifying product concepts that are most likely to yield successful products. The steps are:

1. Statement of Benefit Proposition
2. Identification of Customer Needs and Functional Requirements
3. Identification of Enabling & Complementary Technologies
4. Conceptual Design
5. Concept Evaluation

3.1 Benefit Proposition

A benefit proposition statement usually guides the concept Generation and Evaluation phase of a project. This short statement describes how the product offering delivered by the current project will attract customers away from competitive offerings or create new customers. It is important that the benefit proposition be based on a clear and accurate understanding of the various customer desires that effect the product's success as well as the short and long term goals of the corporation. Some possible purposes for a new product program might be to satisfy an un-addressed customer need, fill out a company's product portfolio, increase the volume and therefore reduce the per part cost of an expensive production process, or help the company or customer transition to the next generation of technology in an industry. For this reason, in an established

corporation, a team representing the Engineering, Finance, and Marketing functions best handles the task of generating a balanced and realistic benefit proposition. Also, in an established organization, the benefit proposition statement is generated during an activity called Portfolio or Market Attack Planning that occurs on a regular basis to specify the company's plans for each of the market spaces it operates in. In the case of a startup company or a new venture idea in an established company, the benefit proposition is not necessarily constrained by an established structure and can be considered part of the concept generation phase as is the case in this project.

A good way to elicit the benefit proposition statement is to ask, What will the product do for the company or the customer and how will it do it? The following benefit proposition statement was used as a guide for this project.

A low cost product that offers a chatter reduction solution for

operations requiring long tool overhangs (greater than 5:1) that can

be used in all existing machine tools without expensive modifications

to the machine or to customer processes.

3.2 Customer Needs and Functional Requirements

The target customer groups for this product are job shop managers and machine operators who mill aluminum molds and deep pocketed prototype parts. This group would have the most incentive to purchase a product that could improve the achievable material removal rate. Most job shops working with aluminum are still milling at conventional speeds, but sales of higher speed machines are increasing and awareness of the benefits of high-speed machining is growing. For this reason, the product should

35

benefit the large installed base of conventional speed operations, but also be able to ride the growth in high speed machining by providing benefits in that regime as well.

3.2.1 Performance

<u>3.2.1.1 Dynamic Stiffness</u>

The dynamic stiffness of the tool is the inverse of the deflection/force transfer function measured at the tool tip and is therefore frequency dependent. In relation to chatter, the most important value is the dynamic stiffness at the resonant peak frequency. Dynamic stiffness is measured in lbs/inch and can also be represented as a ratio, Q, to the static stiffness of the tool.

$$Q = \frac{K_S}{K_D} \qquad Eqn\ 3.1$$

Q is known as the quality factor or the amplification factor. Since it normalizes the dynamic stiffness relative to the static stiffness, Q, is a good indication of the damping in the system. Q is related the damping factor ζ by : (Slocum)

$$Q = \frac{1}{2\zeta\sqrt{1-\zeta^2}} \qquad Eqn\ 3.2$$

For very small damping factors <.2 found in machine tool systems, Q can be approximated as

$$Q = \frac{1}{2\zeta} \qquad Eqn\ 3.3$$

In machining aluminum, the most common limiting factor to material removal rate is the onset of chatter at the machine tool system's natural frequency so by increasing

36

the damping, which is analogous to reducing Q, the chatter-free material removal rate limit will be increased.

3.2.1.2 Static stiffness

The static stiffness of the tool determines the deflection due to sustained or low frequency input forces, the smaller the deflection, the higher the accuracy of part being produced. Since a high static stiffness yields better part accuracy and surface finish, the tool holder should maintain the static stiffness available through currently available tool holders.

3.2.2 Functionality

Long slender end mills are used in cutting deep pockets in prototype parts or injection molds or when cutting complex parts on NC machines. In these applications, shorter tools that are less prone to chatter cannot be used because the machine tool spindle would interfere with the work piece. The tool holder developed in this project should maintain that functionality by keeping features external to the tool holder should be small enough that they will not cause problems in the tight cutting geometries encountered by the end user.

3.2.3 Costs

While certain members of the customer group are able to select products based on performance only, the majority of customers in this group place a high weighting factor on cost in their decisions to purchase tooling and tool holder systems. A product that introduces even slight cost increases will be received with skepticism and must therefore

provide a dramatic performance increase. In particular, the economic benefit of the higher material removal rate allowed by the product must more than offset the product's cost. If significant costs are introduced, however, it could jeopardize the initial salability of the product regardless of the performance increase. After chatter is removed as a bottleneck to the material removal rate (MRR), the limiting factor becomes the available spindle power. Since most spindles in use today are designed for conventional speeds and feeds there is a limit to the material removal rate they could achieve without expensive modifications even if chatter were completely eliminated. The factors affecting the allowable cost are illustrated in Figure 3.1.
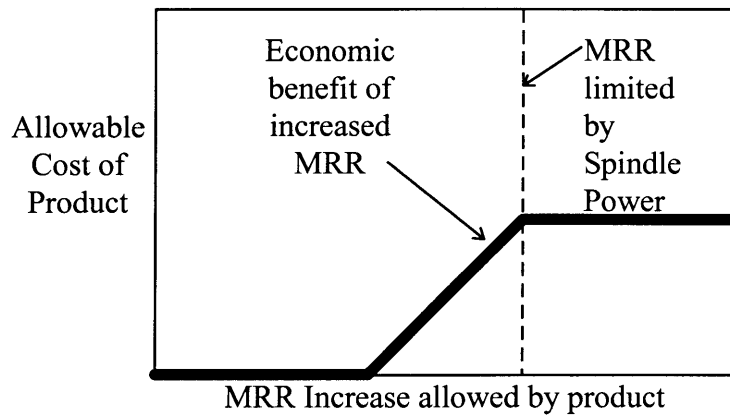
Figure 3.1: Allowable product cost vs. Material Removal Rate (MRR) performance

enhancement

3.2.3.1 Tool costs

Since tools are expendable, it is possible to spend more on tooling than on the machine tool during the life of the machine. As a result, a tooling cost increase of only a few percent can, over time, mean a significant increase in overall costs. Due to their high

38

sales volume, tools of standard form are relatively inexpensive when compared to custom-made tools. For this reason, tool holder that requires modifications to the tool should be avoided.

3.2.3.2 Machine tool modifications

While small modifications to the machine tool might be allowable, the tool holder should not require modifications involving a significant investment of money or time

3.2.3.3 Tool replacement time

In environments with significant machine uptime, the time required to replace a worn tool with a new one can become an important part of the overall lead-time for a part if the replacement time is long. In the tool holder under development in this project, the time required to replace the tool should be kept to a minimum.

3.3 Enabling Technologies

To catalyze product concepts that would be able to increase the damping of the machine tool system, three technologies that well known for their damping properties were explored. Those technologies are introduced in this section.

3.3.1 Hydrostatic Bearings

Hydrostatic bearings are a class of non-contact bearings that use a thin film of externally pressurized oil or water based coolant to support a load. A journal type hydrostatic bearing could find application in the cylindrical geometry of the interface between the tool and the tool holder. A self-compensated rotary hydrostatic bearing could resist deflections to the tool shank by diverting the external pressure from the

surface retreating from the tool holder to the opposed region advancing to the tool holder, thereby exerting a force on the tool shank that is opposed to the deflection. Kevin Wasson [3]and Alex Slocum of the Precision Engineering Research Group at MIT developed the self-compensated rotary hydrostatic bearing[4] that serves as the basis for the concept pictured in Figure 3.3 (Wasson 1996).

The damping capacity of a hydrostatic bearing comes from the energy dissipating viscous flow developed when the bearing is deflected. The liquid in the bearing gap is forced over restrictive lands that separate the pressurized region from atmospheric pressure. Since the clearance of the restrictive lands is on the order of 0.001", and the opposing pressure generated for a given amount of flow is inversely proportional to the cube of the gap, hydrostatic bearings can have huge damping constants. However, a small gap also generates higher self-compensation pressures to resist the deflection because the percent change in the flow exit area is increased. This can limit the deflection available to generate the fluid flow that results in damping. As a result, an optimal design will balance the stiffness of the hydrostatic bearing with the damping factor of the bearing.

---

[3] Dr. Wasson is now Chief Engineer at Aesop, Inc. (Bedford, NH). klwasson@aol.com

[3] See U.S. Patent Numbers: 5, 700, 092 &5,674,032

3.3.2 Constrained Layer Dampers

Constrained layer dampers are completely passive and operate by subjecting a viscous material to the relative motion between a stable structure and a vibrating structure. As a result, the energy in the vibrating structure is dissipated by the forces developed in deflecting the viscous material.

3.3.2.1 Viscous

Completely viscous constrained layer dampers are found in lubricated journal bearings. The damping mechanism is similar to that in hydrostatic journal bearings, but since there is no bearing pocket, the restrictive land acts on the entire area of the fluid layer. This means that the damping factors achievable in plain journal bearings are larger than those achieved in hydrostatic bearings with the same gap. Closed end journal bearings restrict the fluid flow in the axial direction and thereby generate larger flow forcing pressures. As a result, closed end journal bearings develop larger opposing forces than open end journal bearings with the same gap size.

3.3.2.2 Viscoelastic

Viscoelastic damping materials can also be used in constrained layer dampers. Here, the damping factor depends on the loss factor of the material. A higher loss factor results in more damping. Because the material is also elastic, the design can be balanced for the proper combination of stiffness and damping. The damper can be made stiffer by using a thinner layer of material.

3.4 Complimentary Technologies

Complimentary technologies are strong or emerging technologies that are related to the product. The product will be more successful if it utilizes or is at least compatible with these technologies because of the their favored or quickly emerging status in the market place.

3.4.1 Shrinker™ tool holding system

The Shrinker™ shrink fit tool holding system is quickly gaining market share due to the stiffness improvements it provides. The tool holder design should incorporate a shrink fit interface since it is the stiffest tool holding approach currently available. We should also note that the increased stiffness comes at a cost. Since the Shrinker tool holder is all one piece, the tool holding geometry is not interchangeable. Instead of switching the collet for a different diameter tool, a different tool holder must be purchased. This could require a significant investment in a shop where several tool holders in a variety of diameters are required.

3.4.2 HSK coupling

The HSK tool holder interface offers a definite improvement in stiffness over the traditional CV taper at high spindle speeds. Its use is currently limited, but if the trend toward higher spindle speeds continues, as it is expected to do, the HSK coupling may become the dominant coupling system. The tool holder product should be compatible with this coupling system as well as the traditional CV taper system.

3.5 Design Concepts

3.5.1 Concept Tree

The concept tree in Figure 3.2 shows the different chatter reduction solutions that were considered during the course of this project. Short descriptions of each conceptual design are given in the following section.

```
                    ┌──────────────────────────┐
                    │ Chatter Reduction Concepts │
                    └──────────────────────────┘
        ┌───────────────┬──────────┴──────────┬───────────────┐
  ┌───────────┐  ┌──────────────┐   ┌────────────────┐  ┌──────────────┐
  │ Hydrostatic │  │ Visco-elastic │   │ Tapered end-mill │  │ Squeeze film │
  └───────────┘  └──────────────┘   └────────────────┘  └──────────────┘
        ┌──────────────┴──┐              ┌─────────┴──────┐
  ┌──────────────┐  ┌────────────────┐  ┌─────────────┐  ┌──────────────┐
  │ Rear clamped │  │ Forward clamped │  │ Collet style │  │ Sleeve Style │
  └──────────────┘  └────────────────┘  └─────────────┘  └──────────────┘
                        ┌───────────────┼───────────────┐
                  ┌──────────────┐ ┌────────────────┐ ┌──────────────┐
                  │ Waisted Shank │ │ Augmented Shank │ │ Straight Shank │
                  └──────────────┘ └────────────────┘ └──────────────┘
```
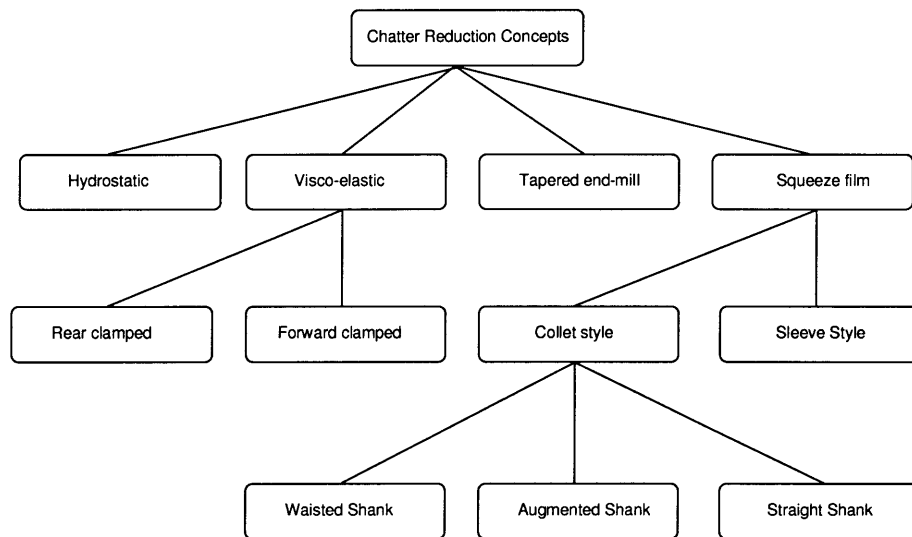
Figure 3.2: Chatter reduction taxonomy.

3.5.2 Concept Descriptions

3.5.2.1 Hydrostatic damper

The hydrostatic damper[5] concept shown in Figure 3.3 consists of a standard tool heat

shrunk into a bearing housing which itself is heat shrunk into a solid collet. A possible

benefit of the hydrostatic bearing design is that the fluid in the bearing pad, or pocket,

provides static stiffness and damping to the tool shank.
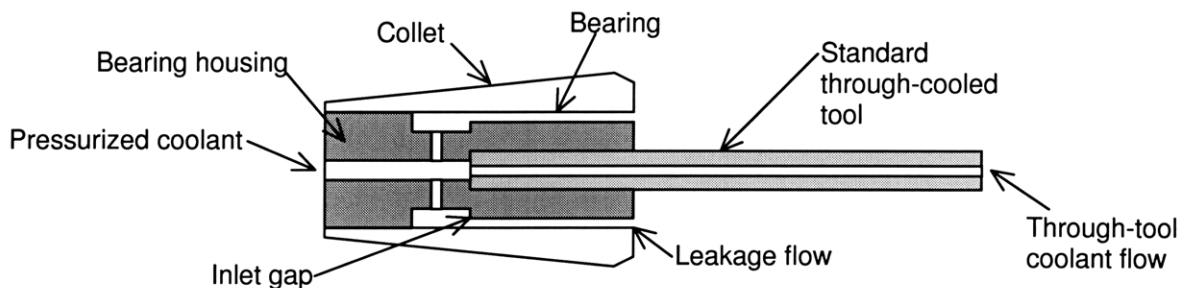
Figure 3.3: Hydrostatically damped tool holder.

The static stiffness is realized when pressurized coolant flows through the feed

hole through the inlet gap and to the bearing pads located around the circumference of the

bearing. Each bearing pad is connected to the inlet gap on the opposite side of the

circular bearing housing with a flow channel and is separated from other bearing pads by

a restricting land. When the tool shank is deflected upward, the bottom inlet gap opens

while the upper inlet gap closes. This changes the relative restriction to the fluid flow

through each bearing pad and provides a pressure differential on the tool shank that

results in a net downward force to oppose the deflection. The static stiffness of the

bearing pad can be estimated by: (Slocum)

_____

[5] Aesop, Inc patent pending.

$$K_{HS} = \frac{P_S A_{TOT}}{2h} \qquad\qquad Eqn\ 3.4$$

Where P_S is the source pressure and A_{TOT} is the total bearing pad area and h is the nominal

inlet gap or radial clearance of the hydrostatic bearing.

The damping factor of a rotary hydrostatic bearing depends on the land to pocket

ratio of the bearing. Only the fluid flow across the axial and radial land regions is

responsible for the dissipative damping effect since flow across the pocket region is

relatively unrestricted. For a completely smooth (no pockets) hydrostatic bearing with

open ends, the damping constant is:

$$C_{HS} = \frac{\pi R L^3 \mu}{h^3} \qquad\qquad Eqn\ 3.5$$

Where R is the radius of the bearing, L is the length of the bearing and μ is the dynamic

viscosity of the fluid.

The pressurized fluid required for the hydrostatic bearing could be supplied by the

pressurized through-tool coolant systems found on many modern machine tools. The

design requires a negligible amount of additional pumping power because the leakage

flow through the bearing clearance is insignificant compared to the coolant flow through

the tool.

In trying to package a hydrostatic bearing into a collet, the area of the bearing is

constrained so the source pressure required to give any appreciable stiffness benefit will

be very high. While through-tool coolant systems with supply pressures up to 5000 psi

are available, they are still exceedingly rare. The coolant filter would also have to be

made more efficient since particles that might normally be allowed in normal high

pressure coolant systems could mar the smooth surface finishes required for the

hydrostatic bearing to function properly. In addition, the design must be balanced since too much static stiffness will not allow enough deflection to generate appreciable damping flow. The fact that this design requires a custom-made solid collet could be another obstacle to its market acceptance if a complementary manufacturer cannot make solid collets readily available.

\

3.5.2.2 Viscoelastic damper

The viscoelastic damper designs shown in Figure 3.4 consist of a steel clamp ring and a damper ring[6]. The clamp ring is shrunk fit onto the tool or is split so it tightens onto the tool shank as the collet is tightened. The damper ring consists of a layer of visco-elastic material between two steel rings. The outer steel ring prevents the visco-elastic material from being extruded between the fingers of the spring collet. The inner steel ring reduces the friction between the damper ring and the tool shank and thereby eases assembly. The damping material is compliant, so the damper ring conforms to the space between the tool shank and the collet to evenly distribute the grip force of the collet.

a) Rear Clamped
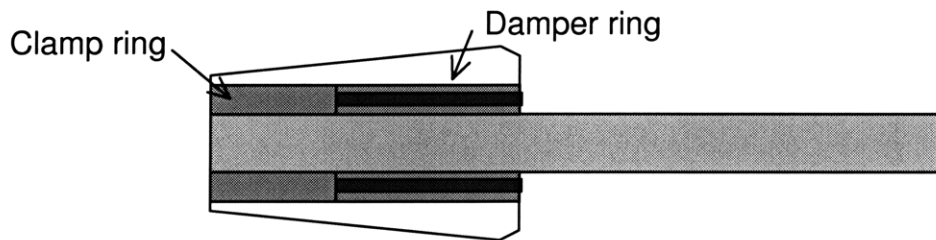
b) Front Clamped
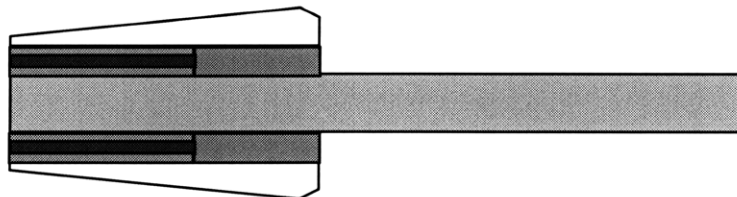
Figure 3.4 a & b: Toolholder designs damped with viscoelastic material can be clamped in the rear (a) or the front(b).

The performance of the damping material in this design is indicated by its loss factor and elastic modulus. The stiffness of a layer of damping material is hysteretic. This means that the strain of the material lags the stress placed on the material and the stiffness of a constrained layer is expressed as a complex value:

$$K_L = \frac{E_{VE} A_L}{t} (1 + \eta \cdot i) \qquad\qquad Eqn\ 3.6$$

where E_{VE} is the elastic modulus of the viscoelastic material, A_L is the area of the constrained layer, t is the thickness of the material and η is the loss factor.

All materials exhibit hysteretic damping which is also known as material damping. The material damping in metals commonly used for tooling is orders of magnitude lower than the material damping found in specialty damping materials. For this reason, there is opportunity to improve the damping of the machine tool system by introducing a damping material in collet's tool shank support mechanism.

The benefit of this design is that it is compatible with the majority of machine tool and tool holder systems installed today. It requires little to no extra equipment and tool replacement is kept simple.

In this design, a damping material with a high loss factor and high modulus is desired to give good damping and static stiffness respectively. Such a material may be difficult to find since most materials with high loss factor have a low modulus.

It is unclear which of the concept's variations, shown in Figure 3.4 a & b, will perform best. The rear clamped design allows more tool tip deflection for a given amount

---

[6] Aesop, Inc patent pending.

of damping than the front clamped design but the front clamped design might not allow enough deflection of the constrained layer to yield sufficient damping.

3.5.2.3 Tapered End-mill

In deep pocketed molds and slotted parts, there is usually a draft angle allowance that allows the tool to be slightly tapered. The recommended allowance for deep pocket molds is about 5 degrees. The tapered tool pictured in Figure 3.5 takes advantage of the draft angle allowance by increasing the diameter at the root of the tool while keeping the cutting diameter small to enable detailed work-piece geometries.
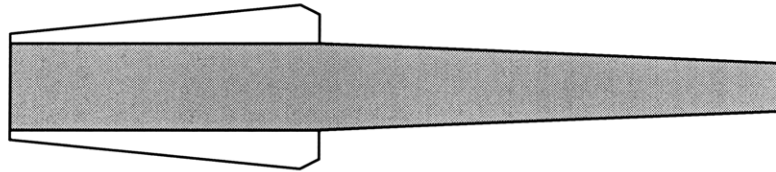
Figure 3.5: Tapered tool for maximum static stiffness.

The benefit of a tapered end mill is the increase in static stiffness over a conventional straight shank tool. A straight tool with a circular cross section has tip stiffness:

$$K_{straight} = \frac{3\pi E d^4}{64 L^3} \qquad Eqn\ 3.7$$

where d is the diameter of the tool and L is the overhung length of the tool. In comparison, a tapered tool with equivalent tip diameter but larger base diameter, D, has tip stiffness:

$$K_{tapered} = \frac{3 \pi E D^3 d}{64 L^3}$$
<div align="right">*Eqn 3.8*</div>

For a 5 inch long tool with ½ inch tip diameter and a taper of only 5 degrees, the tapered tool is about 20 times more statically stiff than the straight tool which has a constant diameter equal to just the tip diameter. This increased stiffness should reduce the amplitude of vibration for a given amount of cutting force and result in a smoother surface at conventional speeds.

The major drawback of this concept is that the high cost tool is not re-usable. The cost of the solution cannot be amortized over many cycles of tool wear. Also, the solution does not introduce any damping to the system, so the dynamic stiffness of the tapered tool may not be significantly higher than a standard tool.

3.5.2.4 Squeeze film damper

The viscous squeeze film designs shown in Figures 3.7-10 consist of a tool shrunk fit in a stepped bore tool housing such as a solid collet or sleeve. The rear portion of the housing interferes with the tool to allow the shrink fit while the forward portion of the housing has a clearance fit relative to the tool. The gap in the forward portion of the housing is filled with a viscous fluid through the fill ports. The fluid is trapped with self sealing screws in the fill ports and with a seal on the collet face.

In this design, the damping is a result of the viscous flow generated when the tool deflects and displaces the fluid from it's leading surface. Since the ends of the damper are closed, the fluid is constrained to flow around the thin annular clearance between the tool and the collet. In order to drive this flow, a driving pressure (P_D) is generated at the leading surface of the tool to oppose the motion of the tool as shown in Figure 3.6.
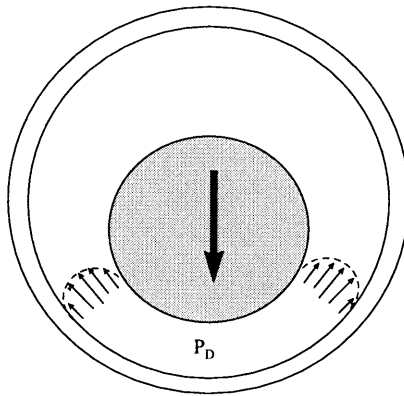
Figure 3.6: Illustration of viscous flow and retarding pressure generated by tool deflection in the squeeze film.

This driving pressure acts against the advancing area of the tool and results in a force opposing the tool's motion that is proportional to the tool's velocity. For a completely smooth, cylindrical squeeze film with closed ends, the damping constant is linear with respect to the length of the squeeze film and is equal to:

$$C_{SF} = \frac{6\Pi R^3 L \mu}{h^3} \qquad\qquad Eqn\ 3.5$$

4 variations of the squeeze-film-damped tool holder are discussed below.

Collet style

The collet style squeeze-film-damped tool holder employs a solid collet to replace the split collet usually found in collet style tool holders. The solid collet is required to provide a smooth continuous surface for the fluid to flow along. Three variations of the collet style squeeze film damped tool were investigated.

The simplest variant of the squeeze film design employs a standard, straight-shank tool and is shown in Figure 3.7. The static stiffness of this design is much lower than a comparably overhung standard tool because the tool is unsupported for the length of the clearance and stiffness is inversely proportional to the cube of the length. This design does not allow the user to control the amount of damping or the static stiffness since the diameter of the tool root, which undergoes the maximum strain and is the site of the damping layer, must be equal to the tool diameter required for the desired cut.
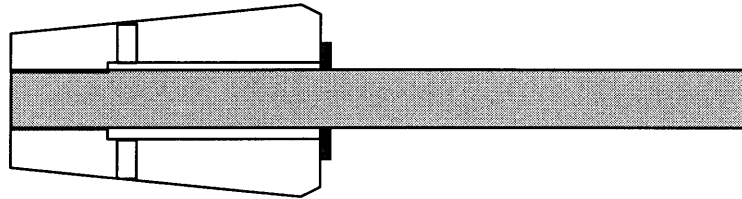
Figure 3.7: Squeeze-film-damped tool with straight tool shank.

The augmented shank design, shown in Figure 3.8, allows the tool to have greater static stiffness than in the straight shank design. The root diameter of the tool root is de-coupled from the cutting diameter of the tool so its static stiffness and damping performance can be tuned to a certain degree. However, the large root diameter could reduce the deflection at the damping layer and result in diminished damping performance since the damping diameter and root diameter are still coupled.
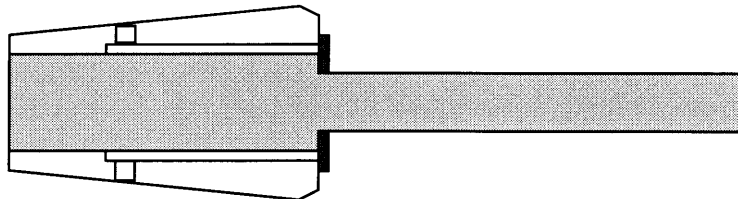
Figure 3.8: Squeeze-film-damped tool with augmented tool shank.

The waisted tool shank design shown in Figure 3.9, allows the static stiffness and dynamic stiffness of the tool to be tuned independently because the tool root diameter, the damper diameter and the cutting diameter are all de-coupled. This design requires a tool shank with multiple steps in diameter which could make the tool very expensive.
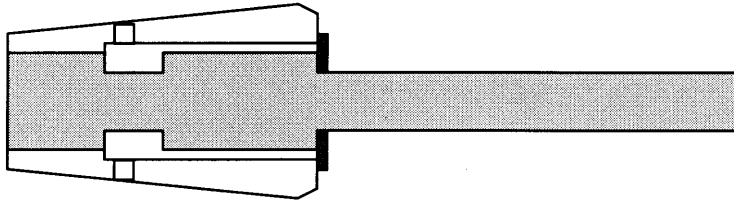
Figure 3.9: Squeeze-film-damped tool with waisted tool.

Sleeve style

In sleeve-supported squeeze film design, shown in Figure 3.10, a standard spring collet can be used since the smooth surface for the squeeze film damper and the tool support is provided by a steel sleeve which is in-turn held in the collet . In this design, the static stiffness can be equal to that of the standard tool in a collet since the effective overhang length is the same with the squeeze film extended completely outside the collet.
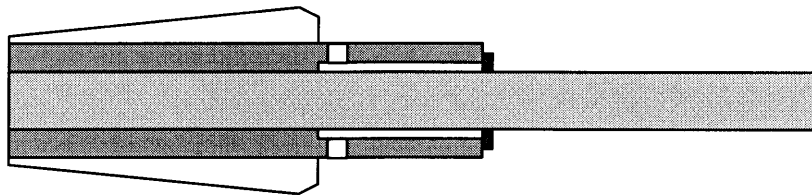
Figure 3.10: Sleeve-supported squeeze film design.

In designing the sleeve supported squeeze film, the sleeve wall should be made thin enough so as not to interfere with the minimum allowable tapers in deep pocketed molds. This design pressure will have to be balanced with the desire for a rigid sleeve. If the sleeve walls are too thin, it will not be able to support the large pressures necessary in the squeeze film to damp the vibrations of the tool shaft.

3.6 Concept Evaluation

Based on this initial discussion of the concepts available, we are ready to evaluate the concepts based on the functional requirements. A Pugh chart, shown in Figure 3.11, is a good way to organize the evaluation. Here, the product concepts are evaluated relative to the 'baseline design' and decisions are made whether to pursue the concept further or halt its development.

	Standard Tool	Hydrostatic	Visco-Elastic	Tapered	Collet	Sleeve
Dynamic Stiffness	0	+	+	?	+	+
Static Stiffness	0	-	-	+	-	0
Functionality	0	0	0	0	0	0
Tool costs	0	0	0	-	-	0
Modifications	0	--	0	0	-	0
Tool replacement time	0	-	-	0	-	-

Figure 3.11: Pugh chart used for initial evaluation of chatter reduction concepts.

Based on the Pugh Concept evaluation, we see that the market acceptance of the hydrostatic design will be limited by the fact that, in the majority of installed machine tool systems today, major modifications would be needed to accommodate a hydrostatic tool holder. The other concepts also incur some cost in offering enhanced performance, but since the relative performance of each concept is not yet known, it is impossible to

make decisions based on value considerations. The rest of the concepts will have to be

developed further through modeling and rapid prototyping before a decision can be made.

Chapter 4: Critical Parameters and Modeling

4.1 Critical Parameters

	Standard	Tapered	Collet: Straight	Visco-elastic	Collet: Augmented	Collet: Waisted	Sleeve	Hydrostatic
Cutting Diameter	X	X	X	X	X	X	X	X
Tool Length	X	X	X	X	X	X	X	X
Tool Material	X	X	X	X	X	X	X	X
Damper Length			X	X	X	X	X	X
Clearance			X		X	X	X	X
Fluid Viscosity			X		X	X	X	X
Shrink Fit Pressure			X		X	X	X	X
Root Diameter		X			X	X		X
Damper Diameter				X		X		X
Root Length					X	X		X
Sleeve Density							X	
Sleeve Diameter							X	
Sleeve Length							X	
Source Pressure								X
Visco-Elastic Loss Factor				X				
Visco-Elastic Modulus				X				
Visco-Elastic Thickness				X				

Table 4.1: Critical Parameters of each conceptual design

Table 4.1 above shows the critical parameters that control the static stiffness and dynamic stiffness performance of each of the conceptual designs discussed in the previous chapter. In modeling the conceptual designs, we seek an accurate and inexpensive tool that will predict the deflection/force transfer function at the tool tip. This way, many different designs can be tried and an optimal design can be found without the expense of actually building and testing all of them.

4.2 Dynamic Response Analytic Approach

Since the tool is flexible, motion at the tool tip can be out of phase with the deflections at the tool root where the damping is applied. As a result, the dynamic response at the tool tip is a function of the deflection at the tool root and the state of the

system must be represented by a vector, $\underline{X}$, of degrees of freedom at points along the length of the tool. The equations of motion for the tool system can be given in matrix form as:

$$[M]\underline{\ddot{X}} + [C]\underline{\dot{X}} + [K]\underline{X} = \underline{F} \qquad\qquad Eqn\ 4.1$$

where [M] is the mass matrix, [C] is the viscous damping matrix, [K] is the stiffness matrix and $\underline{F}$ is the vector of input forces corresponding to the degrees of freedom in $\underline{X}$.

The mass, damping and stiffness matrices of the system can be formulated by modeling the tool and damper as a collection of finite elements. Figure 4.1 is a generic representation of the finite element model used to predict how the critical parameters listed above affect the performance of each design. The formulation of each element property with respect to the critical parameters is discussed in the section below.
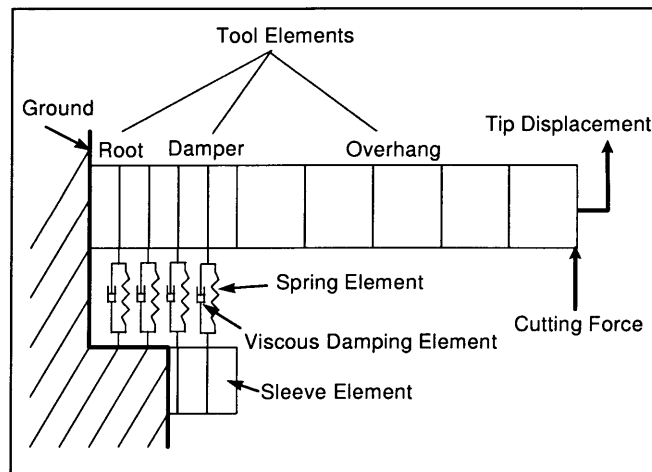
Figure 4.1: Schematic representation of the finite element model used in the study.

4.2.1 Tool and Sleeve Elements

Timoshenko Beam Finite Elements were used to model the flexibility of the tool and the sleeve. Timoshenko beams differ from Euler-Bernoulli type beams in that they account for sheer deformations as well as deformations due to bending. For this reason, Timoshenko elements yield more accurate results for beams with a length to diameter ratio less than 5. Since beams with a small length to diameter ratio will be useful in modeling the deflections in the damped region of the tool, Timoshenko beam elements are preferred in this application.

One-dimensional Timoshenko beam elements have 8 degrees of freedom. At each of the element's two ends, or nodes, the state of the element is defined by the total displacement (x), the total slope (x'), the bending slope (ϕ), and the first derivative of the bending slope (ϕ') as shown in Figure 4.2.
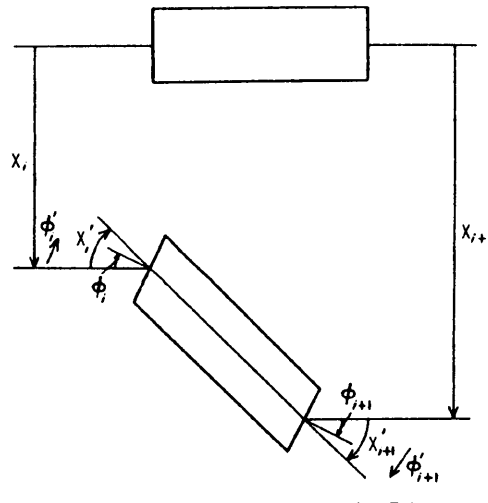
Figure 4.2: Timoshenko beam element degrees of freedom.(Abbas 1975)

4.2.1.1 Tool and Sleeve Element Stiffness: $[K]_{el}$

For an element with nodal displacement vector $\underline{X}_{el}$ such that:

$$\underline{X}_{el}{}^T = \begin{bmatrix} X_1 & X'_1 & \phi_1 & \phi_1 & X_2 & X'_2 & \phi_2 & \phi_2 \end{bmatrix}$$

The element stiffness matrix is given by:

$$[K]_{el} = \frac{E \cdot I}{420 \cdot L} \begin{bmatrix} \dfrac{504S}{L^2} & \dfrac{210S}{L} & \dfrac{42S}{L} & \dfrac{42S}{L} & \dfrac{-504S}{L^2} & \dfrac{210S}{L} & \dfrac{42S}{L} & \dfrac{42S}{L} \\ & 156s+504 & -42S & 22S+42 & \dfrac{-210S}{L} & 54S-504 & 42S & -13S+42 \\ & & 56S & 0 & \dfrac{-42S}{L} & 42S & -14S & -7S \\ & & & 4S+56 & \dfrac{-42S}{L} & 13S-42 & 7S & -3S-14 \\ & & & & \dfrac{504S}{L^2} & \dfrac{-210S}{L} & \dfrac{-42S}{L} & \dfrac{42S}{L} \\ & & & & & 156S+504 & -42S & -22S-42 \\ & & & & & & 56S & 0 \\ & & & & & & & 4S+56 \end{bmatrix}$$

Eqn 4.2(Abbas 1975)

Where I, the cross-sectional moment of inertia for a solid circular beam, is a function of the beam's diameter:

$$I = \frac{\pi D^4}{64}$$

Eqn 4.3

and S, the non-dimensional sheer deformation parameter, is:

$$S = \left(\frac{kG}{E}\right)\left(\frac{AL^2}{I}\right)$$

Eqn 4.4

in which k is the cross section's sheer coefficient (0.85 for a circular beam), G is the sheer modulus of the material, E is the elastic modulus of the material, A is the cross sectional area, and L is the length of the element.

Since the stiffness at a node is determined by the two adjoining elements, the system stiffness matrix [K] can be assembled from the individual element stiffness matrices as shown below.

$$K_{el} = \begin{bmatrix} \boxed{} \end{bmatrix}$$

$$K = \begin{bmatrix} & & & \Leftarrow \text{Tool} \\ \text{Sleeve} \Rightarrow & & & \end{bmatrix}$$
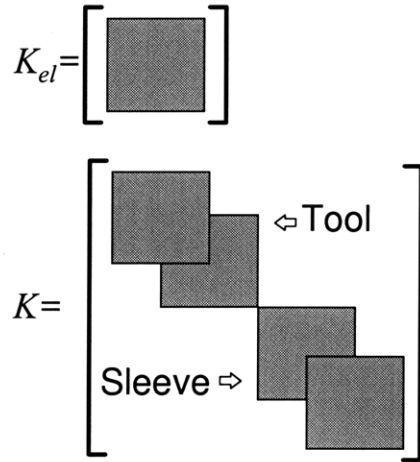
Figure 4.3: Assembling the system stiffness matrix from the individual element stiffness matrices

4.2.1.2 Tool and Sleeve Element Mass: [M]el

The mass of the tool is distributed, not concentrated at the nodes. To account for the beams linear and rotational inertia, a distributed mass matrix is used. The distributed mass matrix for an element with degrees of freedom:

$$\underline{X}_{el}^{T} = \begin{bmatrix} X_1 & X'_1 & \phi_1 & \phi_1 & X_2 & X'_2 & \phi_2 & \phi_2 \end{bmatrix}$$

is given by:

60

$$[K]_{el} = \frac{\rho \cdot A \cdot L^3}{420}
\begin{bmatrix}
\dfrac{156}{L^2} & 0 & \dfrac{22}{L} & 0 & \dfrac{54}{L^2} & 0 & \dfrac{-13}{L} & 0 \\
 & 156R & 0 & 22R & 0 & 54R & 0 & 13R \\
 & & 4 & 0 & \dfrac{13}{L} & 0 & -3 & 0 \\
 & & & 4R & 0 & 13R & 0 & -3R \\
 & & & & \dfrac{156}{L^2} & 0 & \dfrac{-22}{L} & 0 \\
 & & & & & 156R & 0 & -22R \\
 & & & & & & 4 & 0 \\
 & & & & & & & 4R
\end{bmatrix}$$

Eqn 4.5(Abbas 1975)

Where ρ is the material density, A is the cross sectional area, L is the length of the

element, and S, the non-dimensional rotary inertia parameter of the element is:

$$R = \frac{I}{AL^2}$$

Eqn 4.6

in which I is the cross sectional moment of inertia.

Since the equivalent mass at a node is determined by the two adjoining elements,

the system mass matrix $[M]$ can be assembled from the individual element mass matrices

just as the system stiffness matrix is assembled from the element stiffness matrices as

shown in Figure 4.4.

$$M_{el} = \begin{bmatrix} \blacksquare \end{bmatrix}$$

$$M = \begin{bmatrix} \blacksquare & & & \\ & \blacksquare & \Leftarrow \text{Tool} & \\ & & \blacksquare & \\ \text{Sleeve} \Rightarrow & & & \blacksquare \end{bmatrix}$$
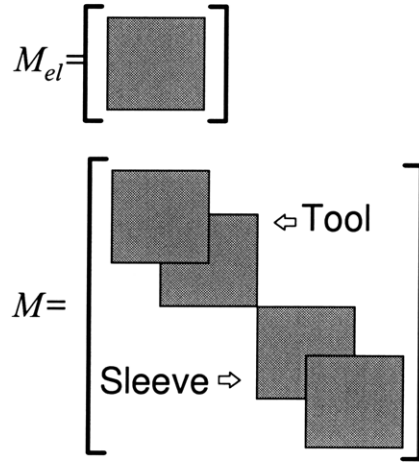
Figure 4.4: Assembling the system mass matrix from the individual element mass matrices.

4.2.2 Spring Element Stiffness: K_{ext}

The portion of the tool supported by the hydrostatic bearing or the visco-elastic material is modeled as a collection of beam elements of equal length. This allows the stiffness of the hydrostatic bearing or the elastic material to be distributed among each of the interior nodes of the supported region. For a region divided into n elements, there are n-1 interior nodes.

For a hydrostatic bearing, the spring constant for the force acting at a node due to the displacement of the node at the fluid inlet can be derived from Equation 3.4:

$$\frac{F_{HS}}{X} = K_{ext} = \frac{P_S A_{TOT}}{2h(n-1)} \qquad\qquad Eqn\ 4.7$$

where P_S is the source pressure, A_{TOT} is the total projected area of the hydrostatic bearing, and h is the clearance at the inlet height.

For a visco-elastic material, the spring constant at each node is a complex value and is derived from Equation 3.6:

$$\frac{F_{VE}}{X} = K_{ext} = \frac{E_{VE} A_L}{t(n-1)}(1 + \eta \cdot i) \qquad\qquad Eqn\ 4.8$$

The approach to incorporating the external stiffness into the system stiffness matrix differs slightly between the hydrostatic and visco-elastic supports. In the hydrostatic concept, the force applied to each node is determined by the pressure in the hydrostatic pocket and the area of the pocket. This pressure is constant throughout the pocket and is determined only by the deflection of the beam at the inlet restriction. As a result, the spring constant K_{ext} is incorporated into the system stiffness matrix along a column associated with the displacement at the inlet node and at each row associated with the linear force at an interior node as follows.

$$K_{ext} = \blacksquare$$

$$K = \begin{bmatrix} & & & & \\ & \blacksquare & & & \\ & \blacksquare & & & \\ & \blacksquare & & & \\ & & & & \end{bmatrix}$$
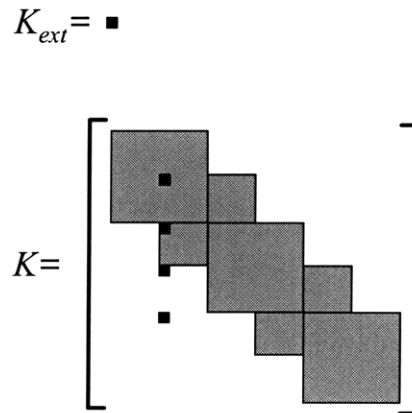
Figure 4.5: Incorporating the stiffness of an external hydrostatic bearing into the system stiffness matrix.

For a visco-elastic material, the force at each node is determined by the deflection at that node so K_{ext} is added along the diagonal of the matrix at each row-column pair associated with the linear displacement at that node.

$$K_{ext} = \blacksquare$$

$$K = \begin{bmatrix} & & & \\ & & & \\ & & & \\ & & & \end{bmatrix}$$

Figure 4.6: Incorporating the stiffness of and external visco-elastic damping layer into the system stiffness matrix.

4.2.3 Viscous Damping Element Damping Constant: C_{ext}

In the squeeze-film damped tool, the damping factor of the squeeze film area must be divided among the nodes within the damped region since the deflection velocity of the tool varies at points along the tools length. The deflection velocity at the root of the tool is smaller than the deflection velocity closer to the tip of the tool. Therefore, more damping force will be generated in the squeeze film near the tip of the tool than at the base of the tool. For the n-1 interior nodes of the n elements representing the tool in the squeeze film. For a squeeze film with closed ends, the damping factor for the force acting at a tool node is proportional to the velocity of the tool node relative to the velocity of the outer boundary of the squeeze film and can be derived from Equation 3.9:

$$\frac{F_{SF}}{\dot{X}_{TN} - \dot{X}_{OB}} = C_{EXT} = \frac{6\pi R^3 L \mu}{h^3 (n-1)} \qquad \text{Eqn 4.9}$$

where R is the radius of the squeeze film layer, L is the total length of the squeeze film, μ is the dynamic viscosity of the fluid, and h is the clearance between the tool and the outer boundary of the squeeze film.

64

In the case where the outer boundary is supported by the collet, we assume the velocity of the outer boundary to be zero. If the outer boundary of the squeeze film is supported by a sleeve, the velocity of the outer boundary is the velocity of the corresponding node in the sleeve. Based on this analysis, the system damping factor can be formulated from the viscous damping element damping constant as follows:

$$C_{ext} = \blacksquare \qquad -C_{ext} = \square$$

Figure 4.7: Incorporating the viscous damping of a squeeze film into the system damping matrix for (a) a tool node supported by ground and (b) a tool node supported by a sleeve node.

4.2.4 Boundary Condition: Ground

For long overhang tools, the deflection at the tool tip is dominated by the tool flexibility and is only slightly effected by the tool grip pre-load of the tool holder. For the purposes of modeling the tool, the tool nodes held in the collet or heat shrunk in the tool holder are regarded as ground. This means all 4 degrees of freedom at the grounded node are set to zero. Grounding a node is analogous to eliminating the rows and columns representing the degrees of freedom associated with that node in the system stiffness, mass, and damping matrices.

65

4.3 Model Implementation

To be a useful design tool, the model must be flexible, compatible with PC hardware commonly available in today's engineering environment, and cost very little to set-up and run. For these reasons, the proposed designs were modeled using MATLAB.

MATLAB is capable of an eigenvalue or frequency domain analysis of a first order state space representation of a system. The frequency domain analysis allows the designer to generate a complete frequency response for each tool design by evaluating a system at many different frequencies. The eigenvalue and frequency domain analysis together allow the designer to compare the static and dynamic stiffness of many designs by quickly finding the natural frequency of the first mode of vibration and then accurately determining the amplitude of the response at that frequency. MATLAB's use of M-files allows the designer to code automated loops that vary a design parameter in increments and seek the optimal output performance of the system. Finally, MATLAB is available at a relatively low cost when compared to more sophisticated modeling and analysis software such as ANSYS and COSMOS. While these software packages may be easier to set up, they do not allow for automated adjust-and-search parameter optimization. Also, due the generality of the underlying code, they require quite a bit of processing time to evaluate the performance of each design.

The second-order state space system of Equation 4.1 is transformed into a first-order state space system by defining a vector of state variables:

$$\underline{X} = \begin{bmatrix} \underline{X} \\ \underline{\dot{X}} \end{bmatrix}$$

Eqn 4.10

Now the first-order system of equations is:

$$\underline{\dot{X}} = [A]\underline{X} + [B]\underline{F}$$

Eqn 4.11

In terms of the system mass, stiffness and damping matrices, and the displacement vector

$\underline{X}$, this is equivalent to:

$$\begin{bmatrix} \underline{\dot{X}} \\ \underline{\ddot{X}} \end{bmatrix} = \begin{bmatrix} 0 & [I] \\ [M]^{-1}[-K] & [M]^{-1}[-C] \end{bmatrix} \begin{bmatrix} \underline{X} \\ \underline{\dot{X}} \end{bmatrix} + \begin{bmatrix} 0 & 0 \\ 0 & [M]^{-1}[I] \end{bmatrix} \begin{bmatrix} 0 \\ \underline{F} \end{bmatrix}$$

Eqn 4.12

where $\underline{F}$ is the vector of input forces and moments. In this analysis, F has only one non-

zero component, the cutting force applied at the tool tip.

The output vector Y of interest consists of only one element, the tip displacement.

For the purposes of the computer simulation, it is formulated as:

$$\underline{Y} = [C]\underline{X} + [D]\underline{F}$$

Eqn 4.13

where [C] and [D] are row vectors. [C] has only one non-zero element corresponding to

the tip displacement and [D] is row vector of zeros.

With this formulation, the MATLAB functions returning the natural frequencies

of the system [eig(A)] and the frequency response [bode(A,B,C,D)] can be applied to the

various designs. A sample of the code used to translate the design parameters into the

state space representation of the system and then predict the system's performance, is

given in Appendix A.

Chapter 5: Rapid Prototyping and Testing

A rapid prototype is a physical model of the product that has one or a few features of the projected final design. Since a rapid prototype is not required to have all the functionality of the product, it is usually much cheaper and quicker to build than a detailed, full-function prototype. Rapid prototyping and testing serves two purposes. First, it is a quick and inexpensive way to determine which design directions will potentially yield successful products. A doomed design direction can be abandoned or a flawed design can be modified based on the results of testing with a rapid prototype. This can save the time and expense of trial and error product development with full-function and full-priced prototypes. Secondly, the data collected from rapid prototype testing can be used to improve the accuracy of product performance models that will be used to design and predict the performance of the optimal product. Model accuracy is important if the model is going to be used in place of physical prototypes to save resources while maintaining confidence in the design during development. Rapid prototypes are a good way to test that the assumptions and fundamental physics captured in the model are sufficient and accurate.

5.1 Dynamic Response Testing

According to metal cutting theory, reducing the resonant amplitude of the deflection/force transfer function of the machine tool structure should increase the chatter free metal removal rate of the machine tool. Impact tests are a simple way to experimentally determine the deflection/force transfer function of a structure. The

deflection/force transfer function at the tool tip is equal to the ratio of the magnitude of the output deflection to the magnitude of the input force over the frequency spectrum of interest. In this study, the transfer function was measured by using a signal analyzer to compare the force input by an instrumented hammer to the deflection indicated by an accelerometer mounted on the tool tip. Each dynamic response measurement was taken with the tool held in a CV40 tapered tool holder in the spindle of a CNC Cincinnati Milacron vertical milling machine. The equipment used in measuring the transfer function at the tool tip is shown in Figure 5.1 and a detailed discussion of the issues that were addressed to ensure accurate and repeatable test results is given in the section that follows.

(a)   (b)   (c)
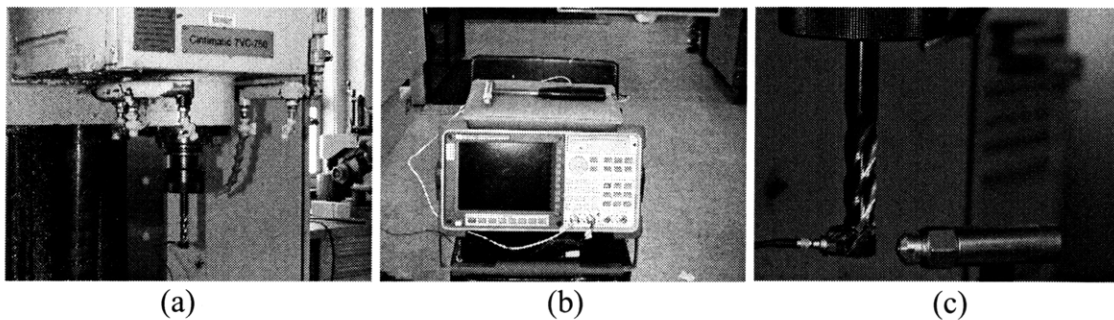
Figure 5.1: Machine tool spindle (a), signal analyzer (b), accelerometer and force hammer (c) used to measure the tool-tip transfer function

Clamping conditions

To replicate actual usage conditions and ensure consistent clamping conditions, all dynamic response measurements were taken while the tool was held in a tool holder in the spindle of the machine tool.

Force input

The impact force input was delivered to the tool tip with a force hammer. The hammer outputs a voltage signal, V_{ham}, proportional to the force, F_{in}, applied at its striking surface. The constant of proportionality is C_{ham} such that:

$$F_{in} = C_{ham}V_{ham} \qquad\qquad Eqn\ 5.1$$

When using the force hammer to excite the tool tip, it is critical to apply the force in line with the direction in which deflection is to be measured. If the force is applied at an unknown angle to the direction of the deflection measurement, it is impossible to know how much of the input force is responsible for the motion. For this reason, an epoxy mold was fashioned to provide a flat target surface perpendicular to the measured deflection direction of the accelerometer, which was mounted to the tool tip through the epoxy. The epoxy mold and the resulting striking surface on the tool tip is shown in Figure 5.2. This flat striking surface in combination with the hemispherical shape of the hammer tip ensured that the force input was in the direction of the measured deflection.
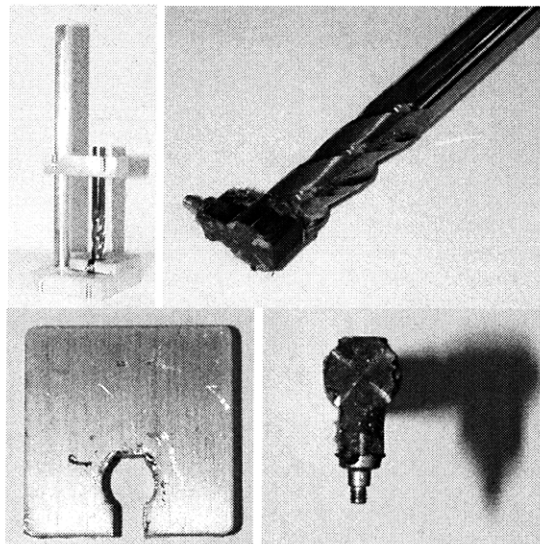
Figure 5.2: Jig, epoxy mold and resulting striking surface and accelerometer mount at the tool tip.

Deflection output

The deflection amplitude was measured by a one axis accelerometer mounted at the tool tip. The accelerometer outputs a voltage signal proportional by the accelerometer constant, C_{acc}, to the acceleration experienced at the tool tip. To determine the deflection, the acceleration must be integrated twice. As a result, the deflection amplitude, $A_x(\omega)$, is a function of frequency, and is calculated from the accelerometer voltage, V_{acc}, by:

$$A_x(\omega) = \frac{C_{acc}}{\omega^2} V_{acc} \qquad\qquad Eqn\ 5.2$$

where ω is the frequency in radians per second.

Due to the intricate geometry of the cutting flutes at the tool tip, epoxy was used replicate a mounting surface for the accelerometer. The epoxy mold shown in Figure 5.2 also incorporated a feature to position and capture the accelerometer in an orientation directly in line with the striking surface. Use of the mold helped minimize the mass of epoxy needed to mount the accelerometer to the tool tip. In addition, the small accelerometer mass and high epoxy stiffness represent a spring-mass structure with bandwidth an order of magnitude higher than the frequencies of interest. As a result, this mounting technique helped ensure that the measured dynamic response was not significantly effected by the additional end-mass of the epoxy and accelerometer or by the addition of the epoxy-accelerometer dynamic system.

Signal Analyzer

An HP signal analyzer was used to compare the voltage signal from the input force hammer to the voltage signal from the accelerometer at the tool tip. Since we are only interested in the first mode of a long overhang tool, a frequency window from 0 to

71

800 Hz was sufficient. The signal analyzer has 800 lines of resolution, which yields a frequency resolution of 1 Hz. The signal analyzer automatically calculates the natural frequency and damping ratio associated based on the measured transfer function. The repeatability of these measurements is discussed in Appendix B. The 95% confidence interval is ± 2.8 Hz and ± 0.0028 for the natural frequency and the damping ratio respectively.

The signal analyzer was also used to average several measurements together. For each tool overhang condition measured, 10 measurements of the transfer function were averaged together to ensure a smooth and accurate trace of the dynamic response of the tool. The signal analyzer also allowed the input force trace to be previewed before including it in the average so that measurements from hammer mis-strikes could be eliminated.

5.2 Rapid Prototypes

During the rapid prototyping phase of the project, three major design directions emerged: fluid damped tools, viscoelastic damped tools, and undamped, large shaft diameter tools. The fluid damped tools are aimed toward offering maximum damping and cutting performance. The viscoelastic damped tools offer damping while simplifying production and use in the machine shop. Finally, the enlarged shaft tools offer increased static stiffness rather than damping as an alternative way to increase the chatter free metal removal rate. Due to the long lead time often associated with the custom manufactured parts needed for new products, the rapid prototyping phases of these design directions

were conducted in parallel. For simplicity, each of the three different design directions

will be introduced and fully developed in chapters 6-8.

Chapter 6: Viscoelastic Damped Tools

6.1 Viscoelastic demonstration prototypes

The prototypes first used to demonstrate the viscoelastic damped concept and validate the model's ability to predict a tools dynamic response are shown in Figure 6.1. They consist of 0.5 inch diameter, 8 inch long aluminum rods turned down to accommodate a layer of viscoelastic material 0.030 inch thick and either 0.6 or 1.2 inches in length. The outer diameter of the viscoelastic layer is flush with the aluminum rod so it can be held in a conventional 0.5 inch collet. The rod is clamped in either the front of the collet or rear of the collet depending on the position of the viscoelastic layer and is overhung 6 inches. The grip length of the collet was 1.875 inches.
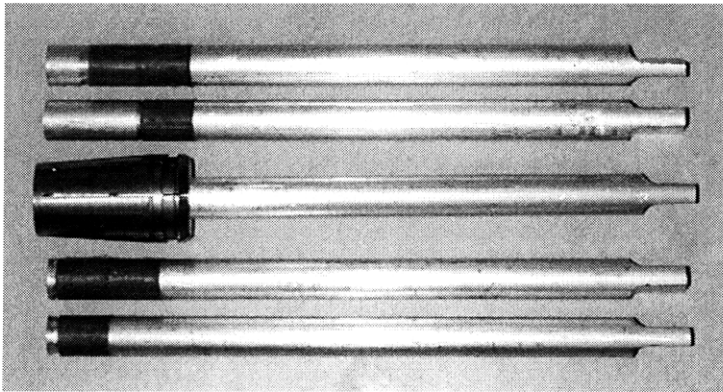
Figure 6.1: Rear clamped (top) and front clamped (bottom) viscoelastic damping concept demonstration prototypes

The damping material used in the test was EAR Specialty Composites C1002. Due to its high loss factor, this material is commonly used in damping machine tool structures.

In order to validate the dynamic model, it was first used to predict the static

stiffness and natural frequency of an undamped tool. Figure 6.2 compares the

experimentally determined dynamic response at the tip of the undamped aluminum rod to

the dynamic response predicted by the finite element model.
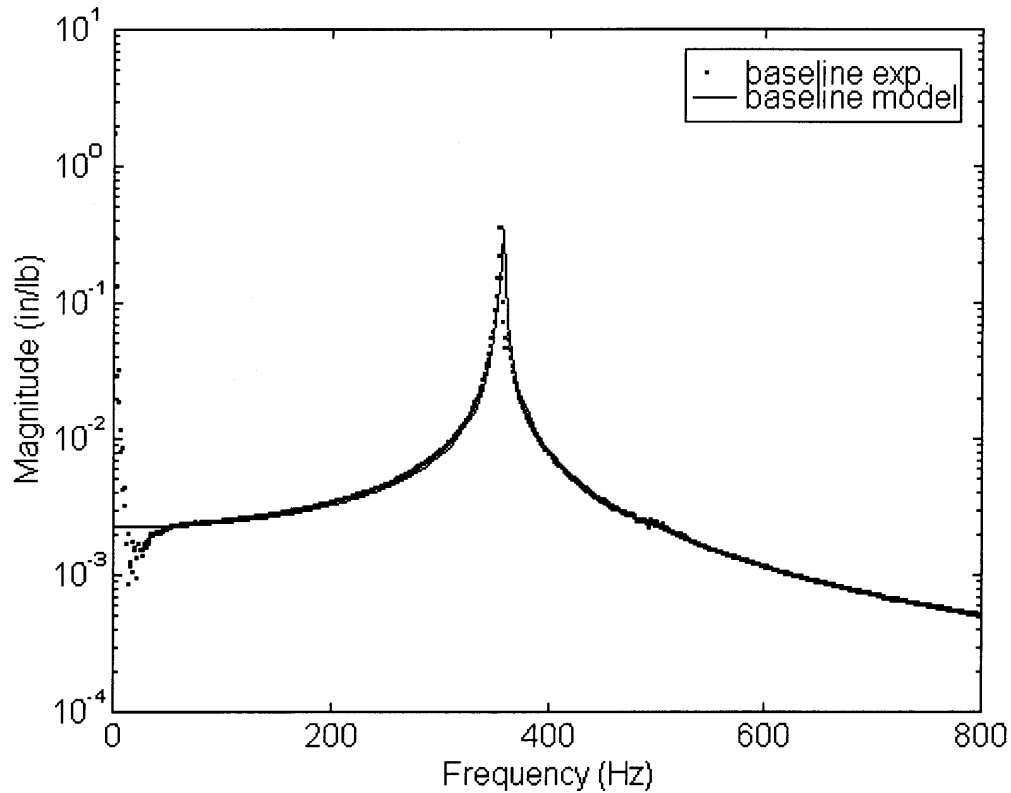
Figure 6.2: Experimentally determined response of an undamped aluminum beam vs. the model's prediction (Q = 153)

Since the effect of the accelerometer end mass is included, the model accurately

predicts the frequency of the first mode. The model also accurately predicts the static

stiffness of the aluminum beam. The model erroneously predicts that the resonant

amplitude of a beam without external damping is infinite because it does not include

material damping . In Figure 6.2, the model appears to accurately predict the resonant

amplitude of the response because the equally spaced frequency points for which the

dynamic response is calculated do not necessarily line up with the resonant peak

frequency, resulting in a finite, false peak. The model is expected to accurately predict

the peak resonant amplitude of the externally damped tool concepts because the effect of

the material damping should be insignificant relative to the effect of the external damping

on the tool response.

To test the viscoelastic material's potential to damp tool vibrations and validate

the model's ability to predict the amplitude of the resonant peak in the damped case,

dynamic response tests were also conducted on the damped aluminum rods. Figure 6.3

compares the response of the baseline aluminum rod to those damped with a long or short

viscoelastic layer and clamped in the front or rear of the collet. The critical parmeters of

the dynamic response are summarized in Table 6.1. The results indicate that a visoelastic

layer between the tool and the collet has the potential to deliver significant amounts of

damping to a long overhang tool.
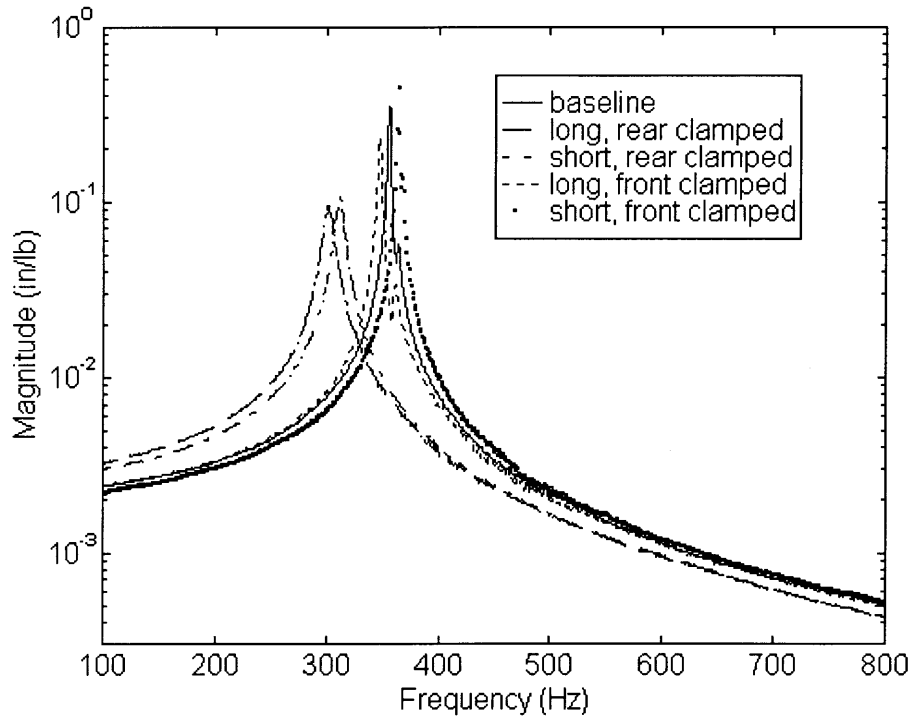
Figure 6.3 comparing baseline and damped aluminum rods

Rod		Resonant Peak Frequency (Hz)	Estimated Static Stiffness (lb/in)	Dynamic Stiffness (lb/in)	Q	Real Negative Max of T.F. (in/lb)	Theoretical increase in stable MRR limit
Undamped	**Actual**	**355**	**435**	**2.85**	**153**	**.246**	**1**
	Model	358	450				
Rear clamped Long damper	**Actual**	**301**	**310**	**10.60**	**29**	**.051**	**4.8**
	Model*	302	290	14.90	19	.035	
Rear clamped Short damper	**Actual**	**311**	**355**	**9.50**	**37**	**.050**	**4.9**
	Model*	310	306	11.30	27	.045	
Front clamped Long damper	**Actual**	**347**	**435**	**4.35**	**100**	**.135**	**1.8**
Front clamped Short damper	**Actual**	**364**	**445**	**2.20**	**202**	**.195**	**1.3**

adjusted model

Table 6.1: Summary of Aluminum Rod Damping Experiment Critical Parameters

Figure 6.3 shows that when the rod is clamped in the front of the collet and the

viscoelastic layer is in the rear of the collet, no damping is exhibited. This may be due to

the fact that very little if any deflection energy is transmitted from the tip of the rod to the viscoelastic layer because the clamped section between them is effectively immobilized. In the case of the rear clamped version of the rod, the dynamic response indicates nearly 4 times more dynamic stiffness than in the baseline case. As expected, there is a reduction in the static stiffness of the rod because the tool is supported by a viscoelastic spring in the collet so, effectively, the overhang length is increased. This also explains why the rod with a long damper in the collet has a lower natural frequency and static stiffness than the rod with a shorter damper. The longer damper does seem to benefit the dynamic stiffness of the rod slightly since the long damper has a longer effective overhang, the viscoelastic material is subject to more deflection and can therefore dissipate more of the tool's vibration energy. The effect of the damper on a steel or carbide tool is expected to be less dramatic because aluminum is relatively poorly damped, still, this initial test showed that it is possible to damp a long overhang tool by introducing a viscoelastic material in the collet.

The next objective was to verify that the model could predict the dynamic response of the damped tool. Figures 6.4 and 6.5 show that the model was unable to accurately predict the dynamic response of the tool using the parameters thought to represent the tool support geometry. The predicted natural frequency and static stiffness were much lower than the actual natural frequency and static stiffness. The predicted dynamic stiffness was much higher than the actual dynamic stiffness as well.

One possible explanation is that the collet collapsed more readily on the viscoelastic material than on the bare shaft. As a result, the viscoelastic material was displaced and extruded through the gaps in the collet or compressed under the fingers of

the collet. This would tend to thin and stiffen the viscoelastic layer between the fingers of

the collet and the tool. The collet is expected to bite into the long damper more than the

short damper because there is less rod length to support the load of the collet, The

parameters for layer thickness and stiffness were adjusted to best fit the experimental data

as shown in Figures 6.4 and 6.5. The parameters used in the predictive model and the

"Squeeze" compensated model are summarized in Table 6.2 . As expected, the long

damper appears to experience more thinning and stiffening than the short damper.

		Rear Clamped Long Damper Prediction	Rear Clamped Long Damper Adjusted	Rear Clamped Short Damper Prediction	Rear Clamped Short Damper Adjusted
Loss Factor		1	1	1	1
Diameter	in.	0.44	0.44	0.44	0.44
Length	in.	1.2	1.2	1.2	1.2
Modulus	PSI	4350	21750	4250	13050
Thickness	in.	.030	.006	.030	.010

Table 6.2: Viscoelastic layer parameters used in predictive and "Squeeze" compensated models
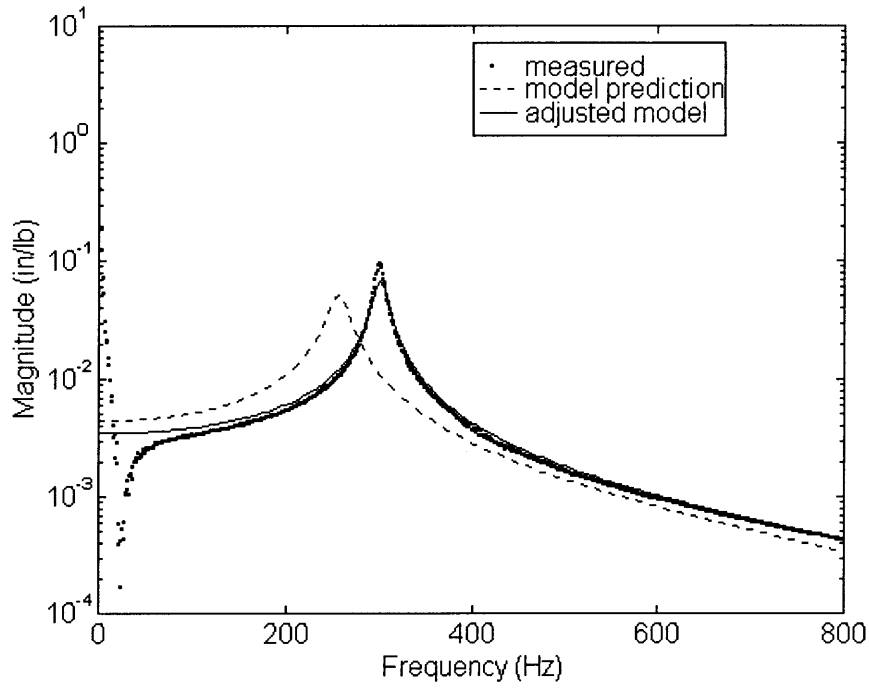
Figure 6.4: Predictive model and" Squeeze" compensated model vs measured dynamic response of rear clamped rod with long damper
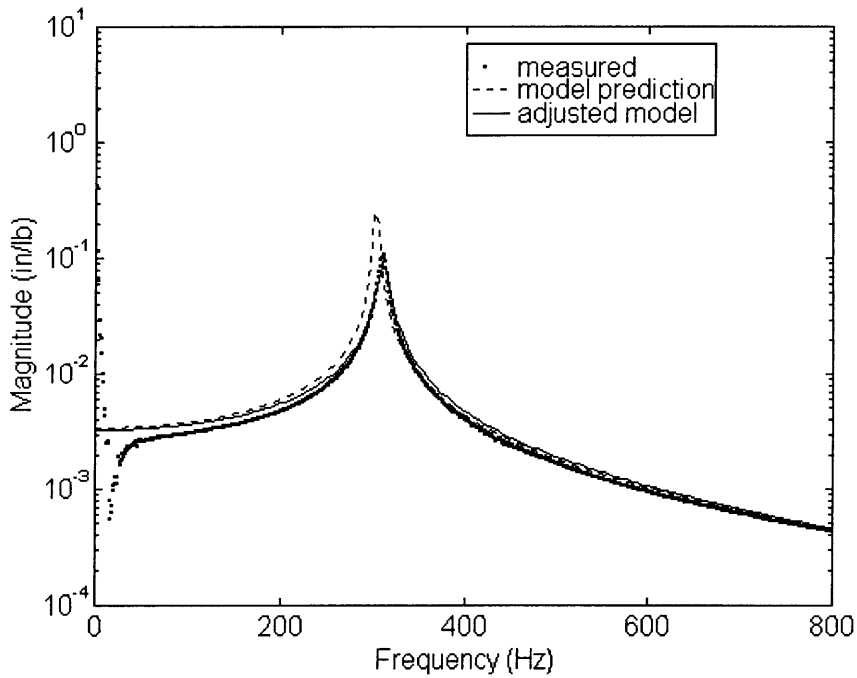

Figure 6.5: Predictive model and" Squeeze" compensated model vs measured dynamic response of rear clamped rod with short damper

80

While the viscoelastic demonstration prototype showed great potential for damping out the resonant amplitude of the first mode of the machine tool system by increasing the dynamic stiffness of an aluminum rod by a factor of 4, a design that allows better control over the viscoeslastic layer stiffness and thickness is needed.

6.2 Viscoelastic Ring Prototype

Once the effectiveness of a viscoelastic damping layer in the collet was demonstrated, a design was needed that could easily be assembled to standared tool shafts and that protected the visco-elastic material from being extruded between the fingers of the collet. These features were embodied in the viscoelastic ring prototype.

The viscoelastic ring prototype, shown in Figure 6.5, is a durable, easy to use implementation of the viscoelastic damped concept. It consists of a solid metal clamp ring and a ring of visco-elastic material sandwiched between two concentric metal spring rings. The rings are each 0.5 inch long and are positioned on a standard 0.5 inch diameter tool shank and are supported in a standard 0.75 inch collet. The sandwich ring is slightly larger than the solid ring and is compressed slightly when the collet clamps down on the solid ring.
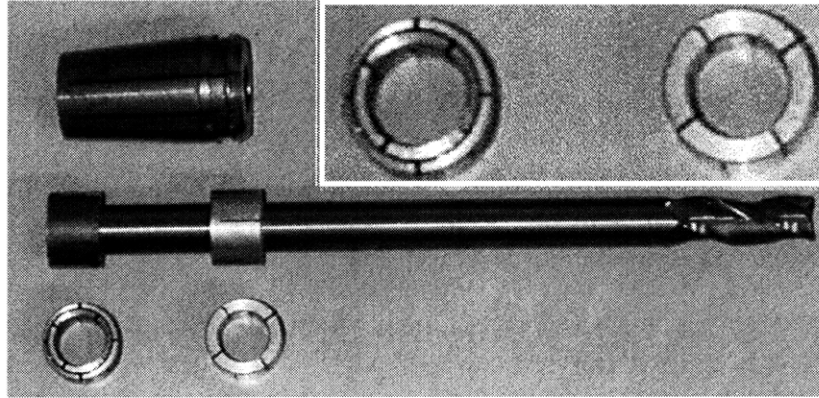
Figure 6.5: Viscoelastic ring prototype

In this design, the viscoelastic material is protected from the wear caused by sliding the ring on and off the tool shaft and from being extruded into the slits of the collet each time the collet is tightened. The concentric metal spring rings take up the frictional forces associated with sliding against the tool shaft during assembly and disassembly and distribute the clamping forces to the viscoelastic layer they surround.

The design is easy to use because the sliding rings can be re-used with any standard tool shaft. They can also be reconfigured to offer either front or rear clamping and viscoelastic layers of various lengths.

Experiments were conducted with a 0.5 inch diameter solid carbide end mill 8 inches in length at an overhang length of 5.5 inches and 6 inches. Both the rear clamped and front clamped orientations were tested. Again, the front clamped orientation yielded little or no damping. In the rear clamped orientation, no significant performance difference could be detected for viscoelastic layers of different lengths generated by stacking one, two or three damping rings side by side in the collet. For the reasons just stated, only data for the rear clamped orientation with one damping ring will be presented.

Next, three different viscoelastic rings with 0.015, 0.030, and 0.060 inch layers of

damping material were made and tested. The results of dynamic response tests are

shown in Figures 6.6 and 6.7 while the critical parameters are summarized in Tables 6.3
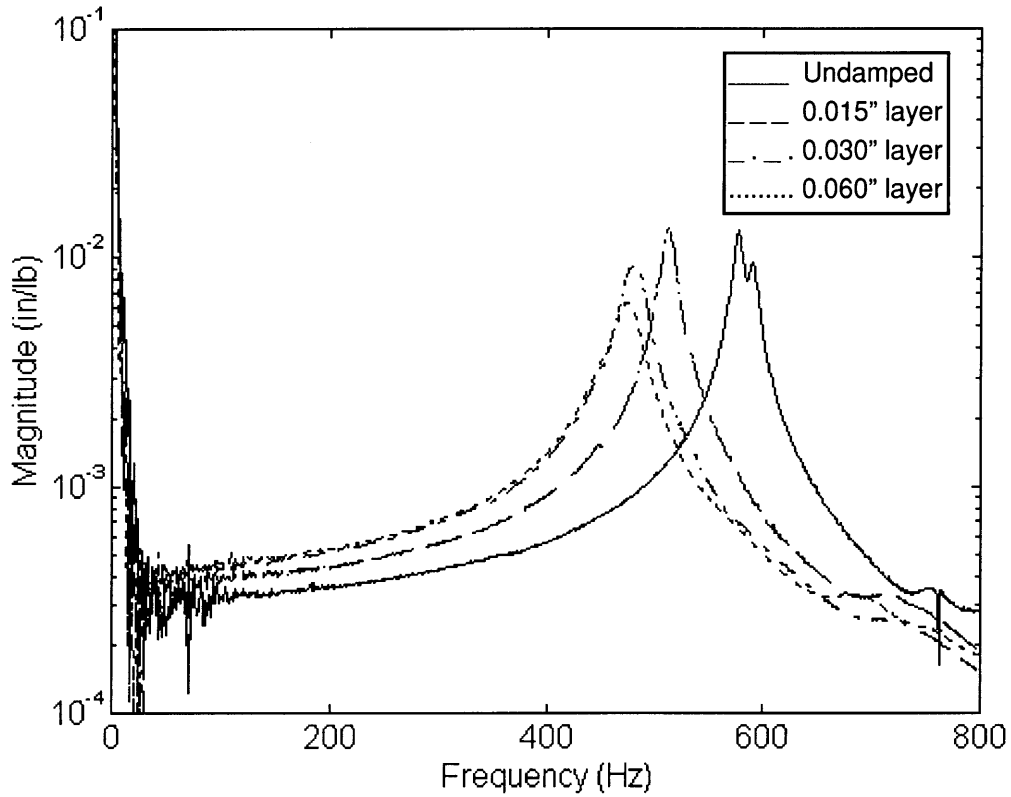
and 6.4.

Figure 6.6: Effect of viscoelastic damping ring on dynamic response of 5.5" overhung 0.5" diameter carbide tool

Tool		Resonant Peak Frequency (Hz)	Estimated Static Stiffness (lb/in)	Dynamic Stiffness (lb/in)	Q	Real Negative Max of T.F. (in/lb)	Theoretical increase in stable MRR limit
5.5" Overhang Undamped	**Actual**	**577**	**2975**	**76.6**	**39**	**.0069**	**1**
	Model	579	3030				
	w/o acc	667					
5.5" Overhang .015" layer	**Actual**	**512**	**2510**	**74.6**	**34**	**.0064**	**1.1**
	Model	406	1810	134.3		.0036	
	PF=15	502	2400	73.0		.0069	
5.5" Overhang .030" layer	**Actual**	**482**	**2210**	**106.6**	**21**	**.0054**	**1.3**
	Model	398	1750	81.5		.0060	
	PF=7	478	2250	104		.0048	
5.5" Overhang .060" layer	**Actual**	**474**	**2105**	**157.9**	**13**	**.0031**	**2.2**
	Model	393	1720	46.0		.010	
	PF=7	470	2190	139.5		.0035	

Table 6.3: Summary of dynamic response critical parameters for 0.5" diameter, 5.5" overhung carbide tool damped with a viscoelastic ring.
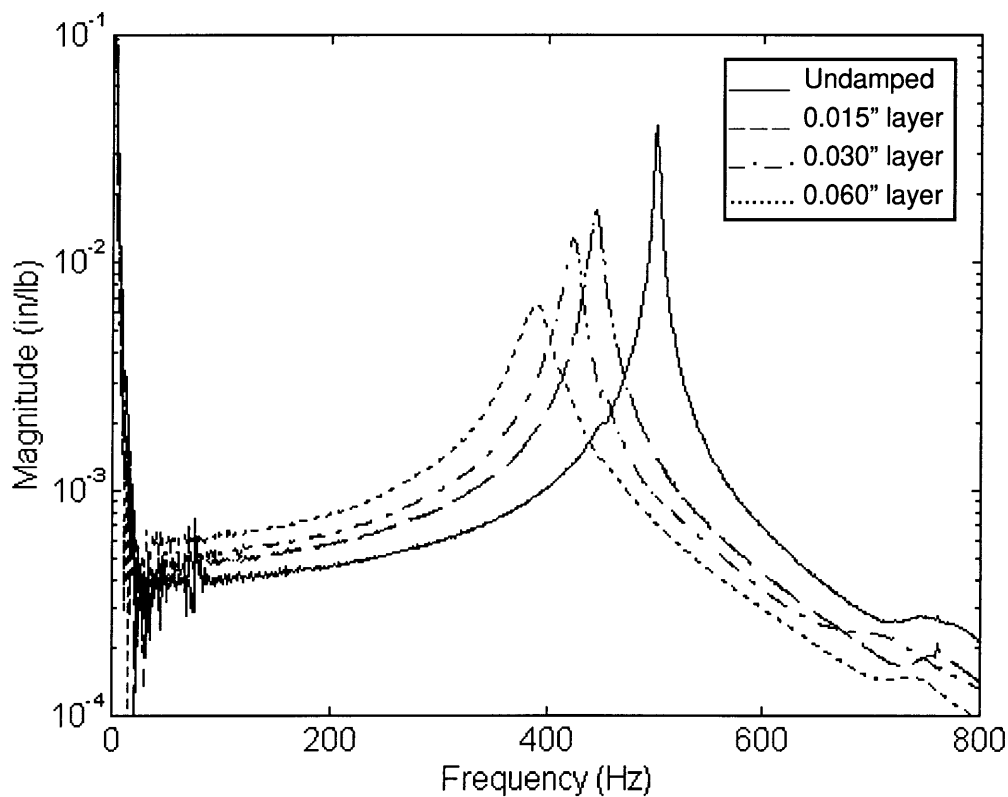

Figure 6.7: Effect of viscoelastic damping ring on dynamic response of 6.0" overhung 0.5" diameter carbide tool.

Tool		Resonant Peak Frequency (Hz)	Estimated Static Stiffness (lb/in)	Dynamic Stiffness (lb/in)	Q	Real Negative Max of T.F. (in/lb)	Theoretical increase in stable MRR limit
6.0" Overhang Undamped	**Actual**	**501**	**2615**	**24.8**	**105**	**.0228**	**1**
	Model	490					
	w/o acc	555					
6.0" Overhang .015" layer	**Actual**	**445**	**2240**	**59.1**	**38**	**.0094**	**2.4**
	Model	362	1495	106.5		.0046	
	PF=15	442	1955	56.5		.0084	
6.0" Overhang .030" layer	**Actual**	**424**	**2080**	**78.2**	**27**	**.0069**	**3.3**
	Model	353	1445	66.0		.0074	
	PF=7	422	1840	79.9		.0061	
6.0" Overhang .060" layer	**Actual**	**391**	**1720**	**152.5**	**11**	**.0032**	**7.1**
	Model	350	1420	39.2		.0130	
	PF=4	390	1665	156.6		.0030	

Table 6.4: Summary of dynamic response critical parameters for 0.5" diameter, 6.0" overhung carbide tool damped with a viscoelastic ring

In modeling a long overhang tool, it is important to model the flutes and accelerometer tip mass for accurate results. The response of a fluted tool with an accelerometer tip mass differs from that of a uniform cylindrical beam in that flutes give the shaft more flexibility thereby lowering the static stiffness while the tip mass of the accelerometer decreases the natural frequency of the tool. The flutes also lower the effective tip mass of the tool but not as dramatically as the accelerometer increases the effective tip mass. The model can be used to project the expected natural frequency of the tool without the tip mass (667 Hz for a 5.5" overhang and 555 Hz for a 6.0" overhang) which is significantly higher than the natural frequency with the accelerometer (577 Hz for a 5.5" overhang and 501 Hz for a 6.0" overhang). For the purposes of this study, the dynamic response parameters determined with an accelerometer in place will be used to characterize the tool dynamics responsible for the surface finish measured in the cutting tests.

The viscoelastic ring concept did not prevent the viscoelastic material from being squeezed as was hoped. The model without preloading does not match the data. In fact, the model predicts a rise in the resonant peak amplitude of the tool tip response and a decrease in the natural frequency of the tool as the viscoelastic layer goes from 0.015" thick to 0.060" thick. However, when the thinning and stiffening of the viscoelastic layer is taken into account by dividing the thickness by a preload factor (PF) and multiplying the stiffness by the same preload factor, the model's predictions corroborate the experimental results quite closely. The preload factors for each tool condition are listed in Tables 6.3 and 6.4. A preload factor of 15 might seem excessive, but the collet can generate a great deal of radial force to squeeze the viscoelastic material and the viscoelastic material stiffness might not exhibit linear behavior under preload conditions. This issue was not explored further as it falls outside the scope and goals of this project and the model did successfully predict the qualitative behavior of the concept's performance.

The viscoelastic ring concept's performance is sensitive to the stiffness of the viscoelastic layer. This stiffness is controlled by the layers thickness and the amount of preload induced by tightening the collet. Figure 6.8 and 6.9 show the effect that increasing the layer's stiffness has on the tool's dynamic response by comparing the parameters predicted by the model to those observed and corroborated with the "Squeeze" adjusted model. They show that the model does predict the dynamic response trend as the viscoelastic layer stiffness increases, but the model must be developed to include the effect of preload before it is quantitatively accurate.
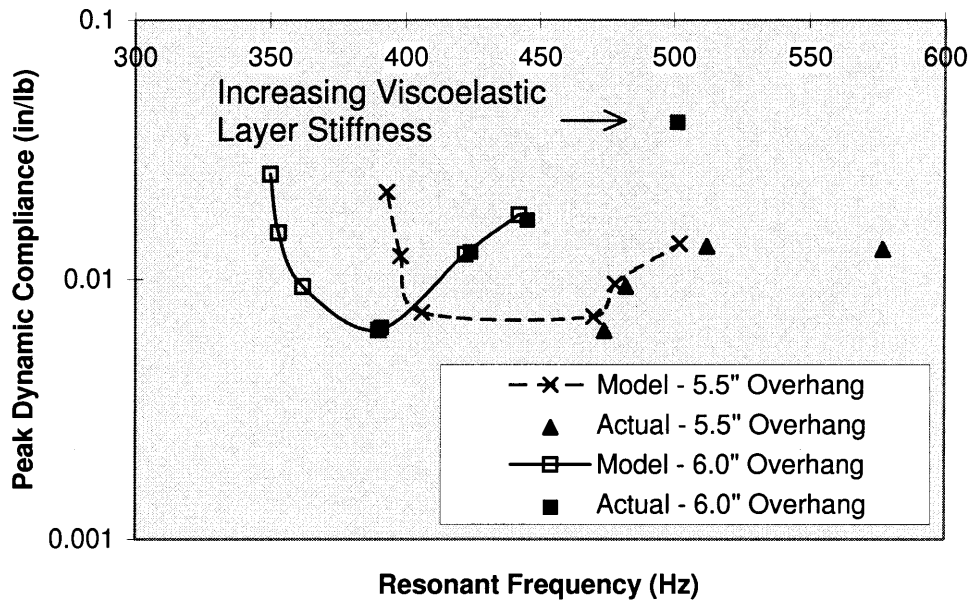
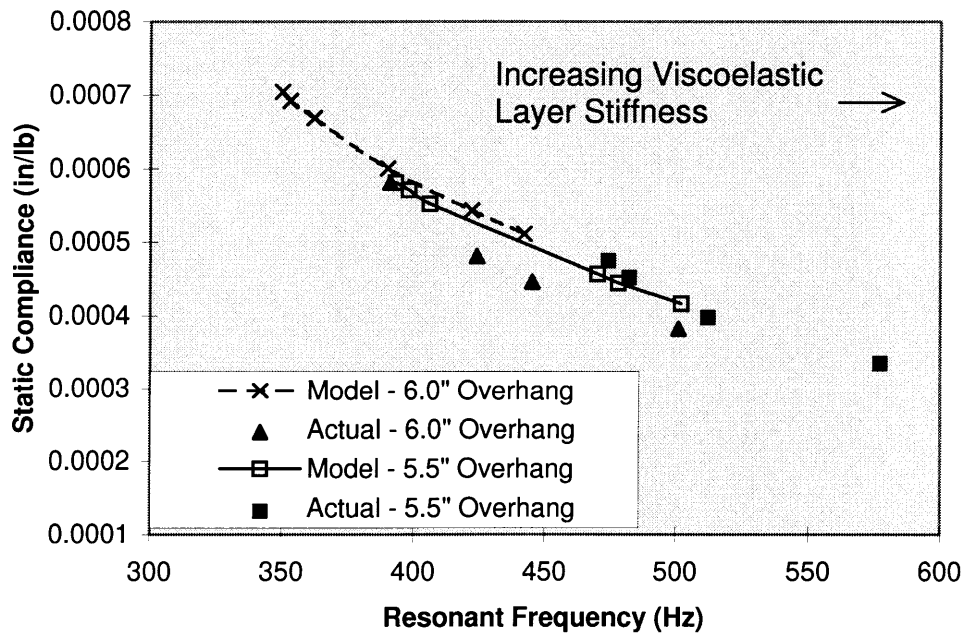*Figure 6.8: Effect of viscoelastic ring layer stiffness on tool tip peak dynamic compliance.*

Figure 6.9: Effect of viscoelastic ring layer stiffness on tool tip static compliance.

87

6.3 Discussion

The simplicity of the viscoelastic ring damped tool eases the manufacturing and use of the design. The product ,consisting of only 4 parts, can simply be manually assembled to the tool shaft by the end user in a matter of seconds. Viscoelastic rings of different lengths and layer stiffness could be sold for tools of different material and overhang length. One problem that must be solved before the successful commercialization of this . The design of the viscoelastic ring damped tool requires that the static stiffness of the tool be reduced in order to decrease the amplitude of vibration at resonance. However, according to the model, there does seem to be an optimal point beyond which further stiffness reduction results in a higher amplitude of vibration at resonance. Currently, it is difficult to control the preload on the viscoelastic layer and , therefore, its resulting stiffness. It may be possible to deterministically set the layer stiffness with tighter control on component tolerances and a calibrated lock locknut allowing the user to "dial in" the desired amount of preload. The issues surrounding the mass production and marketing should be explored more closely if metal cutting tests indicate that trading off static stiffness for dynamic stiffness can yield a better surface finish than a conventional tool.

Chapter 7: Fluid Damped Tools

7.1 Hydrostatically supported tool

In Concept Evaluation, the hydrostatic bearing concept scored poorly since only a small percentage of the machine tools currently in use are equipped with the high pressure through-tool coolant system required by the concept. This also presents an obstacle to testing a rapidly prototyped hydrostatic concept. In addition, the design and production of a hydrostatic bearing requires a significant time and resource commitment and does not lend itself to the trial-and-error approach of rapid prototyping. Although parametric solid models of the concept without the detailed bearing design were produced, a preliminary dynamic model implemented on ANSYS showed that the increase in static stiffness offered by the externally pressurized hydrostatic bearing actually degraded the dynamic response performance of the tool. In fact, the resonant peak response was predicted to increase as the pressure was increased as shown in Figure 7.1. Based on the ANSYS analysis, which favored the minimal external pressure, the development effort was focused on the passive, squeeze film damped concepts.
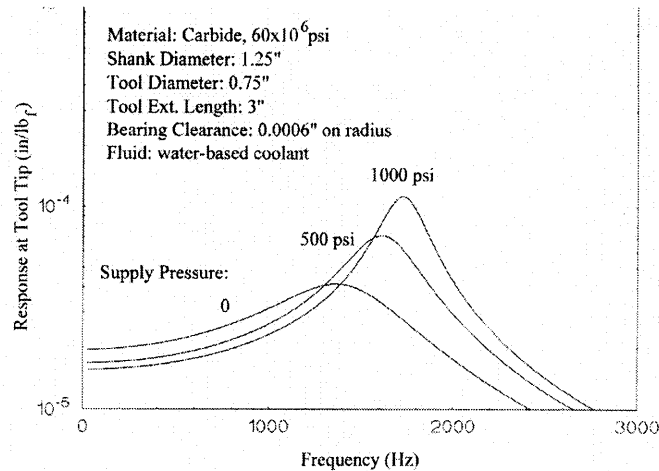
Figure 7.1: *Effect of external pressure on resonant peak amplitude of hydrostatically supported tool.(Wasson 1997)*

This behavior can be explained by solving the equation of motion for a simple spring mass damper system with mass, m, spring constant, k, and damping constant, c, for the damping ratio, ζ,:

$$\zeta = \frac{c}{2\sqrt{mk}}$$
Eqn 7.1

By increasing the stiffness of the system, the amplitude and therefore velocity of the vibration is reduced which means less energy can be dissipated by the viscous squeeze film. For this reason, a passive squeeze film damper should provide the highest dynamic stiffness.

7.2 Collet supported squeeze film damped tool

While parametric solid models and performance models of the collet supported squeeze film concept were created, physical prototypes were never produced. The proprietary nature of various collet system designs available from major manufacturers was the major obstacle that prevented the quick production of a prototype.

In designing the solid collet necessary for the concept, precise information about the dimensions and tolerances of the particular tool holder/collet system was required. There are standard systems whose dimensions and tolerances are well known, but most manufacturers also market their own 'high performance' collet system. Rather than pay licensing fees to another firm to use its technology, most collet system manufacturers have developed their own high performance designs.

The obstacles encountered in dealing with the legal issues surrounding the use of a manufacturer's proprietary collet design information effectively blocked the production of a rapid prototype. In production, the profitability of such a product would suffer from fees paid to license the use of various manufacturer's designs, variety costs associated with producing and stocking solid collet designs compatible with the many different collet systems available, and delays inherent in dealing with the legal departments of the various collet system manufacturers.

Even though the obstacles to production were discouraging, performance models of the concept's three variations (straight, augmented, and waisted shank) were implemented based on the chance that the benefit from improved performance could far outweigh the cost. Although the physical prototypes were never created, the understanding gained in simulating the performance of the concept proved to be valuable in understanding the performance of the sleeve supported squeeze film as well.

7.2.1 Straight Shaft

The straight shaft collet supported squeeze film tool is pictured in Figure 7.2 above. The tool's dynamic stiffness performance at resonance is determined by the length of the squeeze film, the clearance of the squeeze film and the viscosity of the damping fluid.

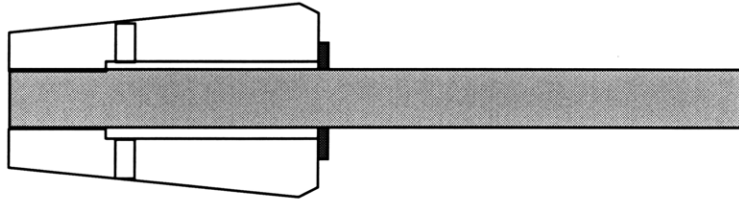*Figure 7.2: Straight Shaft, Collet Supported, Squeeze Film Damped Tool Design*

Figure 7.3 : Effect of squeeze film length and clearance on resonant peak vibration amplitude of a straight shaft, collet supported squeeze film tool. ("light" machine oil)

Figure 7.3 shows the model's prediction of how the resonant peak response of the damped tool varies with damper clearance and damper length for a 0.5 inch diameter

92

carbide tool overhung 5.5 inches from the face of the collet using "light" machine oil (μ = 1.26 x 10^{-5} lb*sec/in^2 at 68° F) as the fluid in the squeeze film. In Figure 7.4 the same design space is simulated using a more viscous fluid, namely glycerin (μ = 2.04 x 10^{-4} lb*sec/in^2 68° F), in the squeeze film.[7]
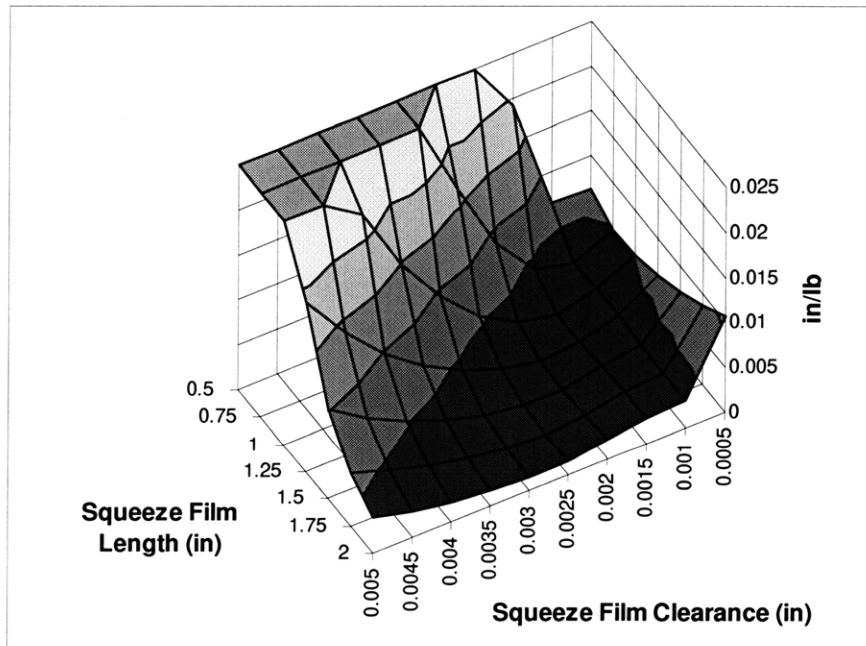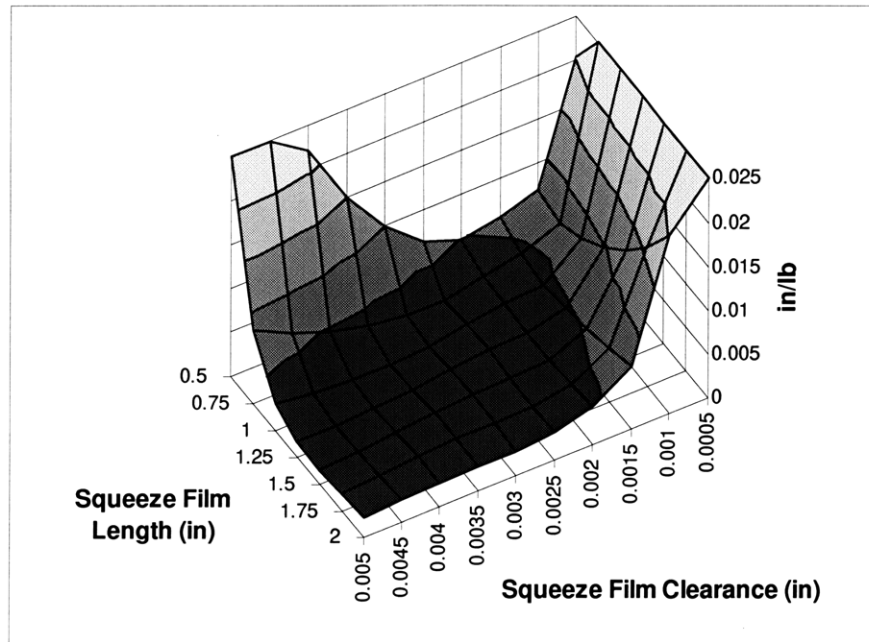

Figure 7.4 : Effect of squeeze film length and clearance on resonant peak vibration amplitude of straight shaft, collet supported squeeze film tool. (glycerin)

The simulation shows that as the viscosity of the fluid increases, the preferred design shifts from a short damper with small clearance (1.25 inch long with 0.002 inch clearance) to a long damper with somewhat relaxed clearance (2 inch long with .005 inch clearance). In both cases, the model predicts an increase in the peak resonant amplitude with long, small clearance dampers and short, large clearance dampers. This indicates that the damping coefficient of the damper has an optimal value and cannot be made

---

[7] Water in comparison has μ = 1.45 x 10^{-7} lb*sec/in^2.

arbitrarily high. The slope of data surface over the design space also shows that the performance of designs with tight clearances, with large slope in the direction of changing clearance, is more sensitive to deviations from nominal clearance caused by tolerance variations than the performance of designs with larger clearance. The static stiffness of the straight shank tool for different damper lengths is shown in figure 7.6 below. While none of the designs compare favorably with a standard tool, the shorter damper designs, due to the resultant decrease in the cantilever length of the tool, exhibit more static stiffness than long damper designs. Based on this analysis, it seems that high viscosity, long damper, large clearance designs offer more robust performance but low viscosity, small clearance designs with their shorter dampers offer greater dynamic and static stiffness performance.

7.2.2 Augmented Shaft

The augmented shaft design, pictured in Figure 7.5, allows the root of the tool to have a larger diameter than the cutting length of the tool. As a result, the deflection amplitude and velocity of the tool in the squeeze film is smaller than in the straight shaft case. This enhances the tool's static stiffness while sacrificing some of its dynamic stiffness.
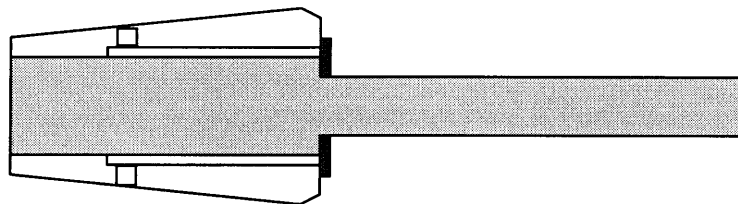
Figure 7.5: Augmented Shaft, Collet Supported, Squeeze Film Damped Tool Design

In Figures 7.6-8, the model's prediction of static and dynamic stiffness for the augmented shaft are compared to the measured parameters for a standard solid carbide endmill 0.5 inches in diameter. Both the model and the experiment represent a tool overhung 5.5" from the face of the collet. Figure 7.7 shows the relative dynamic stiffness using "light" machine oil while Figure 7.8 shows the same using glycerin.

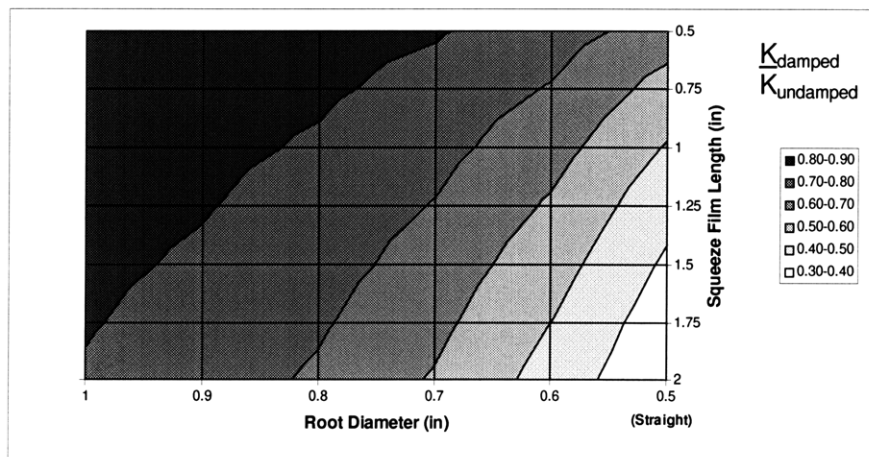

Figure 7.6: Relative Static Stiffness - Various augmented shaft designs versus a standard tool.
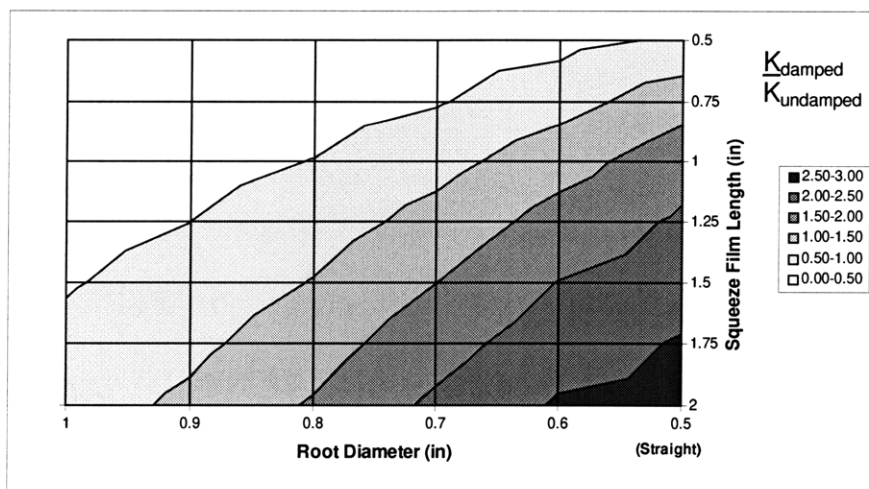

Figure 7.7: Relative Dynamic Stiffness - Various augmented shaft designs using "light" machine oil in the squeeze film versus a standard tool.

After comparing Figure 7.7 and 7.8, it is clear that for the low viscosity oil, there is a direct tradeoff between static stiffness and dynamic stiffness. Using glycerin in the squeeze film, the model's performance output for the design space, shown in Figure 7.8, shows that the peak dynamic stiffness occurs at a shorter squeeze film than with the low viscosity oil. However, in absolute terms, the dynamic stiffness performance with glycerin is either the same or worse than with the low viscosity oil.

In selecting an optimal design, one could assign weights to the importance of dynamic stiffness and static stiffness to determine the weighted peak of a combined performance surface. A normalized performance factor giving equal weight to static and dynamic stiffness is given by:

$$P = \eta_s \left(\frac{K_S}{K_{Sbase}} \right) + \eta_d \left(\frac{K_D}{K_{Dbase}} \right) \qquad \textit{Eqn 7.1}$$

where K_S is the static stiffness, K_D is the dynamic stiffness, η_s and η_d are the importance of static and dynamic stiffness such that $\eta_s + \eta_d = 1$ and P(undamped baseline tool) = 1.

The maximum P for an augmented shaft in the design space is P=1.51. Such a tool has a 2 inch long damper 0.6 inches in diameter allowing it to retain 46% of the standard tool's stiffness. A straight, collet damped tool with a 2 inch long damper has Q = 1.49 and retains 31% of the standard tool's static stiffness. If the tool's static stiffness proves to be of great importance to the surface quality in metal cutting, it is possible that an augmented shaft design could deliver better performance than a damped straight shaft. It is unlikely however, that this marginal increase in performance will justify the marked increase in tooling cost for an augmented shaft in any but the most specific application.
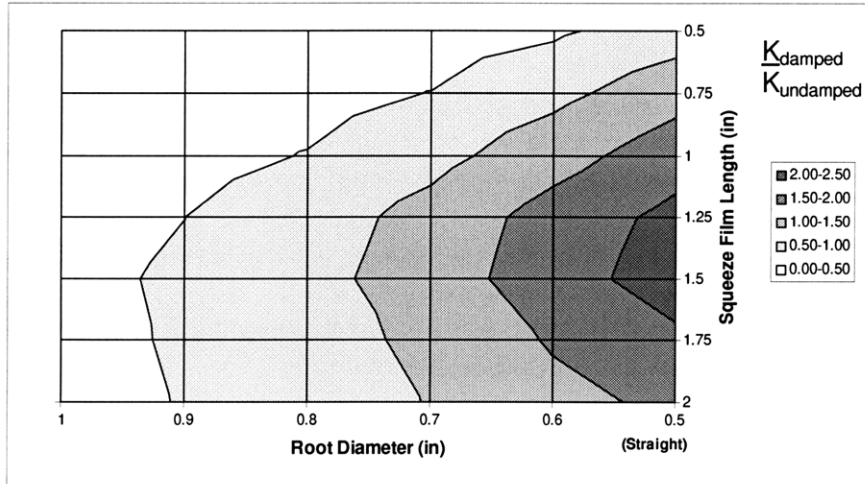
Figure 7.8: Relative Dynamic Stiffness - Various augmented shaft designs using glycerin in the squeeze film versus a standard tool.

7.2.3 Waisted Shaft

The waisted shaft tool, pictured in Figure 7.9, allows the root and damper length to be shortened for optimal static stiffness while maintaining the root flexibility and damper area required for optimal dynamic stiffness.
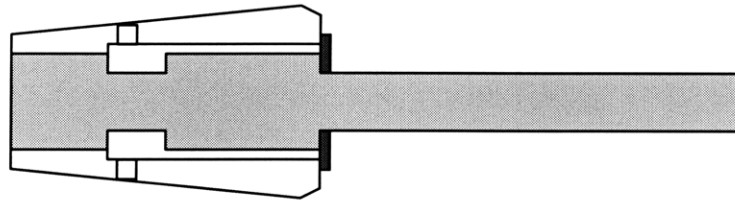
Figure 7.9: Waisted Shaft, Collet Supported, Squeeze Film Damped Tool Design

The performance model was used to determine the static and dynamic stiffness of an augmented shaft tool with 0.5 inch diameter root of various lengths and a 1 inch diameter root of various lengths. The dynamic and static stiffness performance of the waisted tool relative to a comparable standard solid carbide endmill 0.5 inches in diameter and overhung 5 inches from the face of the collet is shown in figures 7.10 and 7.11 respectively.

97
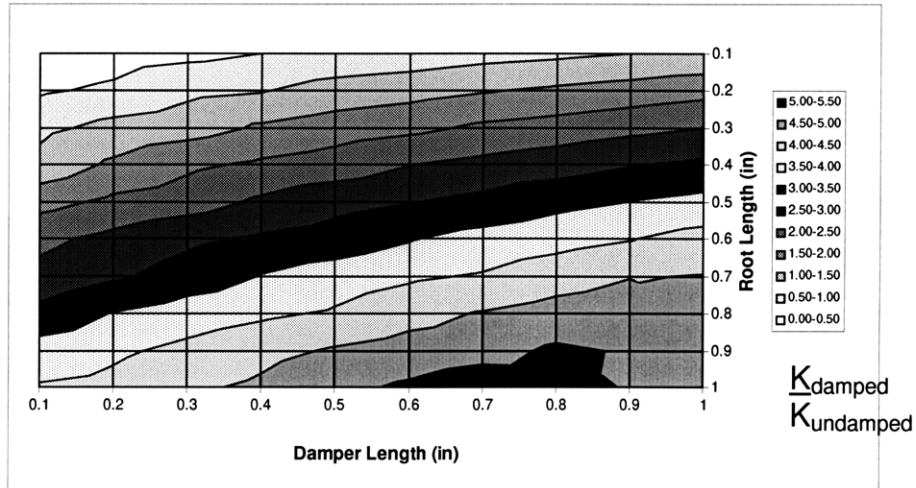
Figure 7.10: Relative Dynamic Stiffness - Various augmented shaft designs (root diameter = 0.5", damper diameter =1") using "light" machine oil in the squeeze film versus a standard tool.
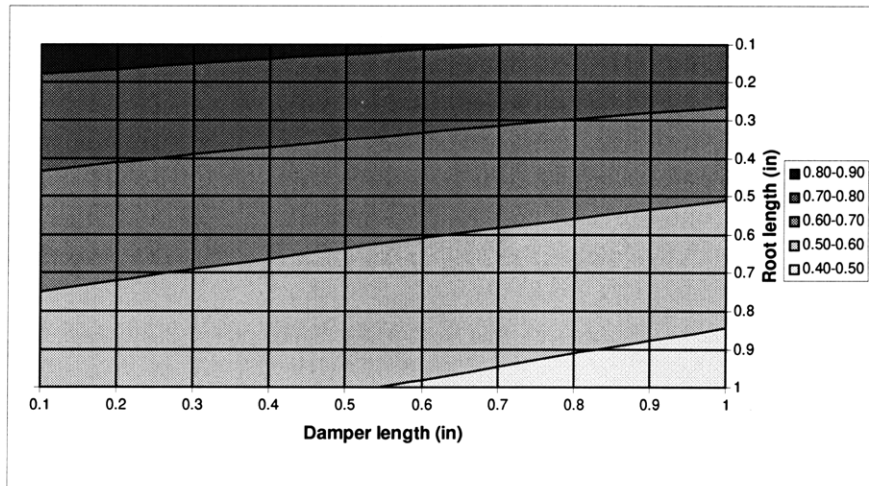
Figure 7.11: Relative Static Stiffness - Various augmented shaft designs (root diameter = 0.5", damper diameter =1") using "light" machine oil in the squeeze film versus a standard tool.

The augmented tool, like the waisted tool, requires that static stiffness be traded off for dynamic stiffness. However, since the root and damper can be designed separately, the design can offer more dynamic stiffness than the augmented shaft tool while retaining the same static stiffness. In the design space, the waisted tool has a P_{max} = 2.88. This particular design has a root length of 1 inch and a damper length of 0.8 inches

allowing it to retain 49% of the standard tool's static stiffness. Table 7.1 summarizes the performance of the optimal straight, augmented, and waisted design relative to the baseline design.

Carbide Tool 5" long 0.5" diameter overhang	Percent of baseline static stiffness	Normalized, equally weighted, combined stiffness (P)	Q
Baseline (undamped)	100	1	20
Straight	31	1.49	2.3
Augmented	46	1.51	3.6
Waisted	49	2.88	1.9

Table 7.1: Performance of ptimal tool designs for various collet supported squeeze film tools using "light" machine oil in the squeeze film.

It is difficult to determine whether the benefit of the collet supported squeeze film designs is worth the cost to produce them. With a better understanding of how dynamic stiffness and static stiffness contribute to increasing chatter free metal removal rate, it is possible that further development of this concept may be justified. Due to the time and budget constraints of this project, this collet supported squeeze film concept was not pursued. Instead a simpler concept, namely the sleeve supported squeeze film, was developed to demonstrate the effectiveness of a squeeze film damped tool.

7.3 Sleeve supported squeeze film

Of the fluid damped tools, the sleeve supported squeeze film concept is the only one that was prototyped. The prototype, as shown in Figure 7.13, simply consists of a steel sleeve in which the front part of the stepped bore offers a slight clearance to the outer diameter of a tool shank and the rear part of the stepped bore is shrunk fit onto the tool shaft. The sleeve is 4 inches long with a 2 inch long shrink fit and a 2 inch long damper. The overall length of the tool was 7.5 inches. The damper radial clearance is

nominally 0.0012 inches. There are three radial holes in the sleeve that allow the damping fluid to be pumped into the clearance. The diameter of the carbide tool and nominal diameter of the sleeve is 0.5 inch and the sleeve's outer diameter is 0.75 inch.

Figure 7.13: Sleeve supported squeeze film prototype

Unlike the other fluid damped tool concepts, the sleeve supported squeeze film is independent of technology from other companies. The smooth outer diameter of the sleeve allows this tool to be used in the same manner as a conventional tool with a smooth shaft. Since the position of the sleeve in the collet can be adjusted, the sleeve supported squeeze film more versatile than the collet supported squeeze film design. By supporting the clearance length of the bore entirely within the collet, as shown in Figure 7.14a, the tool acts as though the squeeze film is rigidly supported. With the clearance length of the bore completely outside the collet, as shown in Figure 7.14b, the tool retains the static stiffness of a standard tool and the dynamic stiffness of a damped tool, unlike the squeeze film collet in which the static stiffness is reduced considerably.
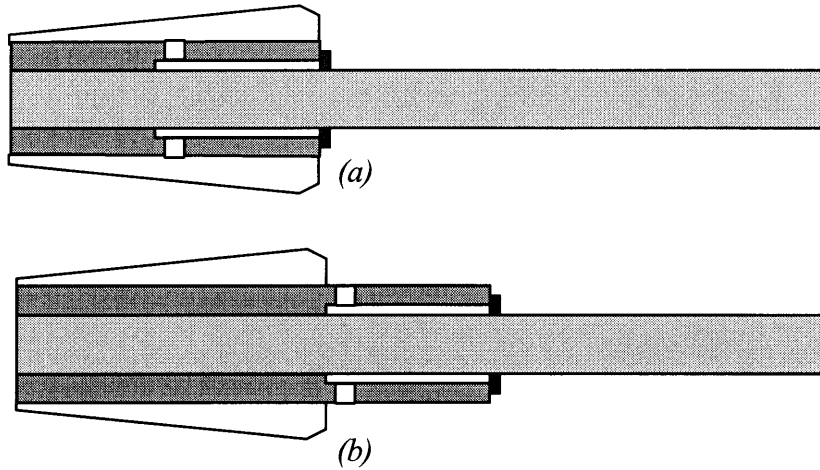
Figure 7.14: The sleeve supported squeeze film can be designed to (a) maximize the rigidity of the sleeve, or (b) minimize the overhang length of the tool.

7.3.1 Effect of sleeve compliance

The deflection of the tool into the squeeze film generates a pressure that opposes the motion of the tool but also pushes on the inner wall of the sleeve. If the sleeve is very compliant, the force pushing on the sleeve can cause it to retreat as the tool advances, thereby reducing the relative velocity of the boundaries of the squeeze film and limiting the effectiveness of the damper. To determine the effect of the sleeve compliance on the dynamic response of the tool, the sleeve was modeled as a collection of finite elements fixed at one end, with nodes connected to the tool nodes by dampers. Figure 7.15 shows the model's predicted dynamic response with sleeves 10, 1 and 0.1 times the stiffness of the tool compared to the measured dynamic response of the undamped and damped tool. For all tools, the overhang length of the 0.5" diameter carbide tool is 5.5". Water is used as the fluid in the squeeze film damped tools which are held in the position of maximum static stiffness (See Figure 7.14 above).
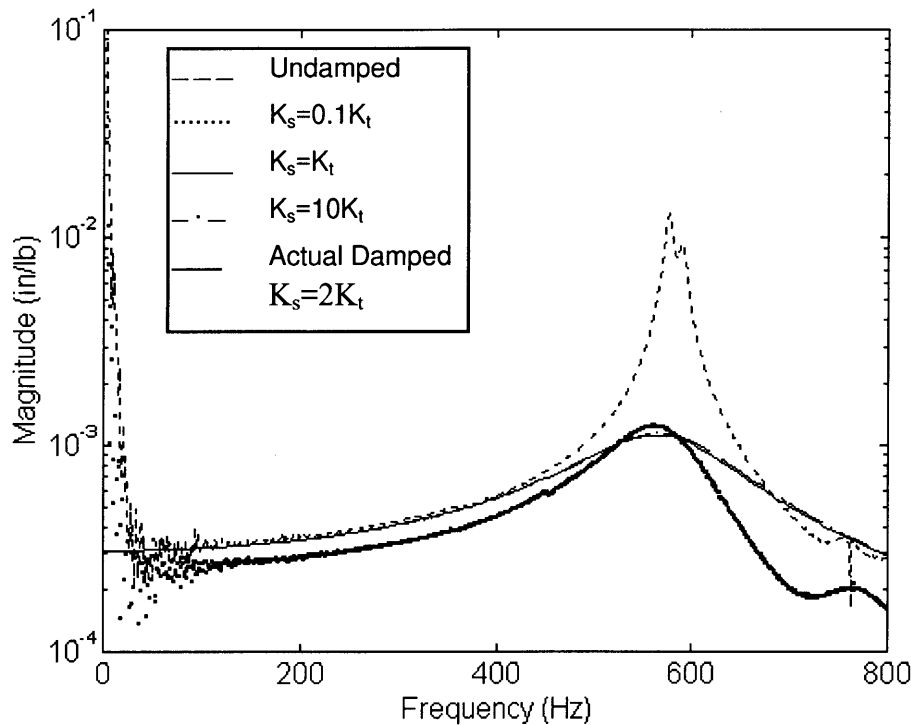
Figure 7.15: Comparison of modeled and actual response of sleeve supported squeeze film tool to standard undamped tool.

Figure 7.15 suggests that there is no significant change in performance as the sleeve goes from 10 times stiffer than the tool to 10 times more compliant than the tool. This is a surprising result. The model also does give a very accurate prediction of the measured response. One possible explanation is that the tool and sleeve are coupled at the point of fixation. Also, the bending slope and its first derivative are not constrained to be zero as suggested by the boundary conditions used in the model. Together, this means that the vibrating tool imparts some displacement to the sleeve surrounding it through the base and the sleeve imparts some additional static stiffness to the tool. This inference is supported by the fact that the sleeve damped tool has higher static stiffness than a comparably overhung standard tool and by the fact that the resonant amplitude of the tools response decreases as more of the clearance length is supported in the collet. Based

102

on this inference, a compliant sleeve more readily "follows" the bending slope than a stiff sleeve. Clearly, the model must be developed further before the effect of the sleeve compliance can be predicted accurately. To avoid the dynamic stiffness performance degradation likely with excessive sleeve compliance, a sleeve with twice the cross sectional stiffness of the tool was deemed sufficient in building the first prototype.

7.3.2 Effect of fluid viscosity

The model of the squeeze film damped concept predicts that there is an optimal viscosity fluid that minimizes the peak dynamic response of the tool. Higher and lower viscosity fluids result in a higher peak dynamic response. The prototype was tested with fluids of different viscosity in the squeeze film by using a water soluble lubricant of different concentrations. The predicted and actual peak response as a function of fluid viscosity are shown in Figure 7.16 below. At higher viscosities, the predicted response closely matches the actual measured response. For less viscous fluids however, the actual peak response is much higher than the predicted peak response. This behavior might be explained by the fact that the fluid flow in the squeeze film tends toward the turbulent flow regime as viscosity decreases or by the fact that the fluid leaks through the seal more readily at lower viscosities. These factors are not included in the model and should be explored more closely upon further development of the concept. For the purposes of demonstrating the performance of the concept, cutting tests were conducted using water as the fluid in the squeeze film as this yielded the minimum peak response at the tool tip.
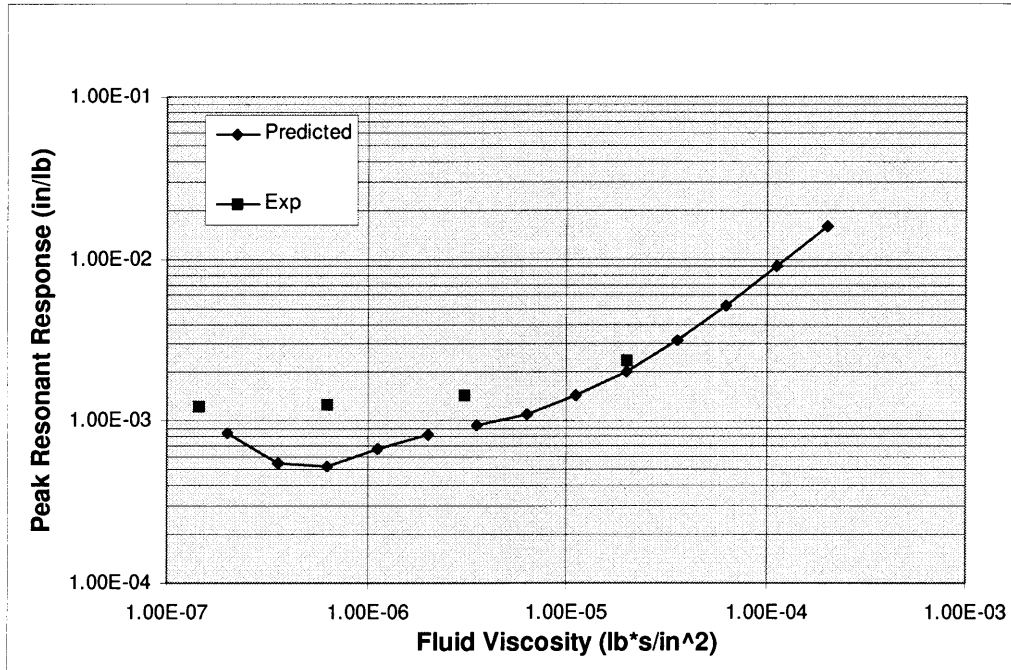
Figure 7.16: Effect of fluid viscosity on peak resonant response at the tool tip.

7.3.3 Dynamic Response Parameters

For the cutting tests and dynamic response tests, the 7.5 inch long carbide tool

was replaced with an 8 inch tool with a more suitable cutting geometry. The tool was

tested under 5.5 inch and 6.0 inch overhang conditions. In the 6.0 inch overhang

condition, the tool offers slightly more static stiffness and much more static stiffness than

the standard tool overhung 6.0 inches. In the 5.5 inch overhang condition, 0.5 inch of the

squeeze film is supported in the collet. Because the tool is still effectively cantilevered

6.0 inches, this results in less static stiffness than the standard tool overhung 5.5 but

yields much more dynamic stiffness. The dynamic response parameters for the standard

tool, the damped tool and the model of the damped tool for both overhang conditions are

compared in Table 7.2.

Tool		Resonant Peak Frequency (Hz)	Estimated Static Stiffness (lb/in)	Dynamic Stiffness (lb/in)	Q	Real Negative Max of T.F. (in/lb)	Theoretical increase in stable MRR limit
5.5" Overhang undamped	Actual	577	2975	76.6	39	.0069	1
5.5" Overhang damped	Actual	559	3080	430	7.2	.0011	6.3
5.5" Overhang damped	Model	490	2370	525		.0008	8.6
6.0" Overhang undamped	Actual	501	2615	24.8	105	.0228	1
6.0" Overhang damped	Actual	553	3000	419	7.1	.0014	16.3
6.0" Overhang damped	Model	490	2370	525		.0008	28.5

Table 7.2: Comparison of dynamic response parameters for sleeve supported squeeze film damped tool using water in the squeeze film and a standard tool.

The results of the dynamic response testing indicates that there is great potential to increase the dynamic stiffness of a long overhang tool and maintaining the static stiffness by using a sleeve supported squeeze film.

7.4 Discussion

The sleeve supported squeeze film damped tool offers the static stiffness of a standard tool and much higher static stiffness. However, before the concept can be introduced profitably to the market, the manufacturing and customer use issues listed below will have to be addressed.

Component tolerances: Component tolerances determine the limits of the tool-sleeve clearance and the shrink fit interference. Variability in the clearance dimension will make it difficult to determine the optimal viscosity for a given tool material, diameter, and overhang length. Variability in the shrink fit interference could effect the

assembled pressure between the tool and the sleeve. Too large an interference can cause the tool to fatigue thermal or mechanical fatigue over many tool change cycles while too small an interference can compromise the rigidity of the tool's support. A spreadsheet that can be used to determine the assembled pressures and assembly temperatures required at the limits of the shrink fit dimension is presented in Appendix C.

Customer owned assembly system: The sleeve must be heated to assemble it to the tool. The sleeve could deform during heating or assembly it is heated non uniformly. Induction heaters that are used for heat-shrink type tool holders are currently very expensive. A low cost and compact induction heater, that could be sold as a system with the damped sleeves, would help the product's acceptance into the market.

Filling the squeeze film: In the prototype, the squeeze film is filled through tiny fill ports using a syringe which are then plugged with screws wrapped in teflon tape. A more convenient filling solution that doesn't compromise the tools dynamic balance must be found. Preferably, this filling system would allow the customer to mix water soluble oil to the desired viscosity "on the fly".

Sealing the squeeze film: The current method of sealing the squeeze film with a bead of silicone sealant will have to be eliminated or made more convenient. A rubber seal retained by a preloading mechanism, such as a threaded ring, would be ideal since the seal must be removed to fill the squeeze film and to heat the sleeve.

The results of the metal cutting tests will show whether the sleeve supported squeeze film damped tool improves the chatter free metal removal rate and whether this improvement is large enough to justify further development of this concept.

106

Chapter 8: Enlarged Shaft Diameter tools

8.1 Tapered and Stepped tool

The tools pictured in Figure 8.1 are designed for maximum stiffness in an envelope that still allows access to deep, slightly tapered pockets and intricate surfaces. Because of their non-standard shape, these tools would be prohibitively expensive for all but the most specialized, "cost is no object' applications. However, if the performance of the statically stiff tools is far greater than that of the standard or damped tools, it could be more cost effective to use tapered tools for certain applications. If these applications grow in popularity, the cost of tapered tools could come down. For this reason, and to fully understand the role of static and dynamic stiffness in metal cutting, the dynamic response and metal cutting performance of these statically stiff tools was measured and compared to the performance of standard and damped tools.
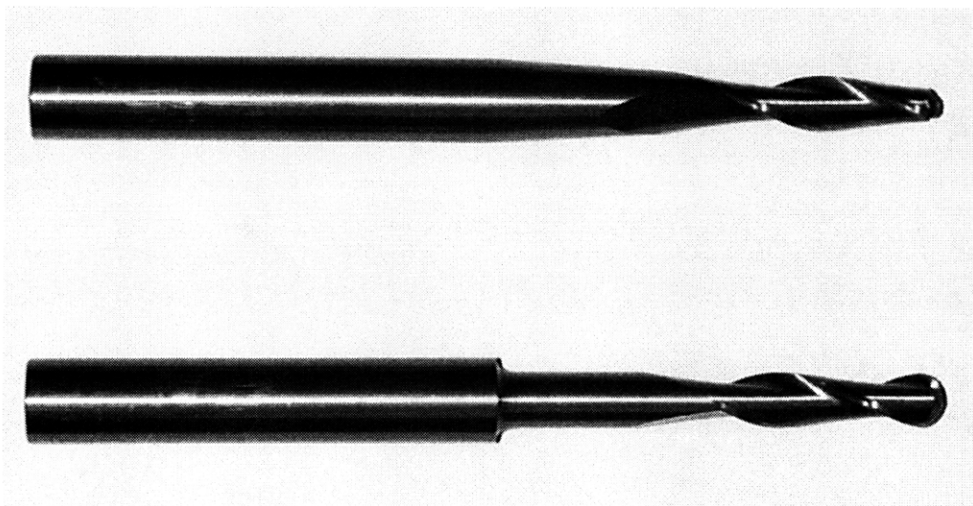
Figure 8.1: Prototypes of tapered shaft (top) and stepped shaft (bottom) tools.

The tools are solid carbide and were tested at overhang lengths of 5.5 inches and 6.0 inches. The end of the tool held in the collet, or the grip length, is 0.75 inches in diameter while the cutting diameter is 0.5". The tools are 8 inches in length with a 4 inch grip length. The taper of the tapered tool is 2 inches long. In both tools, the flutes have a straight profile. The critical parameters of the dynamic response are given in Table 8.1.

Tool	Resonant Peak Frequency (Hz)	Estimated Static Stiffness (lb/in)	Dynamic Stiffness (lb/in)	Q	Real Negative Max of T.F. (in/lb)	Theoretical increase in stable MRR limit
5.5" Overhang standard	577	2975	75	40	.0069	1
5.5" Overhang stepped	694	6265	1105	5.7	.00003	230
5.5" Overhang tapered	670	7375	1600	4.6	.00018	38
6.0" Overhang standard	501	2615	25	105	.0228	1
6.0" Overhang stepped	619	5435	865	6.3	.00038	60
6.0" Overhang tapered	610	6525	1105	5.9	.00033	69

Table 8.1: Comparison of Dynamic Response critical parameters for standard, tapered, and stepped tool.

The results of the dynamic testing show that the statically stiffer tools also have considerably more dynamic stiffness than was excpected. The tapered tool has more static and dynamic stiffness than the stepped tool, but metal cutting tests will have to be conducted to see how significant this difference in performance really is in terms of metal removal rate.

8.2 Discussion

In deep-cavity mold milling applications, the stepped shaft tool , with an envelope equivalent to that of the sleeve damped tool, offers more clearance for intricate surfaces

108

while the tapered shaft tool offers more static stiffness in cases with some constant

minimum draft angle as shown in Figure 8.2.
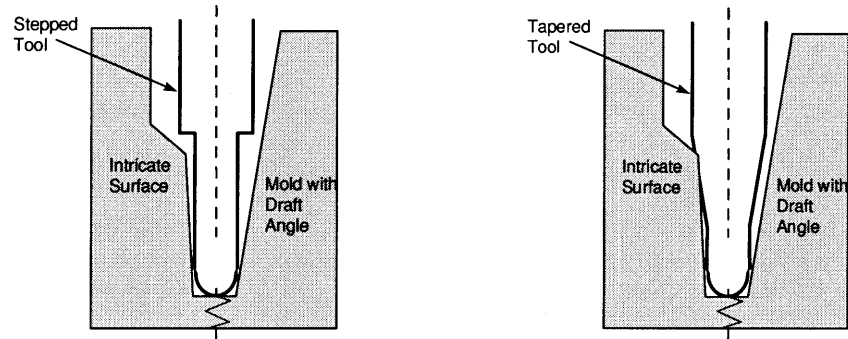
Figure 8.2: Stepped tool offers more clearance for intricate surfaces while tapered tool offers more static stiffness.

Tools with tapered flutes are currently in sold in high volumes for milling mold

cavities with a slight draft angle. Due to the higher static and dynamic stiffness of a

tapered tool, the most readily available solution to increasing metal removal rates may be

to invest in a highly stiff 5 axis machine rather than a 3 axis machine.
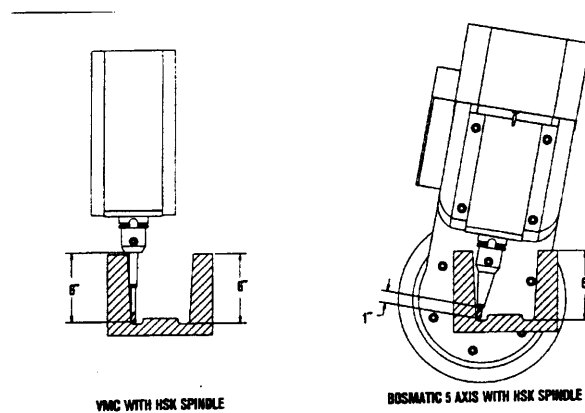
Figure 8.3: 5 axis machine offers deep cavity access with a stiffer tool holder and shorter tool.(Stilwell 1998)

The extra degrees of freedom will allow the machine with a stiff, tapered tool to cut a

deep cavity mold with straight walls(See Appendix D) as shown in Figure 8.3 but will

also introduce some compliance into the machine tool system. In some cases, the increase in chatter free MRR may be well worth the extra initial investment for two additional, highly stiff machine tool axis. This will be determined by the metal cutting tests presented in the next chapter.

Chapter 9: Metal Cutting Tests

9.1 Results

To determine the significance of the dynamic response parameters to the metal removal rate and surface finish in milling, metal cutting tests were conducted in a CNC vertical milling machine. Tests were conducted at 4000 rpm. Faster spindle speeds were not used because a high-speed spindle was not available and the machine used developed a self-induced vibration above 4000 rpm. The material cut was aluminum. The surfaces to be measured were created by taking three successive cuts with 3/8 inch axial depth, on a near-net-shape geometry. The first cut was a 0.008 inch conventional cut, while the second and third were both 0.004 inch climb cuts. The cuts were made at feed rates of 50, 100, 150, and 200 mm/min. A representative test coupon is shown in Figure 8.1 below.
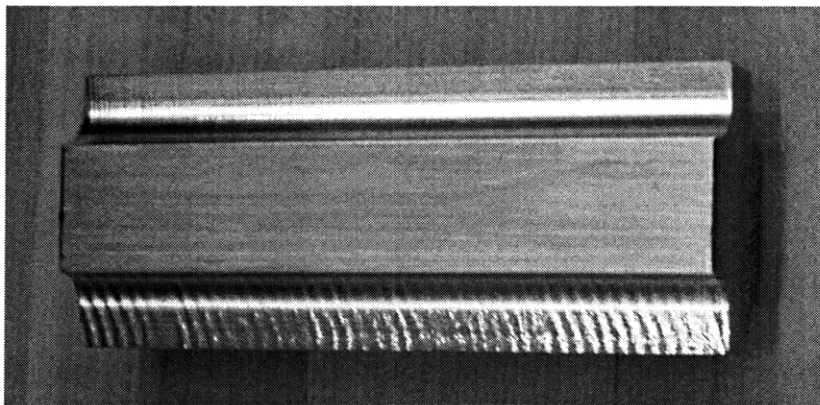
Figure 9.1: representative test coupon

Cuts were made with the standard, sleeve supported squeeze film damped tool, the viscoelastic rings on a standard tool, the stepped tool and the tapered tool at 5.5 and 6

inch overhangs. Tables 9.1 and 9.2 give the measured dynamic response parameters of the tools at 5.5 and 6 inches respectively. Figures 9.2 and 9.3 show the amplitude of the resulting surface roughness, as measured by a profilometer, at the different feed rates. Figure 9.2 is the surface roughness for an overhang of 5.5 inches and Figure 9.3 is the surface roughness for and overhang of 6 inches. Due to their high roughness results, the data for the viscoelastic rings was removed from Figure 9.3 for clarity.

From the surface roughness measurements for cuts at conventional spindle speeds, the surface roughness does not seem to be a linear function of metal removal rate as expected. The surface roughness is more or less constant for the feed rates used. At an overhang of 5.5 inches, the standard tool exhibited some sort of resonance to give its surface a roughness on the order of 250 micro inches. The thicker layer viscoelastic ring also gave a relatively rough surface finish. The sleeve supported squeeze film, viscoelastic rings, stepped and tapered tool did not exhibit this resonance since they have natural frequencies that are very different from the standard tool. The stepped and tapered tool have a surface roughness on the order of 20 micro inches. This represents about half the roughness amplitude of the cuts made with the squeeze film damped tool or the thinner layer viscoelastic ring.

Roughness Amplitude (micro inches) vs **Feed Rate (mm/min)**

Legend:
- Standard
- Damped
- Stepped
- Tapered
- 0.030 Viscoelastic
- 0.060 Viscoelastic
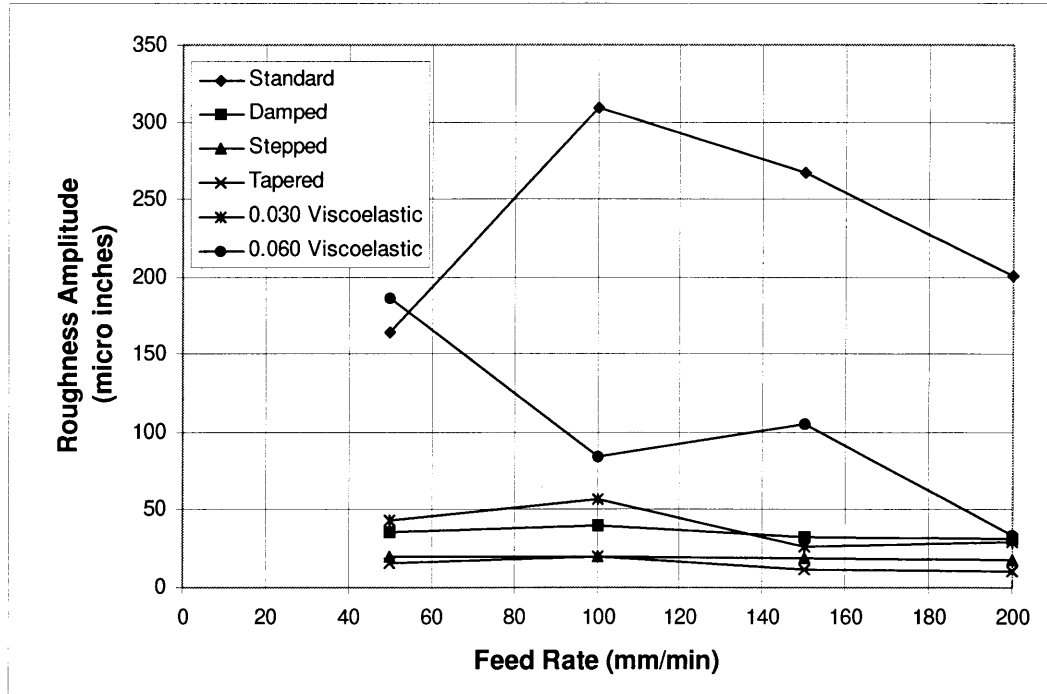
Figure 9.2: Roughness amplitude vs. feed rate for tools overhung 5.5 inches from the collet face.

Tool	Resonant Peak Frequency (Hz)	Estimated Static Stiffness (lb/in)	Dynamic Stiffness (lb/in)	Q	Real Negative Max of T.F. (in/lb)	Theoretical increase in stable MRR limit
5.5" Overhang baseline	577	2975	76.6	39	.0069	1
5.5" Overhang viscoelastic (.030)	482	2210	106.6	21	.0054	1.3
5.5" Overhang viscoelastic (.060)	474	2105	157.9	13	.0031	2.2
5.5" Overhang squeeze film	559	3080	430	7.2	.0011	6.3
5.5" Overhang tapered	670	7375	1600	4.6	.00018	38
5.5" Overhang stepped	694	6267	1105	5.7	.00003	230

Table 9.1: Dynamic response parameters for tools overhung 5.5 inches from the collet face
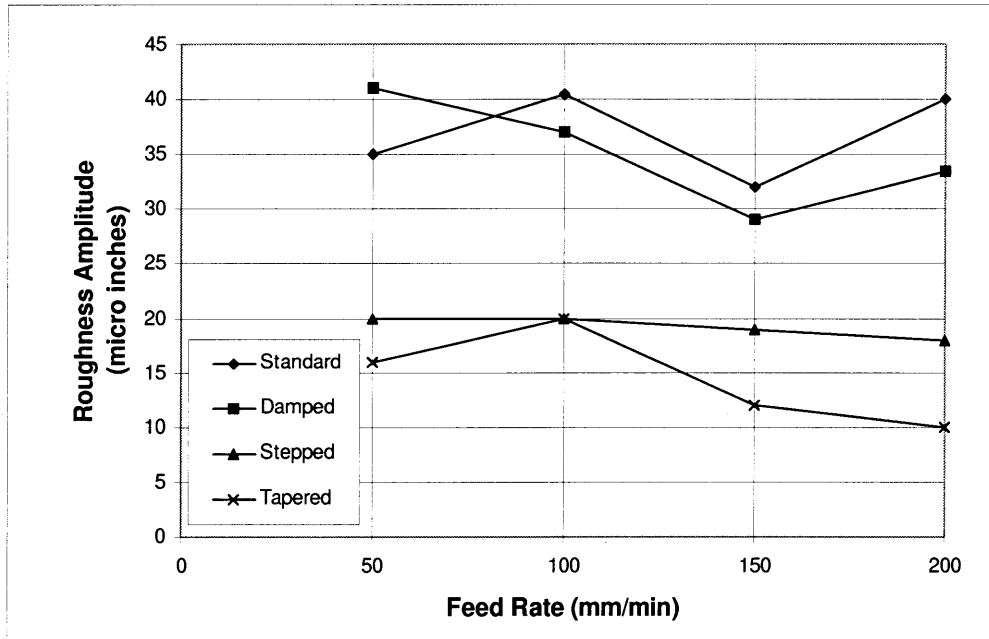
Figure 9.3: Roughness amplitude vs. feed rate for tools overhung 6 inches from the collet face.

Tool	Resonant Peak Frequency (Hz)	Estimated Static Stiffness (lb/in)	Dynamic Stiffness (lb/in)	Q	Real Negative Max of T.F. (in/lb)	Theoretical increase in stable MRR limit
6.0" Overhang baseline	501	2615	24.8	105	.0228	1
6.0" Overhang viscoelastic (.030)	424	2080	78.2	27	.0069	3.3
6.0" Overhang viscoelastic (.060)	391	1720	152.5	11	.0032	7.1
6.0" Overhang squeeze film	553	3000	419	7.1	.0014	16.3
6.0" Overhang tapered	610	6525	1105	5.9	.00033	69
6.0" Overhang stepped	619	5435	865	6.3	.00038	60

Table 9.2: Dynamic response parameters for tools overhung 6 inches from the collet face

At the 6 inch overhang condition, the viscoelastic rings gave a poor surface finish. With all other tools, contrary to what was expected, there was no significant degredation in surface quality in going from a 5.5 inch overhang to a 6 inch overhang. Since the natural frequency of the standard tool at 6 inch overhang is different from that at the 5.5 inch overhang, the resonance and large surface roughness amplitude of the standard tool was not observed in the cutting tests. The sleeve supported squeeze film damped tool and standard tool both had a roughness amplitude around 40 micro inches while the stepped and tapered tool delivered roughness amplitudes of around 20 microinches.

9.2 Discussion

It is surprising that the squeeze film damped tool with slightly greater static stiffness and up to an order of magnitude higher dynamic stiffness did not perform better than the standard tool. One possible explanation is that dynamic stiffness is not as important as static stiffness in milling at conventional speeds. Tests at higher spindle speeds with measurements of the input cutting force frequency spectrum might confirm this hypothesis. Knowing the frequency spectrum of the input cutting force would allow a designer to design a tool best suited to attenuate the response to this input excitation. Another possible explanation for the lack of distinction in the performance of the standard tool and sleeve damped tool is that the viscous fluid may have evaporated from the squeeze film. This was confirmed by the fact that the dynamic stiffness of the squeeze film damped tool went from 430 lb/in as measured when it was just filled to 155 lb/inch as measured after testing for the 5.5 inch overhang and from 419 to 254 lb/inch for the 6 inch overhang. More tests should be conducted at higher speeds and with less

delay between filling the squeeze film damped tool and cutting with it. Also, a better solution for sealing the squeeze film damped tool or squeeze film designs that incorporate a high viscosity fluid should be used to avoid problems with fluid evaporation.

Another interesting result of the cutting tests is that the performance of the stepped and tapered tool do not differ greatly. In this case, the stepped tool is preferred due to its simpler geometry, lower material cost, and greater access to intricate surfaces. The cost could be reduced even further if the stepped tool could be fabricated from a standard tool and a shrink fit sleeve.

Based on the metal cutting tests performed, at conventional milling speeds, static stiffness is the most important parameter of a machine tool system's dynamic response. Under these conditions, a stepped tool offers the best surface finish performance.

Chapter 10: Conclusions

10.1 Outcomes

The goal of the project was to increase the metal removal rate or improve the surface quality of an intricate surface cut by a long overhang tool. The results of the metal cutting tests show that the surface quality of a finish cut at conventional milling speeds can be improved by approximately 50% by using a stepped or tapered tool. In applications with straight walls or intricate surfaces where the larger diameter base of the tool interferes with the workpiece, a high stiffness 5 axis machine can achieve the desired geometry.

Damping treatments such as the squeeze film damped tool and the visocelastic ring were developed that could significantly increase the dynamic stiffness of a long overhang tool. These damping treatments did not improve the workpiece surface finish at conventional milling speeds. However, metal cutting theory indicates that more damping could be beneficial in high speed milling applications in which the vibration amplitude of the tool's resonant cantilever mode limits the stable depth of cut.

This study has also produced an analytic model and damping methods that will enable designers to tailor the dynamic response of a tool to attenuate the vibrations that cause chatter at higher spindle speeds.

10.2 Recommendations for future work

The damped tools presented in this study still hold promise for improving metal removal rates and surface finish at higher spindle speeds where cutting forces are lower

and chatter due to the tools first cantilever mode of vibration limits the depth of cut and feed rate.

The method of data collection in this study could be improved by using a reflectometer, rather than an accelerometer, to determine the machine tool system's dynamic response. This device does not suffer from inaccuracy at low frequency and does not require anything to be mounted to the tool tip. As a result, a more accurate measurement of the true machine tool system response can be made. Another improvement would be to make measurements on the cutting forces between the tool and the workpiece during cutting. With this measurement, the input force spectrum at various cutting speeds could be analyzed and the tool which yielded the lowest amplitude response to the input spectrum could be designed.

Another useful extension of this project would be to explore other applications for the damping treatments presented. For example, by modifying the MATLAB™ code slightly, a more generalized model with a user friendly interface could help in the design of hydrostatically supported jig bore axis capable of creating higher tolerance holes and with longer life than conventional jig bore axes. Also, a more refined model that included the effects of toolholder compliance could aid in the development of advanced tool holding systems.

Finally, work should continue to deliver the improved cutting performance of the stepped tool concept to the marketplace as a reasonably priced product as was discussed in Chapter 9.

Bibliography

Abbas, J. T. a. B. A. H. (1975). "Finite Element Model for Dynamic Analysis of

Timoshenko Beam." Journal of Sound and Vibration 41(3): 291-299.

Diebold Goldring Tooling (1997). Hollow shaft taper (HSK) tooling - overview. website: http://www.hsk.com/toolhold.htm.

King, R., Ed. (1985). Handbook of High Speed Machining Technology. New York, Chapman & Hall.

Lewis, D. (1996). "HSK Status Report." Manufacturing Engineering(January).

Shoffa, R. (1997). Test Data: Relative Cantilever Stiffness of Various Tool Holders. G. Motors. Warren, MI.

Slocum, Alex (1992). Precision Machine Design. Englewood Cliffs, Simon & Schuster Company.

Smith, D. S., S.; Tlusty, J (1994). "High Performance Milling Torque Sensor." Manufacturing Science and Engineering 68(2): 711-723.

Stephenson, D. A. J. (1997). Metal Cutting Theory and Practice. New York, Marcel Dekker.

Stilwell, G. (1998). "Taking the Mystery Out of Hard Die Milling." Manufacturing Engineering(April): 52-59.

Tlusty, J. (1985). Machine Dynamics. Handbook of High Speed Machining Technology. R. King. New York, Chapman and Hall: 49-153.

Tlusty, J., Smith S. (1997). "Current Trends in High-Speed Machining." Journal of Manufacturing Science and Engineering 119(November): 664-666.

Tobias, S. A. (1965). Machine Tool Vibration. New York, John Wiley and Sons, Inc.

Ulrich, K. S., David; Pearson, Scott; Jakiela, Mark (1993). "Including the Value of Time in Design-for-Manufacturing Decision Making." Management Science 39(4): 429-447.

Wasson, K. (1996). Hydrostatic Machine Tool Spindles. Mechanical Engineering. Cambridge MA, Massachussetts Institute of Technology.

Wasson, K. (1997). Hydrostatic Tool: Predicted Dynamic Response, Aesop.

WWW (1997). http://www.hsk.com/toolhold.htm, Diebold Goldring Tooling.

WWW (1998). http://www.toolingsystems.com/univ/shrinker/ueshrink.htm, Tooling Stystems Division.

Appendix A: MATLAB™ code for Timoshenko beam finite element model.

clear

```
%Material Properties for Aluminum
%Elastic Modulus
Modulus(1)=10e6;
%Poisson's Ratio
PR(1)=.332;
%Sheer Modulus
Smodulus(1)=Modulus(1)/(2*(1+PR(1)));
%Density
Density(1)=0.000254;


%Material Properties for Steel
%Elastic Modulus
Modulus(2)=29e6;
%Poisson's Ratio
PR(2)=.29;
%Sheer Modulus
Smodulus(2)=Modulus(2)/(2*(1+PR(2)));
%Density
Density(2)=0.000749;



%Material Properties for Carbide
%Elastic Modulus
Modulus(3)=60e6;
%Poisson's Ratio
PR(3)=.19;
%Sheer Modulus
Smodulus(3)=Modulus(3)/(2*(1+PR(3)));
%Density
Density(3)=0.0013;
```

```
%Select a material (1) Aluminum, (2) Steel, (3)Carbide

%Number of segments used to define tool
segments=4;

%dimension 1 in file
file=1
%for diameter=.5:.1:1;

%dimension 2 in rows
varcount2=2;
for var2=-4:-.25:-7;
var2=2*10^var2

%dimension 3 in columns
varcount1=1;
for var1=0:.2:1.8

% Defining Elements and B.C.

%Describe the Tool in the H.S. Bushing
Dia(1)=.5;
Idia(1)=0;
Len(1)=2;
Els(1)=5;

%Describe the Tool Overhang
Dia(2)=.5;
Idia(2)=0;
Len(2)=2.1;
Els(2)=2;

%Describe the Tool Overhang
Dia(3)=.35;
```

```
Idia(3)=0;
Len(3)=1.2;
Els(3)=2;

%Describe the Tool Overhang
Dia(4)=.6;
Idia(4)=0;
Len(4)=.2;
Els(4)=1;

%Describe the sleeve overhang
Dia(segments+1)=.75;
Idia(segments+1)=.5;
beginoh=var1;
lenoh=2-var1;




%Building Elements
L=0;
D=0;
d=0;

offset=0;

for n=1:segments;

for el=1:sum(Els(1:(segments+1-n)));
D(el)=Dia(segments+1-n);
d(el)=Idia(segments+1-n);
L(el)=Len(segments+1-n)/Els(segments+1-n);




end;
```

```
end;

for el=1:sum(Els(1:segments));
if offset>0 & sum(L(1:el))<=beginoh+lenoh;
L(el+offset)=L(el);
D(el+offset)=Dia(segments+1);
d(el+offset)=Idia(segments+1);
end;

if sum(L(1:el))>beginoh+lenoh & sum(L(1:el-1))<beginoh+lenoh;
L(el+offset)=beginoh+lenoh-sum(L(1:el-1));
D(el+offset)=Dia(segments+1);
d(el+offset)=Idia(segments+1);
end;

if sum(L(1:el))>beginoh & offset==0;
offset=sum(Els)-el+1;
L(el+offset)=sum(L(1:el))-beginoh;
D(el+offset)=Dia(segments+1);
d(el+offset)=Idia(segments+1);
end;

end;

N=sum(Els);
Ntot=length(L)
E=0;
v=0;
G=0;
p=0;

material=3;
for el=1:Ntot;
if el>N;
material=2;
```

122

```
end;
E(el)=Modulus(material);
v(el)=PR(material);
G(el)=Smodulus(material);
p(el)=Density(material);
end;


I=pi*(D.^4-d.^4)/64;
Area=pi/4*(D.^2-d.^2);
%Sheer Coefficient
k=10*(1.+v)./(12.+11*v);
%Shear Deformation Parameter
S=(k.*G./E).*(Area.*L.^2./I);
%Rotary Inertia Parameter
R=I./(Area.*L.^2);



%Defining Nodes
Nodes=length(L)+2;
K=zeros([1,Nodes]);
C=zeros([1,Nodes]);




%Add a spring and/or damper
%K('node') or C('node')=



%Distributed Viscous Damper(SFD with closed ends)
%Radial clearance
h=.0012;
%variable viscosity
visc=var2;
Dampel=6*pi*(Dia(1)/2)^3*(Len(1)*visc/h^3)/(Els(1)-1);
```

```
for n=1:Els(1);
C(n)=Dampel;
end;


%Distributed Hysteretic Damper
%Material thickness
%t=.03;
%Material Elastic Modulus
%EM=4000;
%Material Loss Factor
%LF=.1;
%Dampel=(Dia(1)*(Len(1)*EM/t)/(Els(1)-1)*(1+.1i);
%for n=1:Els(1);
%K(n)=Dampel;
%end;




%Declare the size of the mass, stiffness, and damping matrices
Mass=zeros(Nodes*4,Nodes*4);
Stiffness=zeros(Nodes*4,Nodes*4);
Damping=zeros(Nodes*4,Nodes*4);


%Calculating the Element Mass and Stiffness Matrices
jump=0;

for j=1:Ntot;

if j>N;
jump=4;
end;

Mass(4*j-3+jump:4*j+4+jump,4*j-3+jump:4*j+4+jump)=Mass(4*j-
3+jump:4*j+4+jump,4*j-
3+jump:4*j+4+jump)+p(j)*Area(j)*L(j)^3/420*[156/L(j)^2  0 22/L(j) 0
```

```
54/L(j)^2 0 (-13)/L(j) 0;0 156*R(j) 0 22*R(j) 0 54*R(j) 0 (-13)*R(j);22/L(j)
0 4 0 13/L(j) 0 (-3) 0;0 22*R(j) 0 4*R(j) 0 13*R(j) 0 (-3)*R(j);54/L(j)^2 0
13/L(j) 0 156/L(j)^2 0 (-22)*L(j) 0;0 54*R(j) 0 13*R(j) 0 156*R(j) 0 (-
22)*R(j);(-13)/L(j) 0 (-3) 0 (-22)/L(j) 0 4 0;0 (-13)*R(j) 0 (-3)*R(j) 0 (-
22)*R(j) 0 4*R(j)];
Stiffness(4*j-3+jump:4*j+4+jump,4*j-3+jump:4*j+4+jump)=Stiffness(4*j-
3+jump:4*j+4+jump,4*j-
3+jump:4*j+4+jump)+E(j)*I(j)/(420*L(j))*[504*S(j)/L(j)^2 210*S(j)/L(j)
42*S(j)/L(j) 42*S(j)/L(j) (-504)*S(j)/L(j)^2 210*S(j)/L(j) 42*S(j)/L(j) (-
42)*S(j)/L(j);210*S(j)/L(j) 156*S(j)+504 (-42)*S(j) 22*S(j)+42 (-
210)*S(j)/L(j) 54*S(j)-504 42*S(j) (-13)*S(j)+42;42*S(j)/L(j) (-42)*S(j)
56*S(j) 0 (-42)*S(j)/L(j) 42*S(j) (-14)*S(j) (-7)*S(j);42*S(j)/L(j)
22*S(j)+42 0 4*S(j)+56 (-42)*S(j)/L(j) 13*S(j)-42 7*S(j) (-3)*S(j)-14;(-
504)*S(j)/L(j)^2 (-210)*S(j)/L(j) (-42)*S(j)/L(j) (-42)*S(j)/L(j)
504*S(j)/L(j)^2 (-210)*S(j)/L(j) (-42)*S(j)/L(j) 42*S(j)/L(j);210*S(j)/L(j)
54*S(j)-504 42*S(j) 13*S(j)-42 (-210)*S(j)/L(j) 156*S(j)+504 (-42)*S(j) (-
22)*S(j)-42;42*S(j)/L(j) 42*S(j) (-14)*S(j) 7*S(j) (-42)*S(j)/L(j) (-42)*S(j)
56*S(j) 0;(-42)*S(j)/L(j) (-13)*S(j)+42 (-7)*S(j) (-3)*S(j)-14 42*S(j)/L(j) (-
22)*S(j)-42 0 4*S(j)+56];
end;

Soffset=offset*4+4;
for j=1:Nodes;
%account for linear springs at the NODES!
Stiffness(4*j-3,4*j-3)=Stiffness(4*j-3,4*j-3)+K(j);
%account for linear viscousdamping at the NODES!
Damping(4*j-3,4*j-3)=Damping(4*j-3,4*j-3)+C(j);

%account for the sleeve
if j<=sum(Els)+1;
if (sum(L(1:j-1))>beginoh & sum(L(1:j-1))<beginoh+lenoh);
Stiffness(4*j-3+Soffset,4*j-3+Soffset)=Stiffness(4*j-3+Soffset,4*j-
3+Soffset)+K(j);
Stiffness(4*j-3,4*j-3+Soffset)=Stiffness(4*j-3,4*j-3+Soffset)-K(j);
Stiffness(4*j-3+Soffset,4*j-3)=Stiffness(4*j-3+Soffset,4*j-3)-K(j);
```

```
Damping(4*j-3+Soffset,4*j-3+Soffset)=Damping(4*j-3+Soffset,4*j-
3+Soffset)+C(j);
Damping(4*j-3,4*j-3+Soffset)=Damping(4*j-3,4*j-3+Soffset)-C(j);
Damping(4*j-3+Soffset,4*j-3)=Damping(4*j-3+Soffset,4*j-3)-C(j);
end;
end;


end;


%fix one end rotationally and translationally
Mass=[Mass(5:N*4+4,5:N*4+4)
Mass(5:N*4+4,N*4+9:Ntot*4);Mass(N*4+9:Ntot*4,5:N*4+4)
Mass(N*4+9:Ntot*4,N*4+9:Ntot*4)];
Stiffness=[Stiffness(5:N*4+4,5:N*4+4)
Stiffness(5:N*4+4,N*4+9:Ntot*4);Stiffness(N*4+9:Ntot*4,5:N*4+4)
Stiffness(N*4+9:Ntot*4,N*4+9:Ntot*4)];
Damping=[Damping(5:N*4+4,5:N*4+4)
Damping(5:N*4+4,N*4+9:Ntot*4);Damping(N*4+9:Ntot*4,5:N*4+4)
Damping(N*4+9:Ntot*4,N*4+9:Ntot*4)];
statvar=max(size(Mass));



f=diag(ones(1,statvar),0);
Aa=[zeros(statvar) diag(ones(1,statvar),0);inv(Mass)*(Stiffness*(-1))
inv(Mass)*(Damping*(-1))];
Bb=[zeros(statvar) zeros(statvar);zeros(statvar) inv(Mass)*f];
Cc=zeros(1,2*statvar);
%observe tip deflection
Cc(sum(Els)*4-3)=1;
Dd=zeros(1,2*statvar);
eigenvalues=eig(Aa);
magnitude=abs(eigenvalues);
rval=real(eigenvalues);
ival=imag(eigenvalues);
centfreq=0;
```

```
index=length(eigenvalues);
while centfreq==0;
if ival(index)~=0;
centfreq=magnitude(index)*(1-2*(rval(index)/magnitude(index))^2)^.5;
end;
index=index-1
end;
W=[0 linspace(centfreq-62.8,centfreq+62.8,21)];
%force at tip
[Mag,Phase,W]=bode(Aa,Bb,Cc,Dd,sum(Els)*4-3+statvar,W);
Faxis=W/2/pi;

varcount1=varcount1+1
dynamic(1,varcount1)=var1;
dynamic(varcount2,varcount1)=[max(Mag)];
static(1,varcount1)=var1;
static(varcount2,varcount1)=[Mag(1)];
end;


dynamic(varcount2,1)=var2;
static(varcount2,1)=var2;
varcount2=varcount2+1
end;

%set names of output files
filename=['visceff' num2str(file) '.txt'];
eval(['save ' filename ' dynamic static -ascii -double -tabs']);
%file=file+1

%end;
```

Appendix B: Frequency and damping measurement repeatability

Repeatability of 1/2" diameter 5" overhang carbide tool Dynamic Response Measurements			
Trial	Frequency	Damping	Q
	Hz	Zeta	1/(2*Zeta)
1	657	1.93E-02	25.8
2	659	2.20E-02	22.8
3	655	1.67E-02	29.9
4	654	1.74E-02	28.8
5	656	1.85E-02	27.0
6	657	1.88E-02	26.7
7	655	1.74E-02	28.7
8	657	1.93E-02	25.9
9	657	1.90E-02	26.4
10	656	1.87E-02	26.7
Average	656.3	1.87E-02	26.9
STDEV	1.4	1.45E-03	2.0
95% confidence interval:			
+/-	2.8	2.84E-03	3.9

Appendix C: Heat shrink tolerances EXCEL™ spreadsheet

SHRINK FIT

Variables
Shaft inner diameter   0 in
Shaft E   2.90E+07 psi
Shaft u   0.295

Hub E   2.90E+07 psi
Hub u   0.295
Hub T.E.C   6.00E-06 in/in/F
Hub UTS   7.30E+04 psi

Fit Design
Maximum material condition   Minimum material condition
max shaft od   **1 min shaft od   0.9995**
min hub id   **0.9984 max hub id   0.999**
max hub od   2.001 min hub od   1.999
final hub od   2.003355 final hub od 1.999736

maximum pressure   **17429.0059 psi**
minimum pressure   **5442.48846 psi**
maximum stress   28983.4663 psi
safety factor   2.51867735
Max zero clearance assembly temperature **deg F**
Hub OD tol. range   0.00361903 in

minimum allowance   0.0005
length of shrinkfit   1

dissassembly force   **1708.95727 lbs**
                               from A*Pres*Fcoef(.1)

Max		
Unfit Shaft Dimensions		
Inner Radius	0	a
Outer Radius	0.5	
E	2.90E+07	
Mu	0.295	
Unfit Hub dimensions		
Inner Radius	0.4992	
Outer Radius	1.0005	
E	2.90E+07	
Mu	0.295	
nominal interface radius	0.4996	
interference	0.0008	
pressure	17429.01	
Fit Shaft Dimensions		
Inner Radius	0	
Outer Radius	0.499788	
Fit Hub Dimensions		
Inner Radius	0.499787	
Outer Radius	1.001677	

Min	
Unfit Shaft Dimensions	
Inner Radius	0
Outer Radius	0.49975
E	29000000
Mu	0.295
Unfit Hub dimensions	
Inner Radius	0.4995
Outer Radius	0.9995
E	29000000
Mu	0.295
nominal interface radius	0.499625
interference	0.00025
pressure	5442.488
Fit Shaft Dimensions	
Inner Radius	0
Outer Radius	0.499684
Fit Hub Dimensions	
Inner Radius	0.499684
Outer Radius	0.999868

Appendix D: Article

Stilwell, Gerry, <u>Taking the Mystery Out of Hard Die Milling</u>, Manufacturing

Engineering, April 1998

TAKING THE

OUT OF HARD DIE MILLING

Look closely at the process, and your jobs, before making the leap

Hard die milling can produce mold cavities or dies from hard (R_C 50+) materials to final dimension and finish. eliminating most or all handwork and EDM processes. This very appealing concept has lately become the Holy Grail of machining.

In principle. hard die milling can significantly compress manufacturing lead times. It can reduce the number of operations performed on a part, decrease the amount of hand polishing, and eliminate the need for EDM. While many shops are rushing to embrace this technology. it intimidates others. Although there's no magic to the process, and hard die milling can't provide an answer for every problem, when properly applied it can enhance current shop practice.

If you want to adopt hard die milling, begin by considering cutter requirements. process design, and CNC and machine tool requirements. Also, think about the workpiece and the proper application of hard die milling in the context of "open surfaces" and "intricate surfaces." In general, open surfaces don't have tight corner radii ($\frac{1}{16}$" or 1.6 mm) and steep walls. Gentle changes in curvature, easily accessed by tools. characterize open surfaces. enabling you to employ large-diameter tools and cutter bodies.

If open surfaces call to mind the Great Plains, then intricate surfaces look like the Grand Canyon. They have steep walls with minimal taper and rapid changes in curvature along the part's floor. Consequently, you need small tool radii with long cutter bodies to gain access to the surface. To

GERRY STILWELL
CHIEF APPLICATIONS ENGINEER
BOSTON DIGITAL CORP.
MILFORD, MA

Main/auxiliary spindle combination, which works well for hard-die milling. provides low-end torque and high rpms cost-effectively.

work on an intricate surface. the cutter path requires significantly higher accelerations and decelerations—and a larger number of reversals—than the path followed to machine an open surface. The corner radii are also significantly tighter. These characteristics make intricate surfaces more difficult to produce in hardened steel than open surfaces.

Picking the Right Cutter

Hard die milling in open surfaces is significantly easier, and more practical, than in intricate surfaces. When producing open surfaces. less-capable machine tools and tooling will often prove adequate. while intricate surfaces require more advanced (and expensive) capabilities.

To machine hardened materials successfully. milling cutters must be stiff. tough, and highly heat resistant.

At Boston Digital, we find that TiAlN-coated tools provide the best combination of wear resistance and aggressive material removal for hard die milling applications. TiN-coated tools yield good results, although tool life can't match that of TiAlN-coated tools. This result makes sense because TiN offers only 70% of the hardness and 73% of the heat resistance of TiAlN. Given that TiAlN-coated inserts cost approximately 10% more than TiN, we believe the performance of TiAlN-coated inserts justifies their extra cost.

Standard carbide end mills won't do for machining hardened steels because they wear out so quickly. In tests, they removed material well, and provided good surface finishes on R_c 55 cavities, but tool life was only 1 to 1.5 hours per tool. In comparison, TiAlN tools making similar cuts lasted for 16 hours.

As an example of the benefits of TiAlN tooling, consider a 2 × 3 × 0.5" (51 × 76 × 13 mm) mold cavity for a consumer product cut in S7 tool steel hardened to R_c 55. An intricate surface, the part includes a dozen or so bosses and ribs along its floor. After roughing out the part, the operator switched to a 1/16" (1.6 mm), TiAlN-coated, four-flute ball mill running at 23,000 rpm and 40 ipm (1.0 m/min) in a finish cut with a 0.005" (0.13 mm) depth of cut. The cutter lasted through the entire finish-path length of 9600" (244 m) with no sign of wear at any location other than the bottom of the ball. This cutter produced a surface finish of 10 μin. (0.254 μm) R_a.

When roughing, the benefits of TiAlN-coated tools are also readily apparent. A two-inch-square (51 × 51 mm), R_c 50 cavity 0.75" (19 mm) deep was roughed with high-speed machining techniques using a 0.5" (13 mm) TiAlN end mill costing $200. When machining in a spiral from a 0.75"-diam start hole at the center of the part (employing a 0.01" or 0.25 mm radial stepover and a 0.4" or 10 mm-axial depth of cut), the process achieved average feed rates that exceeded 200 ipm (5.1 m/min). Cooled using pressurized air, the tool exhibited minimal wear and completed the cut in less than three minutes.

By comparison, a 0.375" (9.5 mm) carbide end mill costing $20, employing a conventional coating, machined the cavity using a feed rate of 4 ipm (102 mm/min), a 0.2" (5.1 mm) radial stepover, and a 0.1" (2.5 mm) depth of cut. This conventional roughing process, supported by air-oil-mist lubrication, required more than 20 min. The conventional tool had a life of approximately two parts.

End mills for hard die milling need large central cores and smaller flutes than conventional tools, as well as the proper tool coatings. These changes in tool geometry help to minimize deflection as the tools get longer, as well as provide enough stiffness to resist vibration and premature tool wear.

Process Definition

In addition to selecting appropriate tools, it's important that you define the cutting process. Guidelines to consider include:

Coolant. Flood coolant is not ideal for hard die milling, particularly when working on intricate parts. Air-oil mist or chilled compressed air works better. ITW Vortex produces a chilled air-dispensing unit that runs on compressed air; it's well-suited to such applications.

Toolpath design. When working with hardened materials, you must ensure that the tool sees a constant stock-on condition as it cuts. While cutters can take heavy loads, rapid changes in load "shock" the tool and will break it. To prevent tool breakage, it's important to exit and enter hardened workpieces

smoothly. Best practice calls for beginning the roughing of hardened materials using a start-hole, which can be helical cut. The roughing toolpath is then laid out as a spiral, beginning at the start-hole. Z-level cutting is also a useful approach for hard die milling, particularly when working with open or convex surfaces. By maintaining a constant radial and axial depth-of-cut, it ensures that the tool sees a constant chip load, increasing tool life.

Cornering. When working on intricate or concave parts such as small mold cavities with ribs or bosses, pursuing a Z-level cutting strategy becomes more difficult. In such cases, the toolpath will consist of planar slices along the part. In these cases, you can't use a single feed rate down the wall, across the bottom, and back up the opposite side. As the tool moves into a corner, it experiences more engagement and may break, or at least break down, if the feed rate doesn't decrease.

Consider a case where a machinist used a 1/16" (1.6 mm) TiAlN ball mill to finish a cavity after using a 1/8" (3.2 mm) ball mill to semifinish it. The length of the tool was approximately 6× its diameter. To optimize the cutting process, the machinist employed a feed rate of 10 ipm (254 mm/min) in the down cut as the tool approached
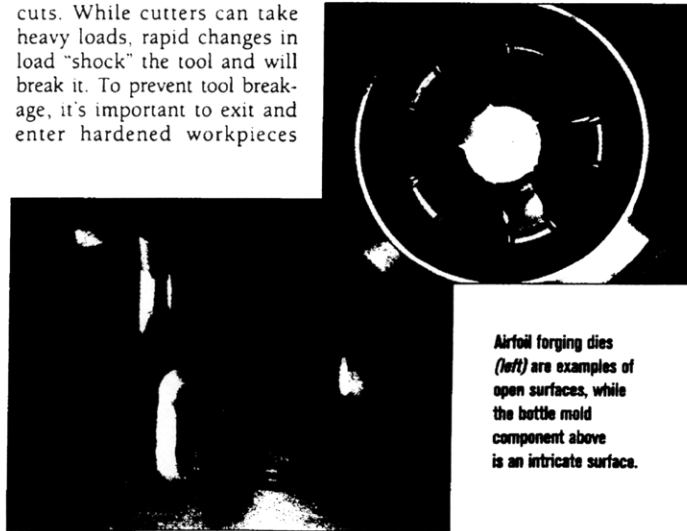
Airfoil forging dies *(left)* are examples of open surfaces, while the bottle mold component above is an intricate surface.

131

Cutter Path and Speeds

128° Cutter Engagement

10 IPM

40 IPM

35 IPM

221° Cutter Engagement
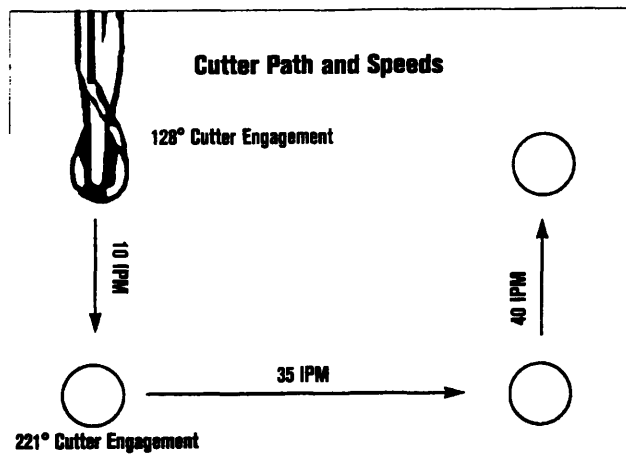
Mold cross section illustrates a change in cutter engagement through a cut.

the corner, 35 ipm (0.9 m/min) across the floor of the cavity, and 40 ipm (1 m/min) up the far wall. Feed rates in the part program were automatically modified using Boston Digital's FMF software, and further conditioned using Contour Optimization software on the BDC 3200X CNC.

A feed rate of 10 ipm ensured that the tool did not see excessive chip load as it entered the corner. Too great an increase in the chip load would place excessive pressure on the tool, causing it to break. Across the part's floor, where the chip load remained constant, the program called for a higher feed rate. To prevent chatter as the tool moved into the far corner and up the wall, a higher feed rate prevented the tool from kicking away from the surface. Because of the cutter's local surface speed at the point where it engages the excess stock in the corner, the case of moving into a corner and up is handled differently than entering a corner moving down.

While many CAM systems generate a single feed rate for an entire cutter path, you must remember to modify the feed rate as a function of the tool vector and the expected chip load. Otherwise tool breakage will occur, a particularly traumatic event when, as in hard die milling, finish operations

can take six hours or more. You must pay similar attention to feed rate when cornering in side-milling situations.

Climb vs. conventional milling. Conventional wisdom says that conventional milling will provide a better finish than climb milling. Tooling manufacturers, and the experiences of our engineers and customers, tell us that climb milling provides the best results in terms of finish and tool life. Remember that the workpiece is not just case-hardened. And when an operation involves conventional milling through hardened materials, the cutter can't "get under" the hard material, and the tool gets pushed away from the part, inducing chatter. Conventional milling in hardened materials also tends to cause burrs as the cut progresses.

Calculating true SFM. Hardened materials prove much less forgiving than conventional steels when it comes to tool life. So you must calculate true SFM when using ball end mills. If the depth of cut is less than the radius of the ball end mill, you can calculate the true cutting diameter (TCD) of the tool using the formula:

TCD=2x[R²-(R-C)²]

R =Cutter Radius

C=Axial Depth of Cut.

Use this diameter to calculate the spindle speed required to achieve the desired SFM. Similar effects apply when side milling, in terms of the true

chip load compared to that encountered during a fully engaged cut.

Trouble with ball mills. At the bottom of a ball mill, cutter velocity equals zero. When ball mills run along horizontal surfaces in a vertical machining center, they provide minimal cutting action. Likewise, on surfaces with only a slight angle relative to the horizontal plane, the tool's surface speed is very low. This low cutter speed matters because the zero-SFM effect degrades surface finish, generates excess heat, and increases part machining times. Particularly when machining hard materials, a process that involves long machining times and stringent surface finish requirements, you must stay off the bottom of ball mills. In some situations you can solve this problem by using cutters such as Millstar's toroid bull nose cutters, which provide two cutting edges and eliminate the area of zero cutting speed.

Another way to skin this cat is to present the machined surface to the cutter at an angle. Putting the part on a sine plate enables you to do so when a single surface dominates the part. With more complex parts, much of the geometry will remain perpendicular to the axis of the cutter, and will be exposed to the cutter's zero-speed area. Alternately, four and five-axis machines can continuously maintain a specific angle (15°, for example) between the tool and the surface normal. Actively controlling tool orientation with respect to the part establishes a constant cutting speed, reducing cycle times and improving surface finish.

BostoMatic five-axis machines machine electrodes, molds, and patterns in this manner. In addition to providing increased cutting speeds, five-axis machines improve access to the part, and allow the use of larger-diameter, shorter tools. Employing five-axis machines further reduces machining cycles by enabling more aggressive machining. But these advantages must be balanced against the potential inaccuracies introduced by the two additional degrees of freedom in a five-axis machine tool.
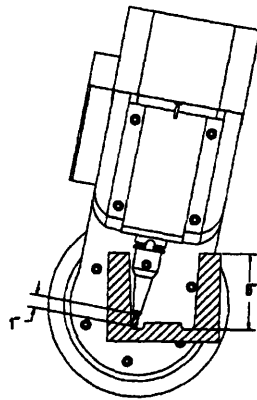
When used with angled tools, five-axis machines can also cut relatively sharp internal corners into parts. For

132
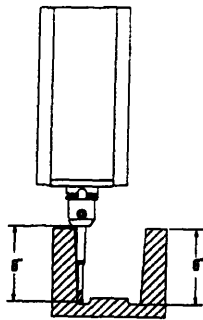
VMC WITH HSK SPINDLE

BOSMATIC 5 AXIS WITH HSK SPINDLE

To access this mold cavity, this BostoMatic five-axis machine uses a stiffer toolholder, and a tool that's shorter by 2" (51 mm), than a three-access VMC would employ.

example, a 90° angled cutter can create an almost-sharp corner in a square cavity. The operator makes the corner by presenting the spindle head at an angle to the part and running the tool up along the previously radiused corner formed by two sides of the cavity.

Machine Tool and CNC Requirements

Many machine tools and CNCs can mill hardened materials, and you need not spend $300,000+ to purchase such capabilities. At last year's European machine tool show, a num- ber of machines on display, some priced at less than $100,000, were machining hardened steels. While most of these machines could remove material as required, and some of them provided good surface finishes, they all had trouble providing high quality crossovers. One machine, which machined a hardened connect- ing-rod forging die, created a part with a beautiful finish. But it left a ripple where the X-axis reversed that appeared to exceed 0.001" (0.025 mm) in size!

To perform hard die machining, a machine should possess the following characteristics:

Stiffness—seek out very rigid machines like C-frame VMCs and hor- izontals. Look for linear roller ways, which are stiffer than hydrodynamic way systems and ball ways. Avoid large axis stackups and overhanging head stocks.

Spindle—running smaller tools requires high speed. Roughing with tools that approach 1" (25 mm) in diam calls for lower rpms, often less

133

than 6000 rpm. A 30-hp (22.4 kW), 30,000-rpm motorized spindle is probably not the answer. These very expensive spindles experience relatively short bearing lives due to the difficulty of combining high-end speed with low-end power and stiffness.

Employing a main/auxiliary spindle pair does the job more economically (with better low-end torque). You might, for example, use a rigid 15-hp (11.2 kW), 8000 or 12,000-rpm main spindle with HSK 63A tooling and a high-speed (25,000+rpm) auxiliary spindle to handle smaller tools. A main/auxiliary spindle pair costs less, and operates more reliably, than a single large motorized spindle, because each spindle is optimized for a more specific speed/torque requirement. Should one spindle go down, you incur lower repair costs, and the machine continues to run in the meantime.

Damping—a well-damped machine structure absorbs vibration created during cutting. Seek heavy iron castings and/or polymer concrete bases; avoid welded structures. The emergence of hydrostatic spindles and way systems promises help in this area.

Accuracy—you need a machine with a high degree of dynamic accuracy. Don't allow static positioning accuracy and repeatability numbers to influence you, unless they are to ISO specifications. Look closely at ball-bar test results and seek machines with better than 0.0003" (0.008 mm) TIR on a 12" (305 mm) ball bar at 20 ipm (508 mm/min). Some builders can provide tighter values (0.00015" or 0.004 mm in some cases) as part of ultraprecision packages.

Feed and Acceleration—hard die milling requires high feed rates, particularly when roughing. But because most of the processing time goes into finishing the part (80% or more for intricate components), acceleration is more important than top-end feed rate. A machine capable of feeding at 600 ipm (15 m/min) with accelerations exceeding 0.3 g will prove less useful in hard die milling than one able to feed at 400 ipm (10 m/min) and 0.7 g. Open parts will tend to favor high feed rates over high accelerations, while the opposite is true for intricate parts.

Motion Algorithms—not all CNC motion algorithms are created equal. Most machines come equipped with a "one-speed transmission" that strikes a compromise between maximum feed rates for roughing and maximum attainable accelerations. Better systems provide a four-speed transmission, allowing the user to shift between roughing mode (high feed rates and low accelerations) and precision or ultraprecision modes (lower feed rates and very high accelerations) for finishing. Using contour optimization and feed rate modification features to slow the machine as it enters areas of increased material and tight corners also proves critical for hard die milling.

Data handling—make sure the CNC has a large hard-disk drive and an Ethernet connection to enable fast transfer and storage of large programs, and to eliminate drip feeding. With a fast enough CNC (1000+ five-axis blocks per second), Ethernet, and a large high-density disk, NURBS becomes unnecessary. Avoid the added complexity and cost if you can.

Practical Hard Die Milling

Hard die milling can economically produce open surfaces in lieu of milling plus EDM processes, if you don't require an EDM-type finish. As parts become more intricate, the use of hard die milling becomes more technically challenging, and options must be weighed carefully.

While hard die milling can reduce the manufacturing lead time for a mold or die. it's a less robust process than EDM. Small tools break more easily in tight corners. Also, milling of soft steel and electrodes, followed by burning, often allows you to hold tighter tolerances than does hard die milling. Further, for shops machining small lot sizes, the time required to optimize a hard die milling process can be excessive.

While hard die milling may require less total process time than a milling plus EDM process. the latter often involves night or weekend work, without operator intervention. Such untended operation is much more difficult to achieve with hard die milling, particularly when your operation produces small quantities of unique pieces. Considering all these factors, it seems clear that EDM will remain a more automated/-untended process than hard die milling.

Not that hard die milling won't prove a viable process for intricate parts. Many machining operations use it successfully today. And in the future, hard die milling will certainly become more robust as machine tool builders, tooling manufacturers, and machine shops become more proficient in its application. If your shop adopts hard die milling, make sure that the machine you choose is well suited to the production of electrodes and other work. Remember that it's difficult to predict the hard die milling content of your work at the onset.

Oddly enough, making good electrodes calls for many of the capabilities you require for hard die milling as well—excellent machine geometry, high dynamic accuracy, a fast CNC, and a high-speed, accurate spindle. To these requirements add greater stiffness and a more powerful spindle to enable hard die milling. Finally, set realistic expectations. In most cases, complete elimination of all EDM and hand finishing is not realistic. Build your justification for adopting hard die milling around a more likely scenario, in which you can reduce, but not eliminate, EDM and hand finishing.■

Gerry Stilwell can be reached at 508-473-4561.